Dissertation zur Erlangung des Doktorgrades
der Fakultät für Chemie und Pharmazie
der Ludwig-Maximilians-Universität München

The Structure of RseB, a Sensor for Periplasmic Stress in *Escherichia coli*

Petra Wollmann
aus Karlsruhe

2007

Erklärung

Diese Dissertation wurde im Sinne von §13 Abs. 3 bzw. 4 der Promotionsordnung vom 29. Januar 1998 von Herrn Prof. Dr. Dieter Oesterhelt betreut.

Ehrenwörtliche Versicherung

Diese Dissertation wurde selbstständig, ohne unerlaubte Hilfe erarbeitet.

München, am 01.10.2007

Petra Wollmann

Dissertation eingereicht am: 04.10.2007

1. Gutachter: Prof. Dieter Oesterhelt

2. Gutachter: Prof. Karl-Peter Hopfner

Mündliche Prüfung am: 07.02.2008

Dedicated to my family

Publications during PhD:

Wollmann, P. & Zeth, K. (2007). The structure of RseB: A sensor in periplasmic stress response of *E. coli*. *Journal of Molecular Biology* **372**, 927-941.

Wollmann, P. & Zeth, K. (2006). Expression, crystallization and preliminary X-ray analysis of the periplasmic stress sensory protein RseB from *Escherichia coli*. *Acta Crystallographica Section F* **62**, 895-898.

Wollmann, P., Zeth, K., Lupas, A. N., Linke, D. (2006). Purification of the YadA membrane anchor for secondary structure analysis and crystallization. *Internationl Journal of Biological Macromolecules* **39**, 3-9.

1. Introduction ... 3
1.1. Stress Response in Bacteria ... 3
1.2. Overview of Extracytoplasmic Stress in *E. coli* ... 5
1.2.1. Envelope of Gram-Negative Bacteria ... 5
1.2.2. Extracytoplasmic Stress Response Pathways in *E. coli* ... 6
1.2.2.1. CpxAR Stress Response Pathway ... 7
1.2.2.2. σ^E Stress Response Pathway ... 8
1.3. Key-Players of the σ^E Stress Response Pathway ... 10
1.3.1. RseA, the anti-Sigma Factor ... 10
1.3.2. DegS, a Stress Sensor and Site-1-Protease ... 11
1.3.3. RseP, a Site-2-Protease ... 12
1.3.4. RseB, a Negative Regulator of σ^E ... 13
1.4. Signals that Activate the σ^E Regulon ... 14
1.5. Conceptual Formulation ... 15
2. Results ... 16
2.1. X-ray Structural Analysis of RseB ... 16
2.1.1. Cloning and Purification of RseB ... 16
2.1.2. Crystallization and Data Collection of RseB ... 17
2.1.3. Phasing and Model Building ... 20
2.1.3.1. Phasing of Data from $P42_12$ Crystals by MIR ... 20
2.1.3.2. Manual Model Building of RseB from Data of $P42_12$ Crystals ... 20
2.1.3.3. Phasing of Data from $C222_1$ Crystals by MR ... 21
2.1.3.4. Quality of the Final Models of RseB ... 22
2.2. Structure of RseB ... 23
2.2.1. Overall Structure of RseB ... 23
2.2.2. Structural Variability ... 24
2.2.3. Structural Comparison ... 26
2.2.3.1. Comparison of the Small Domain with Structural Homologs ... 26
2.2.3.2. Comparison of the Large Domain with Structural Homologs ... 27
2.2.4. Interface of the Large and the Small Domain of RseB ... 29
2.2.5. Conserved Patches on the Surface of RseB ... 30
2.2.6. Oligomeric Assemblies of RseB in the Crystal Lattice ... 31
2.2.6.1. Large Oligomeric Assemblies in the Crystal ... 31
2.2.6.2. Contacts in the Crystal ... 33
2.2.6.3. Co-Crystallization of RseB with Detergent ... 37
2.3. Biochemical Analysis of RseB ... 38
2.3.1. Oligomeric State of RseB in Solution ... 38
2.3.1.1. Analytical Ultracentrifugation of RseB ... 40
2.3.1.2. Small Angle X-ray Scattering (SAXS) of RseB ... 41
2.3.1.3. Electron Microscopy of RseB ... 43
2.3.2. Interaction of RseB and RseA-PP ... 44
2.3.2.1. Cloning, Purification and Biochemical Analysis of RseA-PP ... 44
2.3.2.2. Direct Interaction of Dimeric RseB and RseA-PP ... 46
2.3.2.3. RseB Binds $RseA_{162-186}$ ... 48
2.3.3. Biochemical Properties of the Large and Small Domains of RseB ... 50
2.3.3.1. Cloning and Purification of the Large and Small Domain of RseB ... 50
2.3.3.2. Large Domain of RseB Forms Multiple Oligomers ... 51
2.3.3.3. Small Domain of RseB Interacts with RseA-PP ... 52
3. Discussion ... 53
3.1. RseB Binding Site on RseA ... 53
3.2. RseA Binding Site on the small domain of RseB ... 54
3.3. Function of the Large Domain of RseB ... 55
3.3.1. Lipoproteins as Signals for RseB? ... 59
3.3.2. Model for RseB Binding to RseA and Lipoprotein ... 61
3.4. Oligomeric Forms of RseB ... 64
3.4.1. Possible Role of the RseB Dimers ... 64
3.4.2. Possible Role of the Large Oligomeric Forms of RseB ... 68
4. Summary ... 72

5. Materials and Methods 74
5.1. Material 74
5.1.1. Bacterial Strains 74
5.1.2. Chemicals 74
5.1.3. Enzymes and Proteins 75
5.1.4. Plasmids 76
5.1.5. Oligonucleotides 77
5.1.6. Instruments and Devices 77
5.1.6.1. Centrifuges 77
5.1.6.2. Devices for X-ray Data Collection 77
5.1.6.3. Software 77
5.1.6.4. Consumables 78
5.1.6.5. Additional Instruments and Devices 78
5.1.7. Media and Stock Solutions 79
5.1.7.1. *E. coli* Media 79
5.1.7.2. Stock Solutions 79
5.2. Methods 80
5.2.1. Molecular Biological Methods 80
5.2.1.1. Polymerase Chain Reaction 80
5.2.1.2. Digestion of DNA 81
5.2.1.3. Dephosphorylation of linear DNA Fragments 81
5.2.1.4. DNA Ligation 81
5.2.1.5. DNA Sequencing 82
5.2.1.6. DNA Electrophoresis 82
5.2.1.7. Cultivation of *E. coli* 83
5.2.1.8. Preparation and Transformation of electro-competent *E. coli* 83
5.2.1.9. Transformation of chemo-competent *E. coli* 83
5.2.1.10. Isolation of Plasmid DNA from *E. coli* 84
5.2.1.11. Determination of DNA Concentration 84
5.2.2. Protein Biochemical Methods 85
5.2.2.1. SDS Polyacrylamide Gel Electrophoresis 85
5.2.2.2. Cloning and Purification of C-terminally His_6-tagged RseB 86
5.2.2.3. Cloning and Purification of RseA-PP 87
5.2.2.4. Cloning and Purification of RseB-D1 and RseB-D2 88
5.2.2.5. Determination of Protein Concentration 89
5.2.2.6. N-terminal Sequencing of Proteins 89
5.2.2.7. Size Exclusion Chromatography 89
5.2.2.8. Cross-Linking Proteins 89
5.2.2.9. Binding Studies of RseA and RseB using Ni-chelating material 90
5.2.2.10. Binding of RseB to RseA-Peptide 90
5.2.2.11. High Performance Liquid Chromatography/Mass Spectrometry 91
5.2.2.12. Analytical Ultracentrifugation (AUC) 91
5.2.3. Structure Based Methods 92
5.2.3.1. Small Angle X-ray Scattering (SAXS) 92
5.2.3.2. Negative Staining Electron Microscopy 92
5.2.3.3. Crystallization, Data Collection and Refinement 93
6. References 95
7. Abbreviations 104
8. Acknowledgement 105

1. Introduction

1.1. Stress Response in Bacteria

Prokaryotes consist of a single cell that is responsible for all vital requirements. This fascinating and effective principle of minimal organization has lead to enormous interest for biological, biochemical and medical studies. As a result of the limited cell size, bacteria are forced to accurately manage the production of only essential and needed cellular components. Additionally, useless or damaged elements require a rapid degradation to prevent crowding of the cellular space. The evolutionary consequence is that bacteria have adapted to sense and react to various external stress signals such as repellent compounds, chemicals, toxins, high cell density as well as cold and heat shock with often sophisticated response reactions.

Essential for all responses is at first place the recognition of and the sensibility for existing stress. As unfavourable stress signals mostly lead to accumulation of cellular damaged compounds, monitoring of malfunctions is an important mechanism of sensing stress. Once stress is recognized, the signal has to be processed and transferred to appropriate signal transduction pathways to activate the desired fast response in order to restore cellular integrity. This can be accomplished by repair mechanisms or *de novo* biosynthesis of damaged compounds. Injuries that are beyond repair have to be properly removed by the action of proteases or nucleases.

Bacteria are primarily equipped with two different possibilities of signal transduction pathways. (1) Two component systems, can sense signals with specialized receptors (sensor kinases) and transduce binding of a signal to a response regulator which is usually a transcription factor that in turn activates genexpression (Mizuno, 1997; Mizuno, 1998; Nixon et al., 1986). (2) A broader response to a stress signal is achieved by the activation of the so-called alternative sigma factors. These are normally inactive and only activated in situations where the expression of a subset of genes is required.

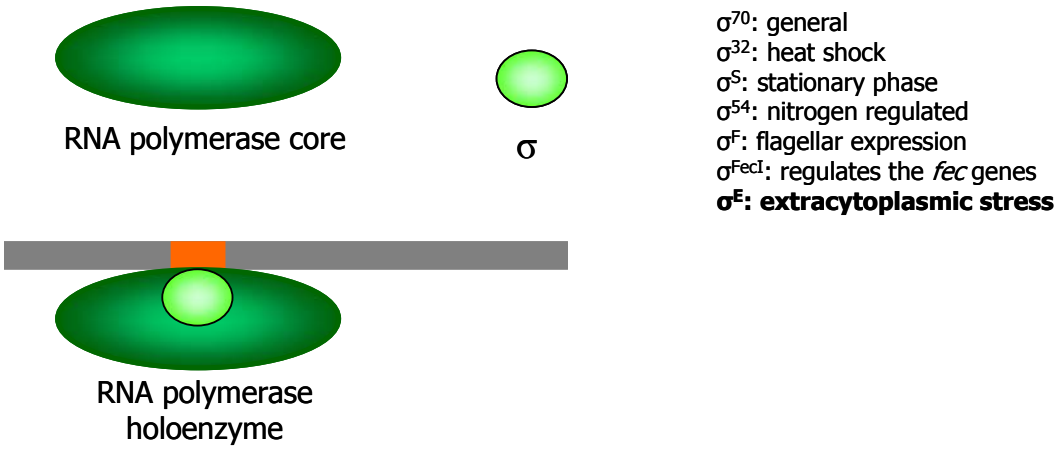

Figure 1. RNA polymerase and sigma factors. Schematic illustration of the RNA polymerase core (dark green) and its assembly with a sigma factor (light green) forming the transcriptionally active holoenzyme. The holoenzyme is able to bind to distinct promoters (orange) on the DNA (grey). Seven sigma factors from *E. coli* are listed on the right.

The prokaryotic RNA polymerase consist of 5 core subunits ($\alpha_2\beta\beta'\omega$) that only forms the transcriptionally active holoenzyme in complex with the sigma subunit which directs the RNA polymerase to the distinct promoters (Figure 1). The existence of more than one sigma factor gives an organism the possibility to change the expression of a set of genes in special situations. A correlation can be observed in the number of sigma factors and the environmental complexity or variability of an organism's habitat (Rhodius et al., 2006). For example *Mycoplasma* (Fraser et al., 1995; Himmelreich et al., 1996) an obligate intracellular pathogen has only a single sigma factor, whereas *Streptomyces coelicolor* has over 60 sigma factors available for specific adaptation functions needed for its complex developmental life style (Hutchings et al., 2004).

In *Escherichia coli*, seven sigma factors are known that can assemble with the RNA polymerase. Whereas the general σ^{70} is responsible for transcription of the housekeeping genes and as such needed under normal growth conditions, six additionally alternative sigma factors exist (Figure 1). The best characterized alternative sigma factor is σ^{32} that mediates the heat shock response (Grossman et al., 1984; Landick et al., 1984; Yura et al., 1984). At elevated temperatures, proteins involved in folding and degradation of proteins are up-regulated. These are commonly termed as heat shock proteins (HSPs) and are transcriptionally controlled by σ^{32} (Bardwell and Craig, 1987; Bardwell et al., 1986; Bukau, 1993). Regulation of σ^{32} is based on chaperones (DnaK/J) that bind to the sigma factor for inactivation under steady-state conditions (Straus et al., 1987; Young and Hartl, 2003). Accumulation of misfolded proteins in the cytoplasm during heat shock need refolding by

chaperones which results in an increased free pool of active σ^{32} (Bukau, 1993; Straus et al., 1990).

Another member of the alternative sigma factors is the σ^{E} that governs the extracytoplasmic stress response in *E. coli*. Here, the scenario for activation is more delicate, as the signal is sensed in extracytoplasmic regions whereas the sigma factor itself is located in the cytoplasm. This requires a signaltransduction cascade *via* the inner membrane.

1.2. Overview of Extracytoplasmic Stress in *E. coli*

1.2.1. Envelope of Gram-Negative Bacteria

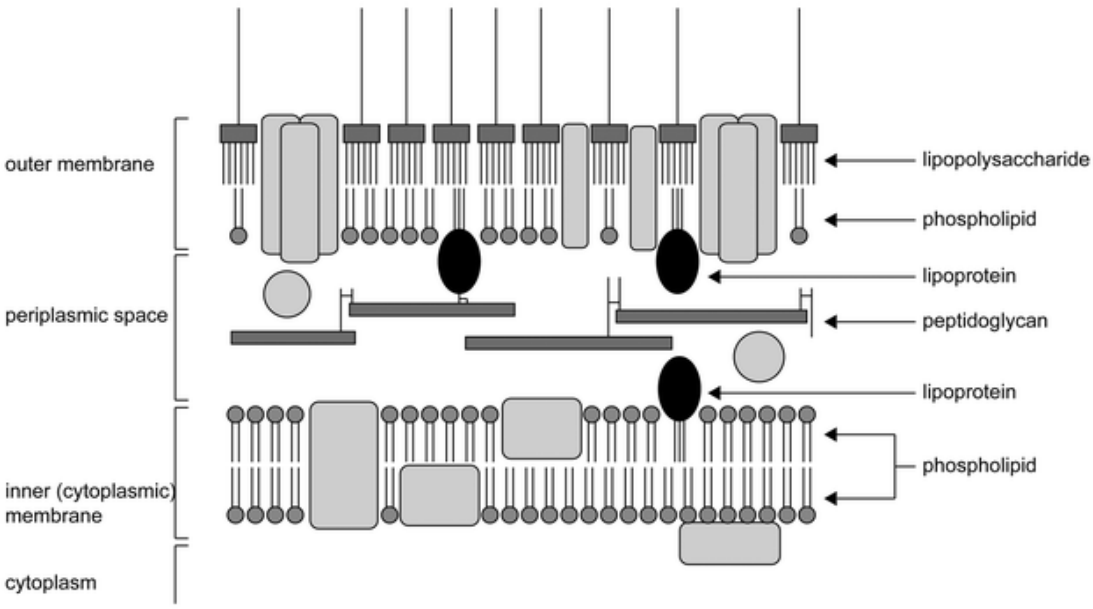

Figure 2. Envelope of Gram-negative bacteria. The envelope of Gram-negative bacteria comprises the inner and the outer membrane and the periplasmic space in between. The inner membrane is a bilayer of phospholipids whereas the outer membrane is composed of an inner layer of phospholipids and an outer layer of lipopolysaccharides. The peptidoglycan, located in the periplasm, confers rigidity to the envelope and is attached by lipoproteins to the outer membrane (illustration from Narita et al., 2004).

The hallmark of Gram-negative bacteria is the organization of the extracytoplasmic regions or the envelope, consisting of an inner and an outer membrane that are separated by the periplasmic space (Figure 2). The inner membrane is made up of a bilayer of phospholipids and contains membrane proteins and anchored lipoproteins. In contrast, the outer membrane exhibits a more asymmetric character, as its inner leaflet consists of phospholipids but its outer leaflet is mainly composed of lipopolysaccharides (LPS) (Kamio

and Nikaido, 1976). Generally proteins of the outer membrane are integral β-barrel forming outer membrane proteins (OMPs) and anchored lipoproteins. Up to 50% of the total mass of the outer membrane consists of OMPs (Nikaido, 1996) which include porins, channel-forming proteins and outer membrane receptors (Seltmann and Holst, 2002). Due to the high amount of channel forming proteins, the outer membrane has a porous character.

The periplasm is a highly viscous compartment with a protein mobility 100-fold lower than in the cytoplasm (Brass et al., 1986). This gel like matrix embeds the peptidoglycan which is a rigid layer forming a sacculus composed of polysaccharides, cross-linked by peptides, and is important for maintaining the bacterial shape (Weidel and Pelzer, 1964). The periplasm moreover differs from the cytoplasm in being devoid of ATP (Raivio and Silhavy, 2001). Furthermore, it exhibits an oxidizing milieu and therefore contains enzymes that catalyze disulfide bond formations (Nakamoto and Bardwell, 2004).

1.2.2. Extracytoplasmic Stress Response Pathways in *E. coli*

Quality control in the periplasm is crucial for the cell, as periplasmic and membrane proteins are synthesized in the cytoplasm and cross the inner membrane mostly as unfolded precursors (reviewed by Driessen et al., 1998; Müller et al., 2001). Additionally, the periplasm is only separated from the surrounding, often changing environment by the porous outer membrane. This is especially important for bacteria during infection, where they become target of the host immune defense system. Therefore, folding must be assisted and controlled to prevent that harmful environmental alterations impair the folding status and proper function of membrane and periplasmic proteins.

Monitoring of incorrectly folded proteins and assurance of intact membrane integrity is an essential function of the extracytoplasmic stress response pathways. These pathways share a common functional feature; the stress signal sensed in the periplasm is conducted *via* the inner membrane to the cytoplasm where the expression of a set of genes is arranged to minimize the defects caused by the unfavorable external condition. In *E. coli* two main and well characterized signaling pathways are known to respond to stress signals sensed in the envelope (Duguay and Silhavy, 2004; Raivio, 2005; Raivio and Silhavy, 2001). One of them (CpxAR) is a two component system whereas the second one acts *via* the alternative sigma factor σ^E.

Although these pathways correspond to unique signals and activate unique target genes they share some overlapping functions (Connolly et al. 1997; Raivio and Silhavy, 1999).

1.2.2.1. CpxAR Stress Response Pathway

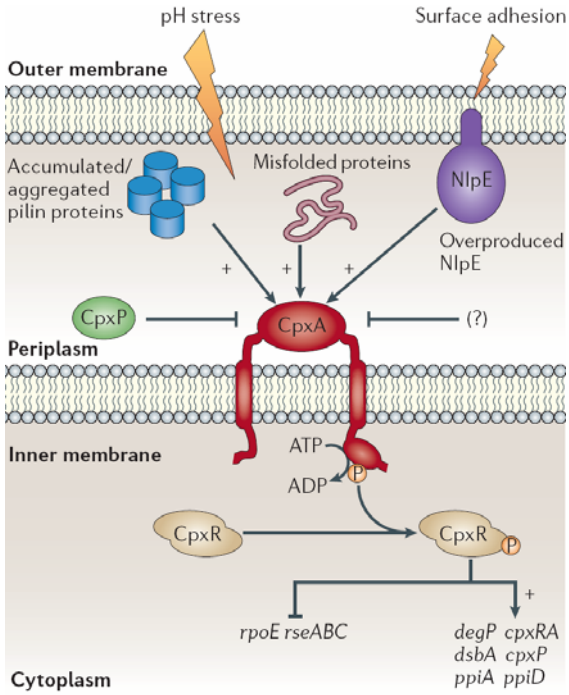

Figure 3. CpxAR two component system. The periplasmic domain of CpxA is suggested to sense stress signals and thereby triggers autophosphorylation of its cytoplasmic domain. The phosphate group is transferred to the response regulator CpxR, which is enabled to bind to specific sites on the DNA to activate transcription of the regulon. CpxP, a periplasmic protein negatively regulates CpxA kinase activity (illustration from Rowley et al., 2006).

As depicted in Figure 3, the CpxAR envelope stress response, composed of the CpxA sensor histidine kinase (Albin et al., 1986) and the CpxR response regulator (Dong et al., 1993), is mainly induced by stress events that result in protein misfolding. For example accumulation of pili subunits in the periplasm was shown to induce the CpxAR system which reflects its role in monitoring and altering the production of pili (Hung et al., 2001; Nevesinjac and Raivio, 2005; McEwen and Silverman, 1980; reviewed by Rowley et al., 2006). Besides this, the outer membrane lipoprotein NlpE specifically induces the pathway which is proposed to be caused by adhesion to surfaces (Otto and Silhavy, 2002; Snyder et al., 1995; Gupta et al., 1995).

Activation of CpxA leads to autophosphorylation and phosphotransfer to the aspartyl of CpxR, which then induces transcription of genes needed in the envelope (Raivio and Silhavy, 1999). Genes activated by phosphorylated CpxR include the periplasmic chaperone DegP (Danese et al., 1995), which is also a target of the σ^E stress response (see below), peptidyl-prolyl-isomerases PpiA and PpiD (Dartigalongue and Raina, 1998; Pogliano et al., 1997) and disulfide oxidase DsbA (Danese and Silhavy, 1997).

A periplasmic adaptor protein, CpxP (Danese and Silhavy, 1998) was suggested to have a role in fine tuning the system (Buelow and Raivio, 2005; Isaac et al., 2005). CpxP, normally down-regulates CpxA activity and is suggested to bind to unfolded proteins which results in enhanced activity of CpxA (Buelow and Raivio, 2005; DiGiuseppe and Silhavy, 2003). The CpxAR pathway is likely to be important for pathogenesis by means of monitoring adhesion to surfaces and for promoting biofilm formation (reviewed by Raivio, 2005).

1.2.2.2. σ^E Stress Response Pathway

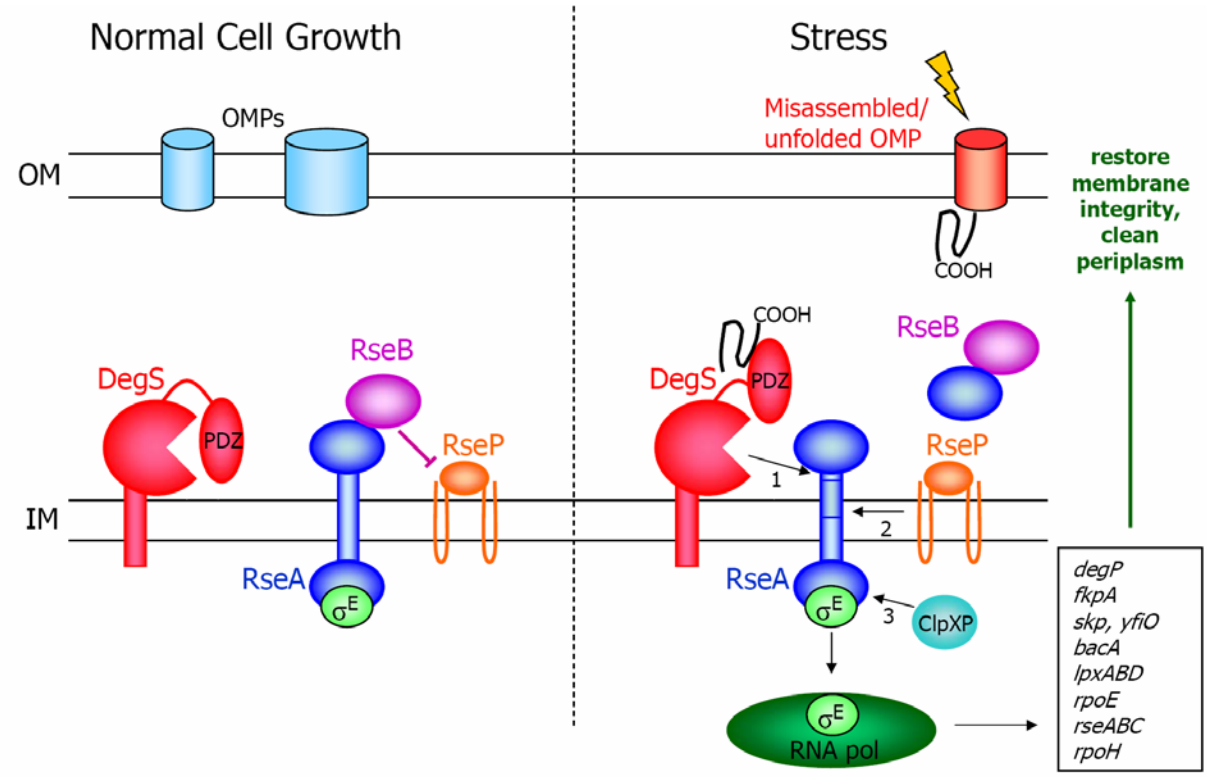

Figure 4. Overview of σ^E regulation. The left part of the scheme, illustrates the off state of key players of the σ^E response under normal cell growth. The σ^E is captured by its anti-sigma factor RseA. The two transmembrane proteases DegS and RseP are inactive. Stress induces misfolding or misassembly of OMPs (outer membrane proteins) leading to exposure of their C-termini which activate DegS (see right part). DegS cleaves RseA in the periplasmic region (1) which enables RseP to process RseA within the membrane spanning domain (2). Cytoplasmic proteases like ClpXP remove the cytoplasmic part of RseA from σ^E (3).This results in free σ^E to activate the RNA polymerase for transcription of a subset of genes (a selection of them are listed in the box), leading to restoration of the envelope integrity. Locations of the outer membrane (OM) and inner membrane (IM) are specified.

The alternative sigma factor σ^E is the only essential sigma factor besides the house keeping σ^{70} (De Las Penas et al., 1997a). It is characterized by being autoregulated and co-transcribed in one polycistronic operon together with its anti-sigma factor RseA, as well as

with the genes encoding for RseB and RseC (De Las Penas et al., 1997b; Missiakas et al., 1997).

In the inactive state, σ^E is captured by the cytoplasmic domain of RseA and thereby prevented from complexation with RNA polymerase (Campbell et al., 2003; De Las Penas et al., 1997b; Missiakas et al., 1997). σ^E activation is governed by a subsequent degradation of RseA that is performed by two PDZ-domain containing, inner membrane-bound proteases (DegS and RseP) (Alba et al., 2002; Ades et al., 1999). After cleavage of the periplasmic domain of RseA by DegS (Waller and Sauer, 1996; Ades et al., 1999), the intramembrane protease RseP (Dartigalongue et al., 2001a; Kanehara et al., 2002) releases the cytoplasmic domain that still sequesters σ^E (Alba et al., 2002; Campbell et al., 2003; Dartigalongue et al., 2001a; Kanehara et al., 2002). Finally, cytoplasmic proteases like ClpXP remove RseA and liberate σ^E for RNA polymerase activation (Flynn et al., 2004; Chaba et al., 2007). A schematic overview is given in Figure 4.

1.3. Key-Players of the σ^E Stress Response Pathway

1.3.1. RseA, the anti-Sigma Factor

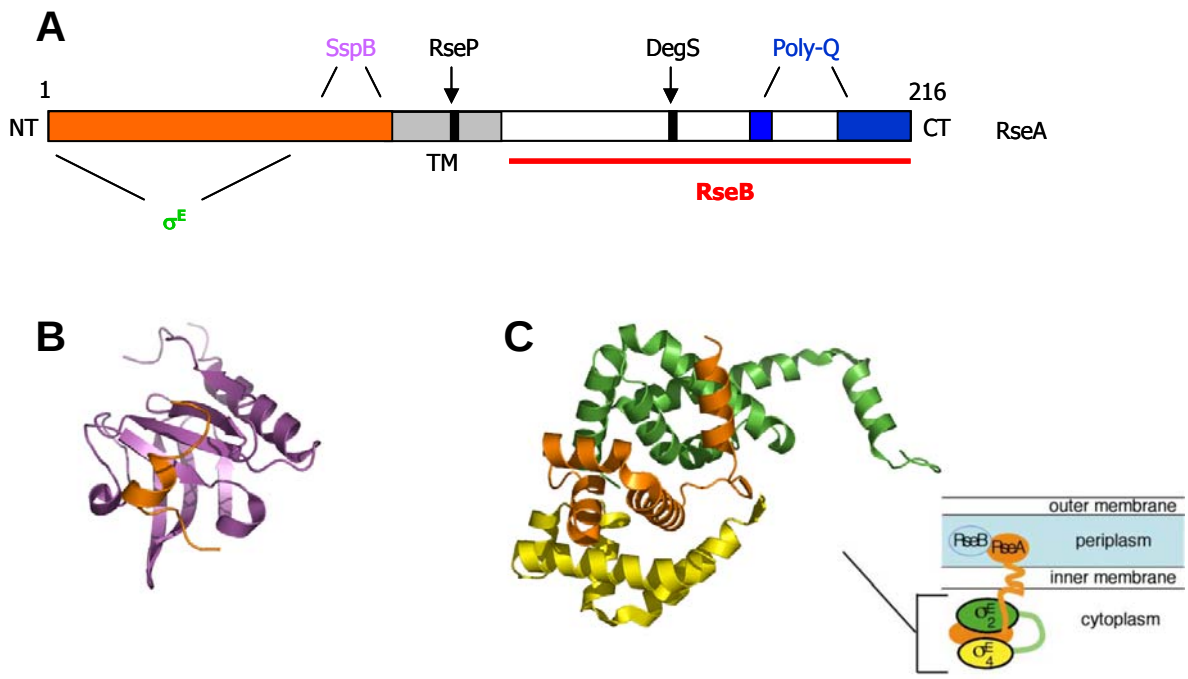

Figure 5. Features of RseA and structures of cytoplasmic regions of RseA. (A) Schematic representation of RseA depicts important regions of RseA from *E. coli*. The cytoplasmic part of RseA, drawn in orange, includes binding sites for σ^E and SspB. RseP cleaves RseA within the transmembrane domain (grey), whereas DegS cleaves in the periplasmic domain (white) of RseA. This domain confers interaction to RseB (red) and contains two stretches that have a high content of glutamines (blue). N- and C-termini are indicated. **(B)** Crystal structure of SspB (purple) with residues 73-95 of RseA (orange) (PDB-entry 1yfn; Levchenko et al., 2005). SspB is required for delivery of RseA to the ClpXP protease (Flynn et al., 2004; Hersch et al., 2004). **(C)** Crystal structure of the cytoplasmic part of RseA (orange) with σ^E (green and yellow; PDB-entry 1or7; Campbell et al., 2003). A cartoon explaining domain organization is given on the right (from Campbell et al., 2003).

The anti-sigma factor RseA is a monotopic integral inner membrane protein of 216 amino acids with a molecular weight of 24 kDa. RseA comprises one transmembrane helix (101-118), a periplasmic domain of 88 residues with two poly-Q stretches and an N-terminal cytoplasmic domain of 100 residues (Figure 5A). The cytoplasmic part directly mediates the interaction to σ^E, which results in inactivation of σ^E (De Las Penas et al., 1997b; Missiakas et al., 1997).

X-ray structural analysis of the N-terminal 90 residues in complex with σ^E (Figure 5C) demonstrated that RseA sterically inhibits formation of the RNA polymerase holoenzyme (Campbell et al., 2003). As only the N-terminal 66 residues of RseA participated in σ^E

binding, it is suggested that flexible parts (67-90) could serve as targets for the cytoplasmic proteases like ClpXP (Figure 5B) (Alba et al., 2002; Campbell et al., 2003; Flynn et al., 2004). The transmembrane region spans residues 101-118 and includes the cleavage site for RseP (Ala108-Cys109). The periplasmic domain of RseA is involved in interaction to the periplasmic protein RseB and contains the DegS cleavage site (Ser149-Leu150).

1.3.2. DegS, a Stress Sensor and Site-1-Protease

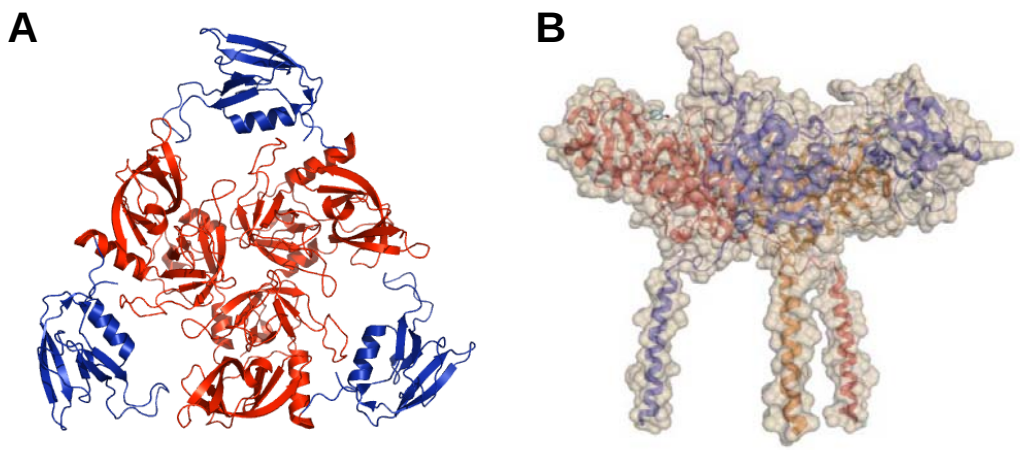

Figure 6. Crystal structure of DegS. (A) Trimeric DegS (PDB-entry 1te0) protease in top view with the protease and PDZ-domains colored in red and blue, respectively. **(B)** Side view of the surface of DegS including modelled membrane helices with different monomers colored in blue, red and orange (illustration from Zeth, 2004).

DegS is an essential inner membrane anchored serine protease, homologous to the family of HtrA proteases (Alba et al., 2001; Bass et al., 1996; Pallen and Wren, 1997; Waller and Sauer, 1996). Under normal conditions DegS is inactivated by its PDZ domain which shields the active site of the protease domain (Figure 6) (Wilken et al., 2004; Zeth, 2004). In the activation process of σ^E, DegS adopts the function of a site-1 protease, meaning that DegS initiates the proteolytic cascade of RseA degradation which is followed by the action of a site-2 protease, RseP. Both proteases, DegS and RseP, possess a PDZ domain, a known module for mediating protein protein interactions and frequently found in signalling proteins (Cho et al., 1992; Kim et al., 1995; Woods and Bryant, 1993). They are reported to recognize either short C-terminal peptide motifs or internal sequences that structurally mimic a terminus (reviewed by Harris and Lim, 2001). Activation of DegS was demonstrated to rely on the accumulation of misfolded OMPs. Further investigations showed that DegS specifically recognizes peptides ending with OMP-like C-terminal sequences like YYF or YQF that can act

as activators (Walsh et al., 2003). These OMP C-termini are proposed to be only accessible in improperly folded OMPs as they are normally embedded in the native β-barrel structure. DegS cleaves RseA in the periplasmic domain between Ser149 and Leu150. By a not clearly understood mechanism RseA1-149 is subsequently a substrate of the zinc metalloprotease RseP.

1.3.3. RseP, a Site-2-Protease

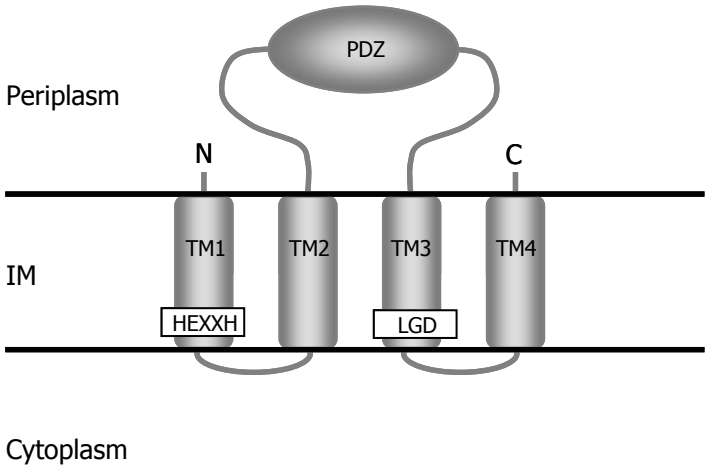

Figure 7. Topology of RseP. RseP is predicted to have four transmembrane regions, one large periplasmic domain including a PDZ domain and two cytoplasmic located domains. The zinc-binding motif (HEXXH motif) and a C-terminal LGD motif are located at membrane-cytoplasmic boudaries. Both termini face the periplasm (abstracted and modified from (Koide et al., 2007).

RseP, formerly known as YaeL, is an essential inner membrane spanning protein with four transmembrane helices, one periplasmic PDZ domain and two active site motifs located at membrane-cytoplasmic boundary regions (Koide et al., 2007; Alba et al., 2002; Dartigalongue et al., 2001a; Kanehara et al., 2001; Kanehara et al., 2002). A topologic model of RseP is illustrated in Figure 7 (Kanehara et al., 2001; Koide et al., 2007). RseP is homologous to S2P (Dartigalongue et al., 2001a), a mammalian site-2-protease that mediates activation of SREBP (sterol regulator element binding protein) located in the endoplasmic reticulum (Brown et al., 2000). Like S2P, RseP belongs to a special group of proteases that can perform regulated intramembrane proteolysis (RIP) which means degradation of targets within the membrane (Akiyama et al., 2004).

For regulation of RseP, three factors are discussed to be important: (1) RseP requires a DegS-processed RseA substrate. (2) Two Gln-rich regions in the periplasmic domain of RseA

seem to play a regulatory role, as deletion of these resulted in uncontrolled activation of RseP (Kanehara et al., 2003). (3) The periplasmic protein RseB is proposed to negatively influence RseP activity (Ades et al., 1999).

1.3.4. RseB, a Negative Regulator of σ^E

RseB (rse for regulator of σ^E), a periplasmic protein, binds to the periplasmic domain of RseA and was shown to exert a negative effect on σ^E activity (Missiakas et al., 1997). RseB is widely conserved among bacteria and reported to be responsible for a controlled progress in the RseA degradation pathway (Grigorova et al., 2004). By interaction with the periplasmic domain of the anti-sigma factor RseA (De Las Penas et al., 1997b; Missiakas et al., 1997), RseB reduces the efficiency of RseP to cleave RseA presumably either by RseP inhibition or RseA stabilization (Ades et al., 1999; Grigorova et al., 2004). In the absence of RseB, σ^E activity raises 2 - 2.3 fold (De Las Penas et al., 1997b; Missiakas et al., 1997), whereas overproduction of RseB results in 30-40% decrease of σ^E activity (Missiakas et al., 1997).
RseB is described to act as a sensor for periplasmic stress (Ruiz and Silhavy, 2005). In this functional model, RseB binding to RseA competes with binding to a stress signal, and RseB could be titrated away from RseA (Collinet et al., 2000; De Las Penas et al., 1997b; Grigorova et al., 2004). A displacement of RseB was shown to enable RseP to cleave RseA (Ades et al., 1999) independent on the action of the site-1 protease DegS. Besides this, σ^E activity was observed to be inducible in a DegS independent manner, which led to the hypothesis, that RseB is involved in a different way to modulate σ^E activity (Grigorova et al., 2004).

1.4. Signals that Activate the σ^E Regulon

Once σ^E is activated, it guides the RNA polymerase to specific promoters on the DNA. About 100 genes were identified to be part of the σ^E-regulon (Alba and Gross, 2004; Dartigalongue et al., 2001b; Duguay and Silhavy, 2004; Rezuchova et al., 2003; Rhodius et al., 2006) including those that encode for periplasmic chaperones like *fkpA* or *degP* (Erickson and Gross, 1989; Lipinska et al., 1988; Raina et al., 1995) and genes whose products are involved in the biogenesis and assembly of the outer membrane components (*skp*, *yfiO*, *bacA*, *lpxABD*) (Dartigalongue et al., 2001b; Onufryk et al., 2005; Rhodius et al., 2006). The expressed proteins can manage the restoration of the membrane integrity, which is the general task of the σ^E stress response.

The σ^E is activated by signals as heat or ethanol that cause a general damage in the envelope by protein misfolding (Erickson et al., 1987; Rouviere et al., 1995). Furthermore, as for the CpxAR or cytoplasmic heat shock response, all events that affect protein misfolding are potent inducers. For example, mutants missing periplasmic folding agents like FkpA, PpiD and SurA show elevated σ^E activity (Raina et al., 1995; Dartigalongue and Raina, 1998). Besides this, conditions that result in overproduction of OMPs were reported to turn on the σ^E response as well (Mecsas et al., 1993). Additionally, mutation or deletion of genes, coding for proteins involved in OMP biogenesis, similarly induces σ^E (Missiakas et al., 1996b; Raina et al., 1995; Rouviere and Gross, 1996). The underlying molecular mechanism is, as described above, the specific activation of DegS by sensing OMP C-termini that are only accessible in not properly folded or unassembled OMPs (Rouviere and Gross, 1996; Missiakas et al., 1996a). Finally, also modified lipopolysaccharides (LPS) were found to induce the σ^E response by an unknown mechanism (Tam and Missiakas, 2005).

First hints that RseB could be titrated away and may act as a sensor for σ^E induction came from experiments with a mutant of maltose-binding protein (MalE or MBP) (reviewed by Shuman and Panagiotidis, 1993). Expression of the *MalE* mutant, *malE31*, results in accumulation of MalE31 in periplasmic aggregates, which was shown to induce the σ^E activity. In these aggregates, RseB was found to be co-localized, which led to the suggestion that RseB may bind to unfolded proteins other than OMPs (Collinet et al., 2000; Grigorova et al., 2004).

1.5. Conceptual Formulation

The σ^E activation of extracytoplasmic stress response is regulated by a successive degradation of its anti-sigma factor RseA. Two inner membrane bound proteases execute degradation in a highly regulated manner. The periplasmic protein RseB is believed to exert a modulatory role in this pathway, but open questions remain to be solved. It is yet unclear how RseB can modulate the stability of RseA and how RseB is able to influence the cleavage efficiency of RseP. In the most popular model for RseB function, RseB is thought to be titrated away from RseA by a stress signal. Neither the nature of the putative signal nor the mechanism for this hypothesis is known to date.

In order to gain insight in the precise function of RseB, the task of this thesis is to solve the molecular structure by X-ray crystallography. Crystallographic and supporting biochemical data should enlighten the mode of RseB action and may help to identify postulated signals which could be sensed by RseB.

2. Results

2.1. X-ray Structural Analysis of RseB

2.1.1. Cloning and Purification of RseB

To produce RseB for crystallization trials, initially full length RseB from *E. coli* was subjected to over-expression. However, expression of RseB in the periplasm did not yield appropriate amounts for crystallization. For cytoplasmic expression, the N-terminal signal sequence was deleted and an N-terminally truncated version of RseB with a His-tag at the C-terminus was cloned as described in Materials and Methods (Figure 8).

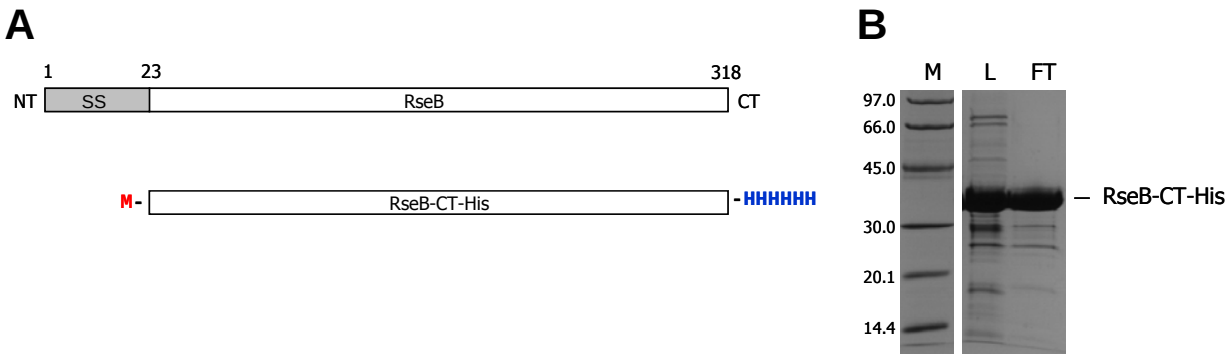

Figure 8. Illustration of C-terminally His-tagged RseB and its purification. (A) C-terminally His-tagged (blue) RseB from *E. coli* missing the signal sequence (SS). The methionine needed for initiation of translation is colored in red. Positions of the N-terminus (NT) and C-terminus (CT) are indicated. **(B)** Final purification step of RseB-CT-His using anion exchange chromatography. Samples of the load (L) and the flow though (FT) of the MonoQ experiment were analyzed by SDS-PAGE together with a molecular weight marker (M). The purity of RseB-CT-His of the flow through was verified by mass spectroscopy.

Initial tests revealed that expression in the cytoplasm gave acceptable amounts of the protein. The purification was performed *via* a two-step procedure (for details see Materials and Methods). Affinity chromatography using Ni-chelating material was done in a first purification step. Final purification of C-terminally His-tagged RseB (for simplicity called RseB) was achieved by anion exchange chromatography as shown in Figure 8. Purified protein was concentrated to 5 mg/ml.

2.1.2. Crystallization and Data Collection of RseB

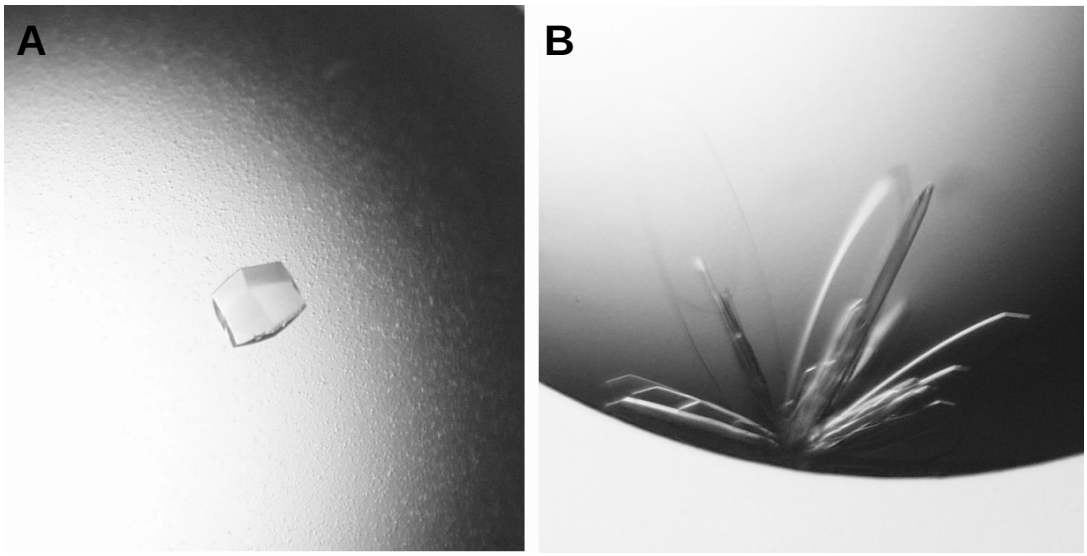

Figure 9. Crystals of RseB. (A) Tetragonal crystal of RseB from *E. coli* with dimensions of 0.25 x 0.25 x 0.05 mm crystallized in space group $P42_12$ (crystal form I). **(B)** Crystals of RseB in orthorhombic space group $C222_1$ with dimensions of 0.2 x 0.8 x 0.02 mm (crystal form II).

Conditions for crystallization of RseB were screened by the hanging drop vapour diffusion method, as described in Material and Methods. The commercially available crystal screens (Hampton Research), applied to the protein (at low protein concentrations, 1 mg/ml), yielded mainly two different crystal forms under a few conditions. The composition of the crystal was analyzed by N-terminal sequencing, which showed that the crystals indeed contain the RseB protein.

Small tetragonal crystals (form I) appeared after two weeks incubation at 291 K. These conditions were further refined using additive screens. Crystals grew in a solution containing 2.4 M sodium malonate pH 7 and 0.3 M dimethylethylammonium propane sulfonate to final dimensions of 0.25 x 0.25 x 0.05 mm (Figure 9A). Orthorhombic crystals (form II) were obtained from a solution containing 0.2 M magnesium chloride hexahydrate, 0.1 M Tris-HCl pH 8.5, 25% (w/v) polyethylene glycol 3350 and 10 mM L-cysteine after 3 weeks. These crystals grew in clusters and had a sickle shaped appearance (Figure 9B). To prepare orthorhombic crystals for synchrotron data collection, single sickles were mounted to avoid overlapping crystal lattices interfering with data processing.

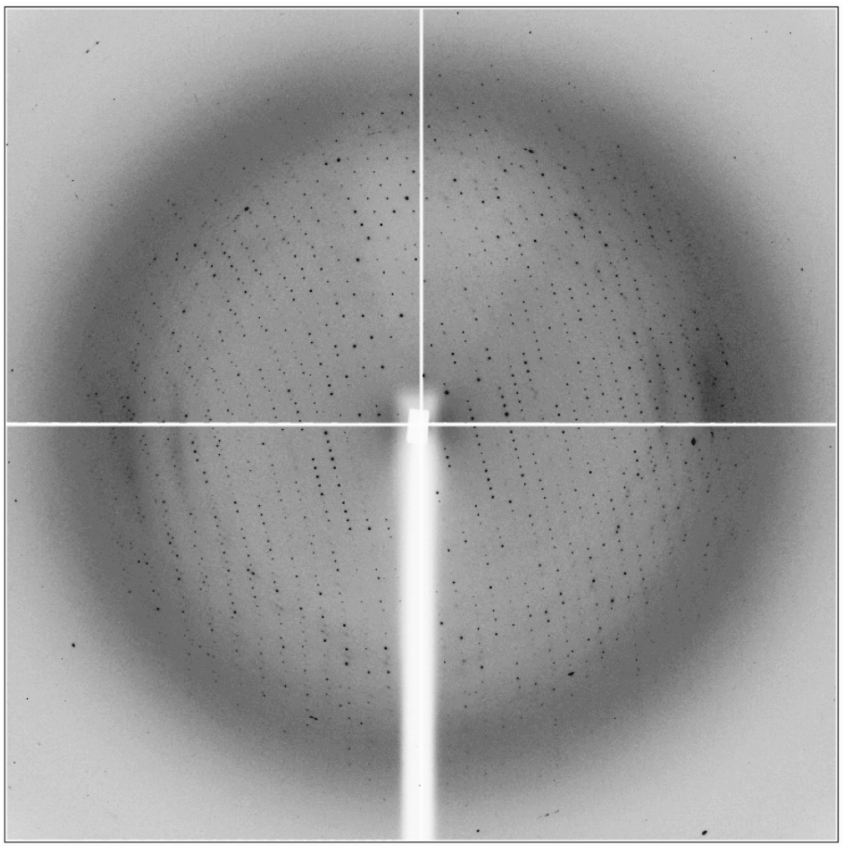

Figure 10. Diffraction image of tetragonal crystal. Diffraction image recorded on a mar225 CCD detector at PXII-X10SA (SLS) showing diffraction of the tetragonal crystal to 2.8 Å resolution.

Data collection statistics of all datasets collected are summarized in Table 1. Tetragonal crystals belong to space group $P42_12$ with a = 164.3 Å, c = 81.5 Å, α = 90° and diffracted to 2.8 Å resolution (Figure 10) with an R_{meas} of 8.7% and I/σ (I) of 18.8. Orthorhombic crystals diffracted to 2.4 Å resolution and belong to space group $C222_1$ with a = 98.6 Å, b = 200.7 Å, c =109.7 Å, α = 90°, with R_{meas} of 11.1% and I/σ (I) of 12.64.

Table 1. Data collection and refinement statistics.

	Native		Derivative			
	Crystal form I	**Crystal form II**	**Pt1[b]**	**Pt2[b]**	**Pt3[b]**	**Pt4[b]**
Data collection						
Space group	$P42_12$	$C222_1$	$P42_12$	$P42_12$	$P42_12$	$P42_12$
a (Å)	164.3	98.6	164.8	164.2	165.0	165.0
b (Å)	164.3	200.7	164.8	164.2	165.0	165.0
c (Å)	81.5	109.7	82.2	81.9	81.8	82.0
Beamline	PXII-X10SA (SLS)	ID23-1 (ESRF)	ID14-4 (ESRF)	ID14-4 (ESRF)	ID14-4 (ESRF)	ID14-4 (ESRF)
Detector	mar225 CCD	Q315 ADSC CCD	Q315 ADSC CCD	Q315 ADSC CCD	Q315 ADSC CCD	Q315 ADSC CCD
Resolution (Å)*	20 – 2.8 (2.9 – 2.8)	20 – 2.4 (2.5 – 2.4)	50 – 3.3 (3.5 – 3.3)	50 – 4 (4.2 – 4.0)	50 – 4.0 (4.2 – 4.0)	50 – 3.6 (3.8 – 3.6)
Wavelength (Å)	0.9790	0.9762	1.07195	1.07195	1.07195	1.00883
Osc. Angle (°)	1	0.5	1	1	1	1
Unique reflections*	28941 (4291)	40893 (4373)	32733 (4856)	18066 (2746)	27396 (4046)	24846 (3831)
Completeness (%)*	97.9 (92.8)	95.2 (89.4)	97.3 (91.1)	92.8 (96.6)	75.1 (69.6)	96.3 (93.0)
Redundancy*	12.4 (12.0)	3.7 (3.8)	7.4 (7.1)	3.7 (3.8)	1.6 (1.5)	3.8 (3.7)
Average I/σ (I)*	18.8 (2.4)	12.6 (2.4)	11.3 (2.5)	9.4 (3.9)	4.7 (1.6)	8.4 (3.0)
R_{meas} [a] (%)*	8.7 (50.9)	11.1 (57.7)	16.9 (88.7)	14.2 (42.9)	20.3 (67.4)	16.8 (54.1)
Refinement						
Resolution (Å)	20 – 2.8	19.9 – 2.4				
Monomers in AU	2	3				
Protein residues	614	1011				
Water molecules	44	194				
Heteromolecules	2	4				
R_{cryst} (%)	21.7	22.8				
R_{free} (%)	25.8	27.8				
RMSD Bonds (Å)	0.011	0.011				
RMSD Angles (°)	1.69	1.41				
Ramachandran plot						
most favoured	443 (88.8%)	641 (90.2%)				
additionally allowed	53 (10.6%)	64 (9.0%)				
generously allowed	2 (0.4%)	3 (0.4%)				
disallowed	1 (0.2%)	3 (0.4%)				

*Values in parentheses correspond to the highest resolution shell
[a] R_{meas} (Diederichs and Karplus, 1997)
[b] Pt1: $K_2Pt(SCN)_6$, Pt2, Pt4: $[Pt_2I_2(H_2NCH_2CH_2NH_2)_2](NO_3)_2$, Pt3: K_2PtCl_4

2.1.3. Phasing and Model Building

2.1.3.1. Phasing of Data from $P42_12$ Crystals by MIR

Multiple isomorphous replacement (MIR) is besides multi wavelength anomalous diffraction (MAD) a common method for determination of initial phases of completely new structures (Terwilliger and Berendzen, 1999). Numerous heavy atom containing compounds must typically be screened before one (or more) is found that binds specifically without damaging the crystal or disrupting the crystal lattice.

For structure solution, phases from heavy atom soaked crystals were obtained. 12 different platinum salts and five different mercury salts, each in two to four varying concentrations were tested for yielding anomalous signals in the soaked crystals. The best isomorphous phases resulted from datasets of RseB type I crystals soaked in reservoir solution containing 0.5 mM K_2PtCl_4, $K_2Pt(SCN)_6$ or $[Pt_2I_2(H_2NCH_2CH_2NH_2)_2](NO_3)_2$ with the derivative data collected at the Pt-edge. From the analysis of heavy atom site occupancies, it became obvious that two monomers (P1 and P2) of the protein build up the asymmetric unit (Matthews coefficient of 4, 69.3% solvent content, (Matthews, 1968)). Phases were determined at 3.2 Å using the program SOLVE (Terwilliger and Berendzen, 1999) and improved by the program RESOLVE (Terwilliger, 2000).

2.1.3.2. Manual Model Building of RseB from Data of $P42_12$ Crystals

An automatic RESOLVE generated model was not helpful as it did not show continuous features and in addition only very few parts had been placed in the initial electron density (Terwilliger, 2002a; Terwilliger, 2002b). Therefore, it was a challenging task to manually build the model of RseB. Severe difficulties in tracing the electron density were encountered because of bad quality especially in less structured areas as loop regions. Initially, pre-built α-helices and β-strands were placed into prominent parts of the electron density. With the help of secondary structure predictions, these parts were connected using the programs O and Coot (Jones et al., 1991; Emsley and Cowtan, 2004).

All regions with connected electron density were interpreted with poly-alanine stretches. However, the docking of the amino acid sequence proved to be a delicate problem, due to

several gaps in the model as well as missing side chain density. A comparison of initial electron density and final density is given in Figure 11.

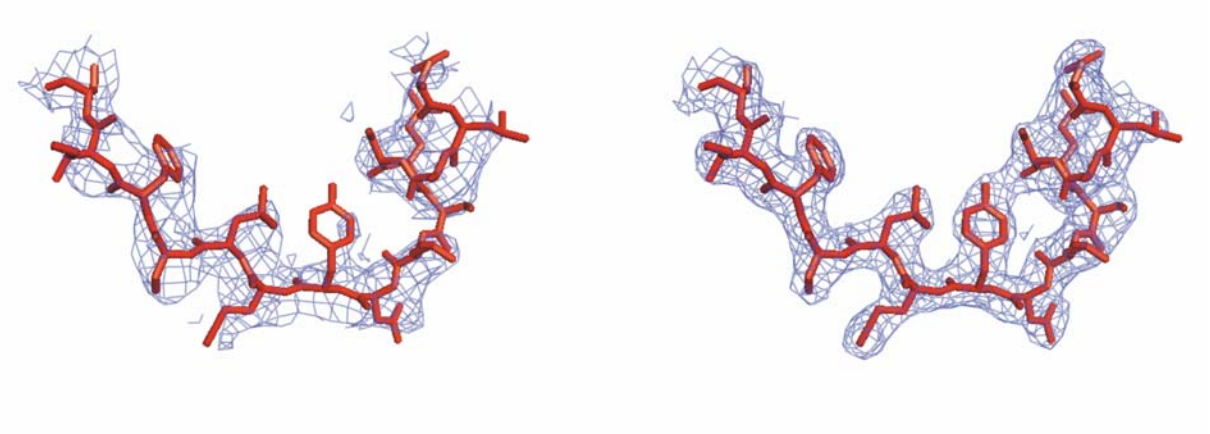

Figure 11. Densities of $P42_12$ data. Initial density is shown on the left, whereas the final density is depicted on the right. The corresponding part of the final model of RseB (Asn35-Ser49) is represented as sticks in red.

2.1.3.3. Phasing of Data from $C222_1$ Crystals by MR

Crystals of the orthorhombic form II diffracted to a resolution of 2.4 Å. They contain three monomers (C1, C2 and C3) in the asymmetric unit at a solvent content of 53.1% (Matthews, 1968). The structure was solved by molecular replacement (MR) in MOLREP (Vagin and Teplyakov, 1997), using the first 200 residues of the tetragonal model. After manual placement of the remaining part of the model, the structure could be refined to 2.4 Å. Improvement of the electron density was done with RESOLVE prime-and-switch phasing to minimize the model bias (Terwilliger, 2000; Terwilliger, 2004).

2.1.3.4. Quality of the Final Models of RseB

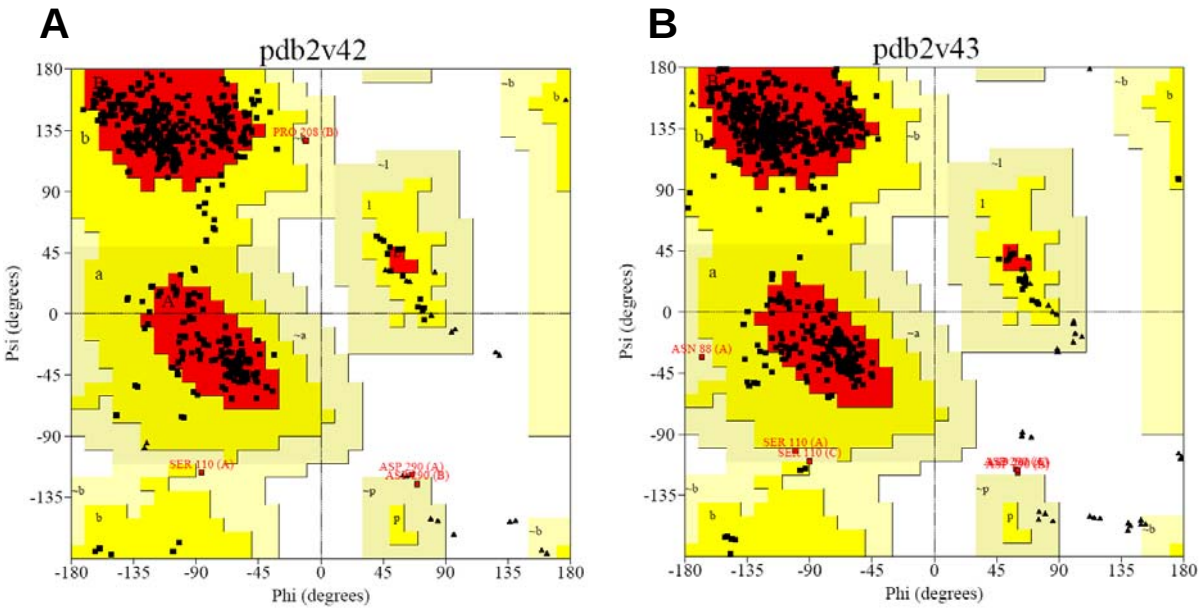

Residues in most favored regions [A,B,L]	443	88.8%
Residues in additionally allowed regions [a,b,l,p]	53	10.6%
Residues in generously allowed regions [~a,~b,~c,~d]	2	0.4%
Residues in disallowed regions	1	0.2%
Number of non-glycine and non-proline residues	499	100.0%
Number of end-residues (excl. Gly and Pro)	8	
Number of glycine residues (shown as triangles)	27	
Number of proline residues	34	
Total number of residues	568	

Residues in most favored regions [A,B,L]	641	90.0%
Residues in additionally allowed regions [a,b,l,p]	65	9.1%
Residues in generously allowed regions [~a,~b,~c,~d]	3	0.4%
Residues in disallowed regions	3	0.4%
Number of non-glycine and non-proline residues	712	100.0%
Number of end-residues (excl. Gly and Pro)	19	
Number of glycine residues (shown as triangles)	42	
Number of proline residues	45	
Total number of residues	818	

Figure 12. Ramachandran plot. The final models were analyzed with PROCHECK (Laskowski et al., 1993) to validate the quality of the model. The Ramachandran plot showed that the models of tetragonal **(A)** and orthorhombic **(B)** crystals have a good stereochemistry as most of the residues are within the most favoured regions.

Subsequent cycles of refinement resulted in an R_{cryst} of 21.7% (R_{free} of 25.8%) and R_{cryst} of 22.8% (R_{free} of 27.8%) for tetragonal and orthorhombic crystals, respectively. Ramachandran plot analysis depicts the distribution of the stereochemistry of peptide bonds in the structures and gives a good estimate for the quality of the model. In both models 88.8% and 90.0% of all residues are in most favoured regions whereas only 0.2% and 0.4% of all residues belong to disallowed regions in $P42_12$ and $C222_1$ models, respectively (Figure 12A and B). Although RseB, crystallized in the orthorhombic space group diffracted to higher resolution, our structure pictures are based on P1 (unless otherwise stated).

The coordinates for RseB (tetragonal and orthorhombic forms) have been deposited in the Protein Data Bank (Berman et al., 2000; Bernstein et al., 1977) under accession numbers 2v42 and 2v43, respectively.

2.2. Structure of RseB

2.2.1. Overall Structure of RseB

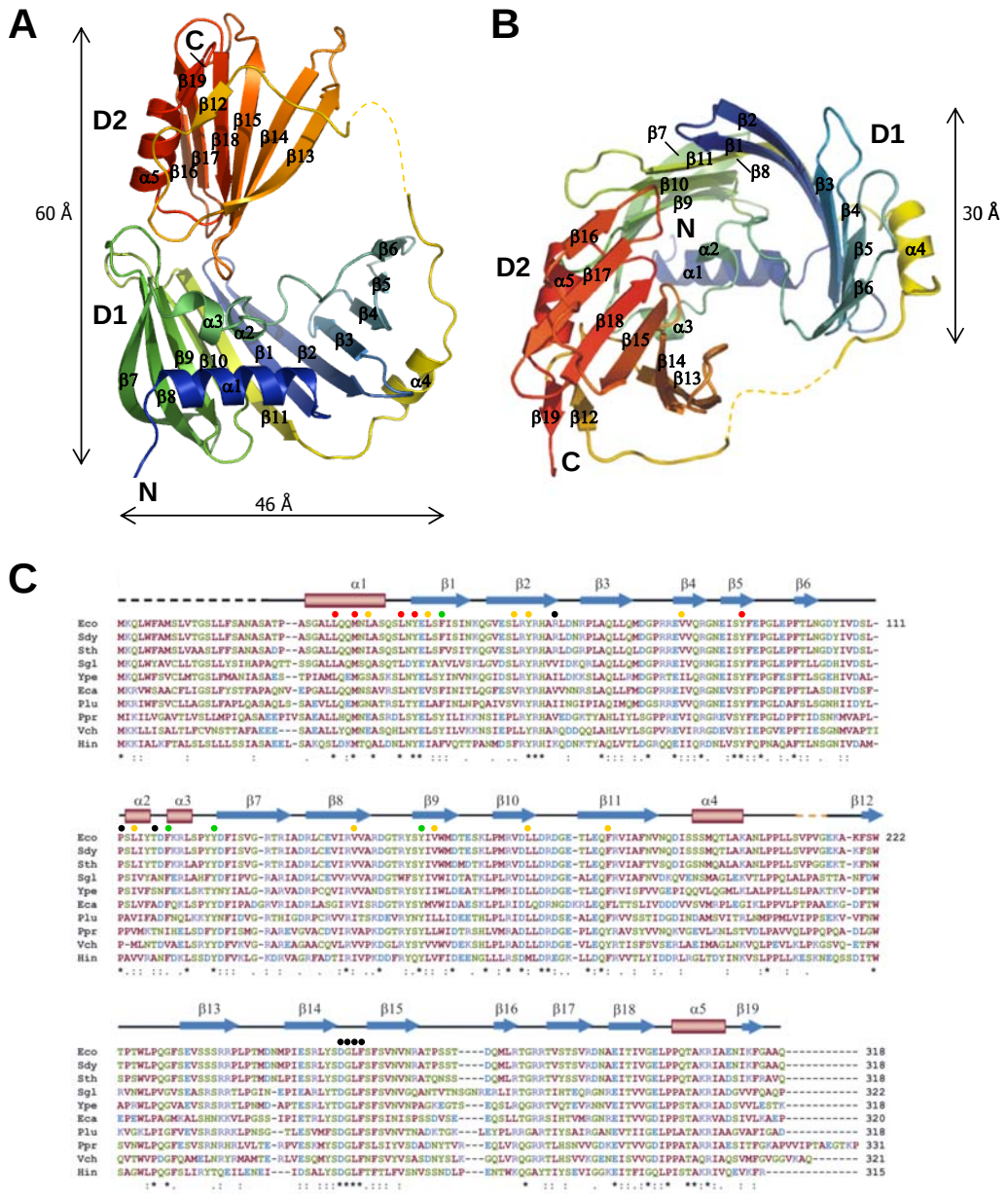

Figure 13. Structure of the RseB monomer and sequence alignment. Cartoon representation of monomeric RseB structure shown in front **(A)** and top view **(B)**, each colored in rainbow from the N-terminus (blue) to C-terminus (red). For both domains (D1, large domain and D2, small domain) individual naming of the secondary elements and positions of the N- and C-termini are indicated. **(C)** Sequence alignment of RseB orthologs, colored according ClustalW output (Thompson et al., 1994) with invariant, conserved and semi-conserved residues specified on the bottom line with '*', ':' and '.' respectively. Abbreviations are as follows: Eco (*Escherichia coli*), Sdy (*Shigella dysenteriae*), Sth (*Salmonella typhimurium*), Sgl (*Soldalis glossinidius*), Ype (*Yersinia pestis*), Eca (*Erwinia carotovora*), Plu (*Photorhabdus luminescens*), Ppr (*Photobacterium profundum*), Vch (*Vibrio cholerae*) and Hin (*Haemophilus influenzae*). Part of the connecting loop (Val212 to Gly215) not traced by electron density is indicated by a yellow dashed line. The black dashed line marks the position of the putative N-terminal signal sequence which was omitted in cloning RseB. Hydrophobic residues of RseB lining the unclosed barrel that are conserved in the structural homolog LolA, are indicated with green and red dots. Additional hydrophobic residues in the RseB half-barrel are specified with yellow squares. Further residues mentioned in the text are marked with black squares (Arg64, Pro112 and Thr117) including a loop of invariant residues (Asp256, Gly257, Leu258, Phe259) of the small domain.

The RseB monomer has an approximate dimension of 60 Å x 46 Å x 30 Å and consists of two domains: one large domain (RseB-D1) and one small domain (RseB-D2). It is composed mainly of β-stands arranged in two anti-parallel β-sheets (Figure 13A and B). The N-terminal D1 domain includes residues Ala23 to Lys203 with an initial long N-terminal helix that is followed by an 11-stranded anti-parallel β-sheet, forming an unclosed β-barrel (strand order: $\beta_7\beta_8\beta_9\beta_{10}\beta_{11}$-$\beta_1\beta_2\beta_3\beta_4\beta_5\beta_6$ see also Figure 16A). Notably, the unclosed β-barrel is composed of two sheets (β_7-β_{11} and β_1-β_6) connected by an internal loop-helix structure (residues Asn103 to Tyr125) with two small helices (α_2 and α_3) that links the two parts from the one (β_6) to the other side (β_7). Both β-sheets show also sequence homology and can be overlaid with a root mean square deviation (RMSD) value of 2.3 Å for the first five β-strands (data not shown). The inner surface of the unclosed barrel has an overall hydrophobic character. The N-terminal helix (α_1) is amphipathic with the hydrophobic residues facing the barrel interior. Helix α_4 evolves from the inner side of the open barrel and extends to a long loop (residues Ala204 to Ser221) connecting RseB-D1 and D2.

The second domain (RseB-D2) spans residues Trp222 to Phe317 (see also Figure 15A) and harbours a six-stranded anti-parallel β-sheet with the strand order $\beta_{13}\beta_{14}\beta_{15}\beta_{18}\beta_{17}\beta_{16}$ and terminates with the C-terminal helix α_5. The two small strands β_{12} and β_{19} are attached on the large β-sheet *via* hydrophobic interactions. Trp222 on β_{12} seems to be a key residue in fixing the preceding connecting loop to the beta sheet of the small domain, as it contacts Glu250 and Arg252 of β_{15}. In analogy to domain D1, this β-sheet is as well an assembly of two separated half sheets (β_{13}-β_{15} and β_{18}-β_{16}), but is less bent than the unclosed barrel domain.

2.2.2. Structural Variability

To evaluate the structural variability of RseB five independent monomers that occurred in the two space groups (monomers P1, P2, C1, C2 and C3) were compared. Figure 14A illustrates superpositions of the RseB-D1 and RseB-D2 domains separately, which were taken for calculation of RMSD values (with P1 as a reference). The superposition of RseB-D2 (Figure 14A), left) shows that all RseB-D2 domains were apparently identical (RMSD for P1/P2 is 0.18 Å; P1/C2 is 0.49 Å), while for D1 (Figure 4(a), right) minor changes were observed (RMSD for P1/P2 0.50 Å and P1/C1 0.88 Å). Structural variations are mainly found in the loop region of β_5 and β_6 and in the loop preceding α_4 which is positioned outside of the

unclosed barrel. As there is no significant rearrangement or conformational change, such deviations are rather in a range reflecting the flexible character of this region and/or resulting from differences in crystal packing.

However, when superimposing the independently built monomers composing the asymmetric unit of the $P42_12$ and $C222_1$ cells, higher positional discrepancies could be observed (RMSD vary between 0.5 Å for P1/P2 to 1.4 Å for P1/C1), that are mostly distributed to one side of the protein. These structural variations can be explained by varying angles of inclination (up to 5 Å) between the two domains in different monomers (Figure 14B). Further investigations revealed that the small domains in $P42_12$ monomers are more down tilted than in $C222_1$ monomers. This suggests that the relative positions of domains are intrinsically flexible which might be of biological relevance. The loop connecting RseB-D1 and RseB-D2 could only be traced by electron density in monomer P1 which reflects its flexible character facilitating movements of the two domains. These observations are further underlined by B-factor distributions which show high values in these flexible areas (parts of the small domain, α_4, connecting loop and part of the internal loop of RseB-D1) (Figure 14C).

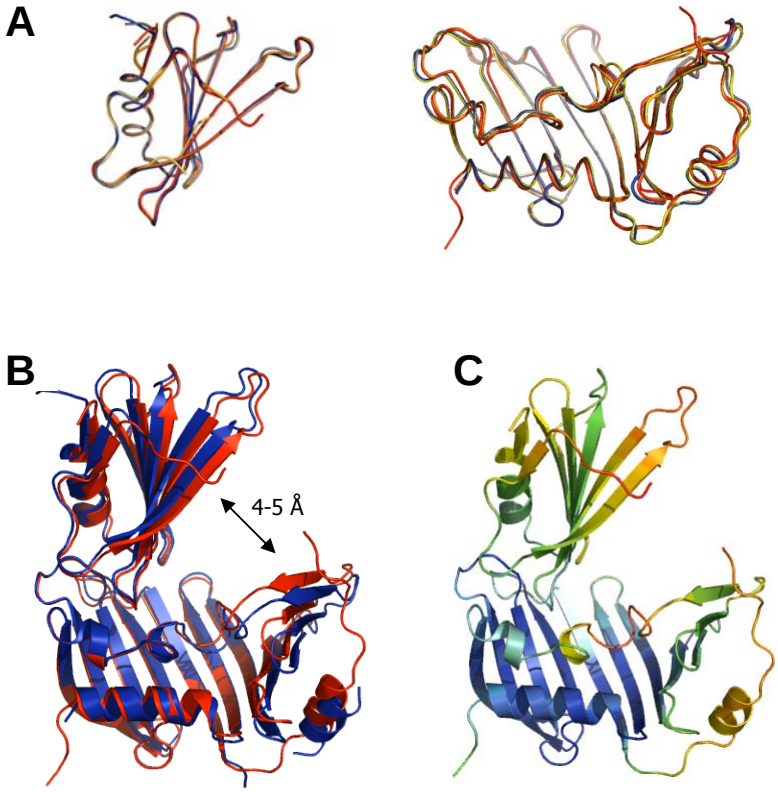

Figure 14. Flexibility of RseB. (A) Structural superposition of the small (RseB-D2, left) and the large (RseB-D1, right) domains of the five monomers of RseB, observed in the two crystal forms, indicates almost no structural variability in the small domain and few variable regions in the large domain. Monomers P1, P2, C1, C2 and C3 are colored in red, orange, yellow, grey and blue respectively. **(B)** Structural superposition of P1 (red) and C3 (blue) indicates that the small domains of $P42_12$ monomers are more inclined than observed for $C222_1$ monomers. For clarity only two representatives are depicted. **(C)** Monomer P1 is colored according to its B-factor distribution, revealing the internal loop and outer parts of the monomer having enhanced B-factor values.

2.2.3. Structural Comparison

2.2.3.1. Comparison of the Small Domain with Structural Homologs

A structural similarity search, performed with coordinates of the D2 domain using the DALI server (Holm and Sander, 1995), indicates that the closest structural homologue is TM1622 (PDB-entry 1vr8, Z-score 7.3, sequence identity 6%), a GTP-binding protein from *Thermotoga maritima* (Xu et al., 2006). The structural similarity of TM1622 and RseB-D2 is due to a similar backbone twist of the β-sheet and the position of the C-terminal helix (Figure 15C). However, the β-sheet of the thermophilic protein is sandwiched by two additional helices, one on each side and equipped with an extra β-strand (Figure 15B). TM1622 and RseB-D2 share only five residues, just three of them are conserved among other RseB homologs (Tyr254, Val265 and Gly280) and seem to play a basic and important role in structural maintenance.

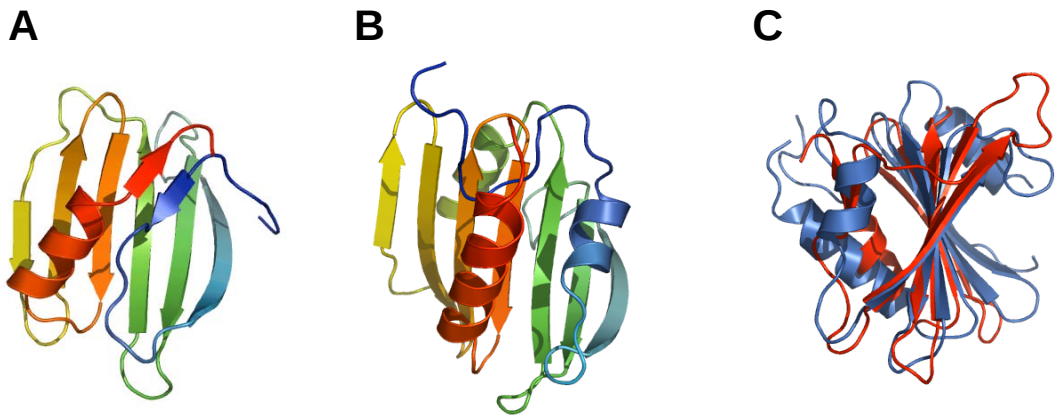

Figure 15. Small domain (RseB-D2) and its structural homolog TM1622. RseB-D2 **(A)** and the structural homolog TM1622 **(B)** from *Thermotoga maritima* (Xu et al., 2006) are colored in rainbow from the N-terminus (blue) to C-terminus (red). Picture **(C)** shows a superposition of TM1622 (blue) and RseB-D2 (red) which reveals a similar twist of the β-sheet.

The next closest structural homolog found was DIP2269 (PDB-entry 2i8g, Z-core 7.1, sequence identity 9%), a hypothetical protein from *Corynebacterium diphteriae*. It has no related protein in BLAST searches (Altschul et al., 1990).

2.2.3.2. Comparison of the Large Domain with Structural Homologs

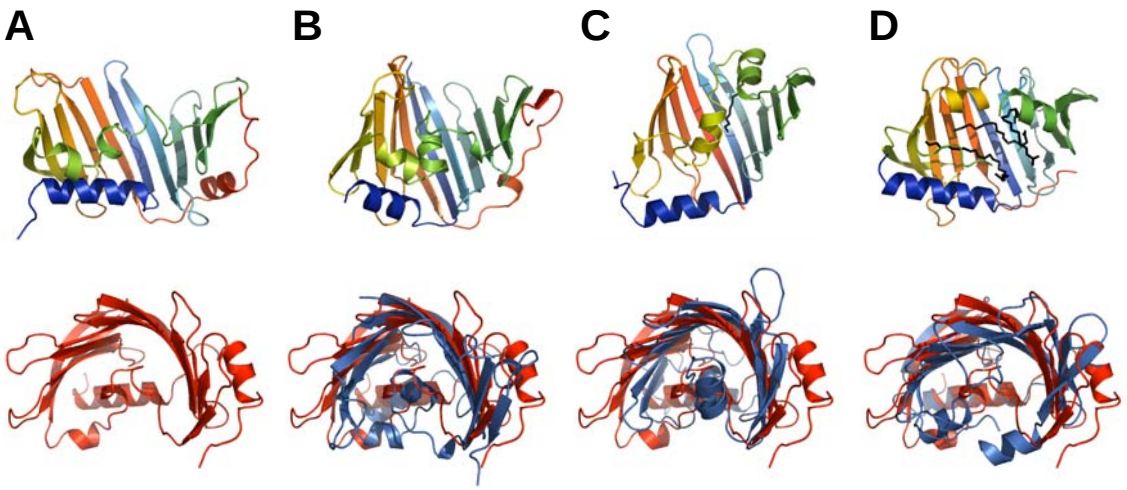

Figure 16. Large domain (RseB-D1) and its structural homologs. For structural comparison, the large domain of RseB-D2 **(A)** and respective homologs, LolA **(B)**, LolB **(C)** (Takeda et al., 2003) and LppX **(D)** (Sulzenbacher et al., 2006) are shown in front view (top). PEGMME2000, co-crystallized with LolB is shown in stick representation (black) in **(C)**; modeled palmitates are drawn as black sticks in **(D)**. The bottom row illustrates RseB-D1 (red) in top view and shows superpositions of RseB-D1 (red) with its structural homologs (blue) in **(B)**, **(C)** and **(D)**.

Three close structural homologs of RseB-D1 were identified which also exhibit the unclosed barrel fold (LppX (PDB-entry 2by0), LolA (PDB-entry 1iwl) and LolB (PDB-entry 1iwm and 1iwn), Figure 16). While the structural similarity is remarkably high for LolA (Z-score of 12.1 *versus* 11.0 for LppX and 8.6 for LolB), the identity on sequence level is highest for LppX (15% *versus* 8% for LolA and 11% for LolB). Noteworthy, also the outer membrane proteins OmpG (Subbarao and van den Berg, 2006; Yildiz et al., 2006) and Tsx (Ye and van den Berg, 2004) were found to be structurally similar to RseB-D1 as they exhibit 'complete' closed β-barrels of similar dimensions. The monomeric LppX (Figure 16D) from *Mycobacterium tuberculosis* is responsible for the translocation of phthiocerol dimycocerosates (DIM) to the outer membrane (Sulzenbacher et al., 2006). The two other structural homologs, LolA and LolB (Figure 16B and C) are involved in targeting of lipoproteins in Gram-negative bacteria (Matsuyama et al., 1995; Matsuyama et al., 1997).

All three structural homologs of RseB-D1 have the common feature to transiently interact with lipophilic compounds and share a deep hydrophobic half-barrel that can accommodate long lipophilic tails. However, none of these three RseB-D1 homologs have any additional domain.

Figure 17. Topology of RseB-D1 and its structural homologs. Topology of RseB-D1 **(A)**, LolA **(B)**, LolB **(C)** and LppX **(D)** drawn with the program TopDraw (Bond, 2003). Helical elements are shown in red, whereas β-sheets are colored in blue. LppX modified from Sulzenbacher et al., 2006.

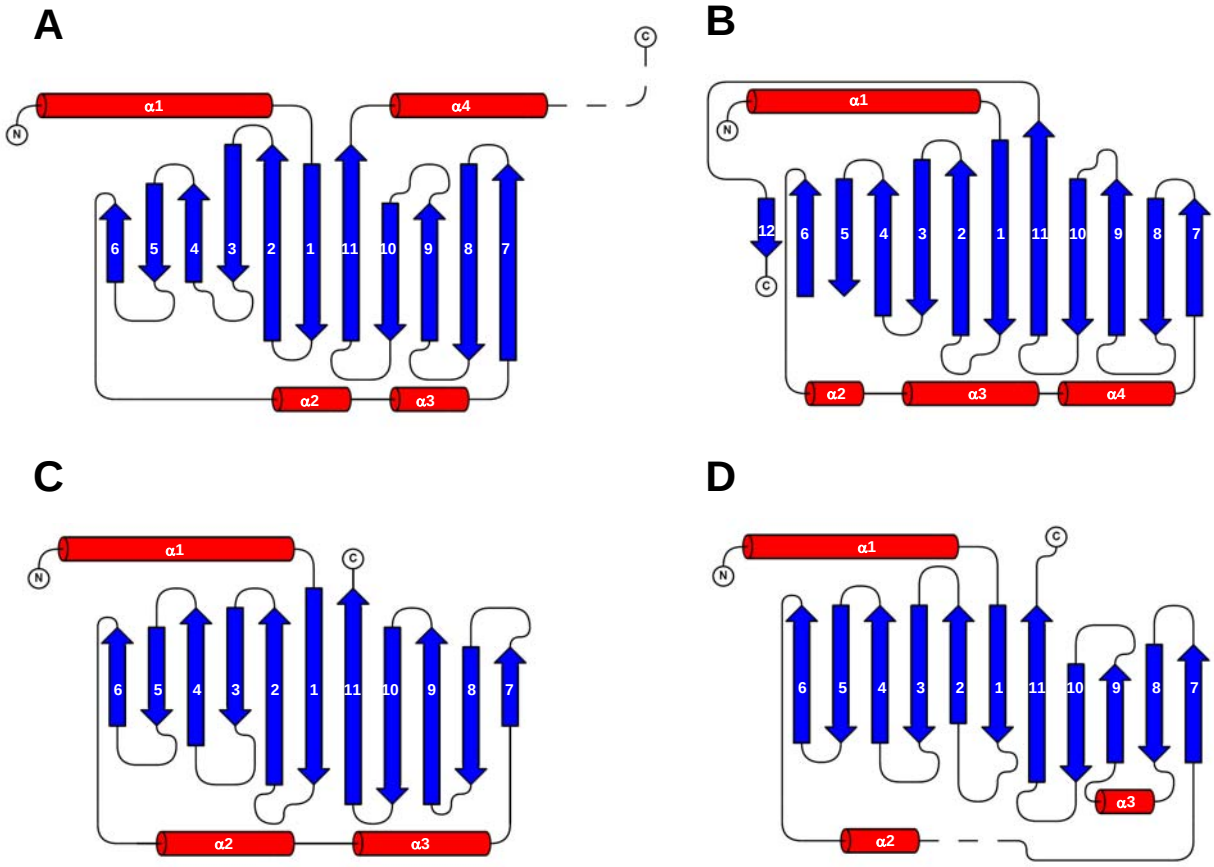

As shown in Figure 16 (bottom row), the structural homology is most distinct in the central part of the unclosed β-barrel. The barrel dimensions of RseB and the three homologs (LolA, LolB, LppX) vary in terms of their relative width and curvature. This deviation is also reflected by the RMSD values between the RseB large domain and LolA (4.4 Å, 155 aligned residues), LolB (3.3 Å, 127 aligned residues) and LppX (3.8 Å, 150 aligned residues). From the overall fold, RseB resembles mostly LolA, although proteins differ in an extra C-terminal secondary element (α_4 in RseB, Figure 17A, and β_{12} in LolA, Figure 17B). LolB differs more significantly from RseB due to an enlarged barrel wall and a more compact structure (Figure 16C). LppX forms a less convex barrel with lower depth. Additional to these differences in the otherwise common topology (Figure 17), LolA has an additional internal helix and LppX has the unique feature of an extra α-helix between β_8 and β_9 (Sulzenbacher et al., 2006).

2.2.4. Interface of the Large and the Small Domain of RseB

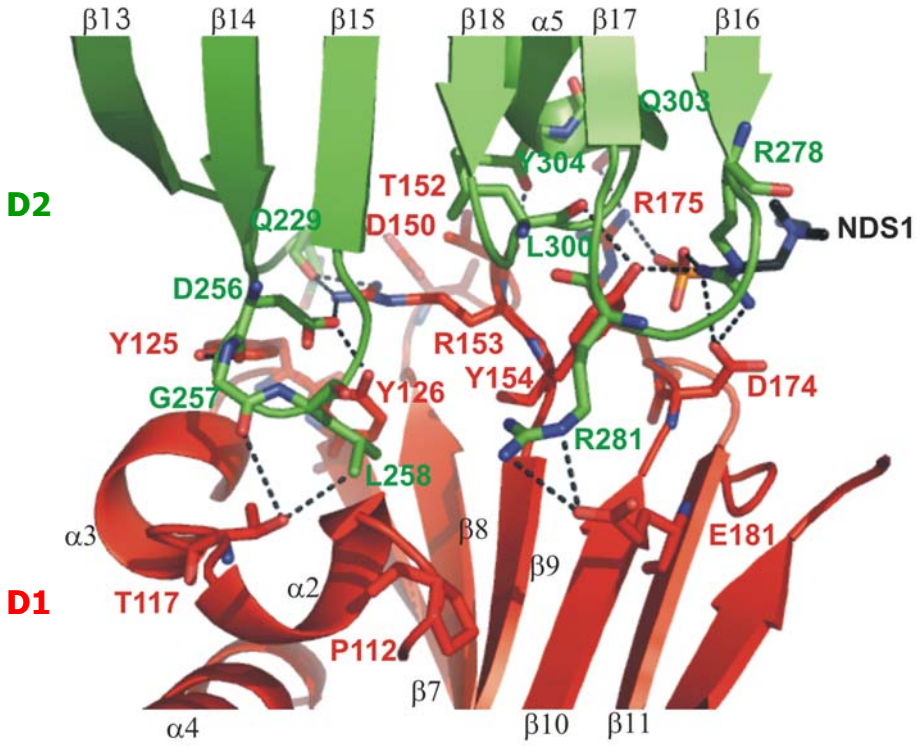

Figure 18. Interface between RseB-D1 and RseB-D2. RseB-D1 (red) and RseB-D2 (green) domains of interact *via* a highly conserved interface. On RseB-D1, residues involved in interface formation are placed in the extended loops β_8/β_9 and β_{10}/β_{11} (except two tyrosines in loop α_3/β_7). On RseB-D2, all loops pointing to the large domain participate in interdomain contacts. A loop in RseB-D2 between β_{14} and β_{15} bearing four invariant residues (Asp256, Gly257, Leu258 and Phe259) interacts with Thr117 of the internal loop of RseB-D1. Another residue (Asp256) of the invariant loop interacts with Tyr125, Tyr126 and Arg153 to stabilize interdomain contacts and to fix it to the barrel wall. Dimethylethylammonium propane sulfonate (NDS1) was present in the crystallization buffer and was found to bind to Arg175 and Arg278.

As depicted in Figure 18, the highly conserved interface (889 Å^2) between the RseB-D1 and the RseB-D2 domain is formed by ten residues on the large domain (Thr117, Tyr125, Tyr126, Asp150, Thr152, Arg153, Tyr154, Asp174, Arg175 and Glu181) and nine residues on the small domain (Gln229, Asp256, Gly257, Leu258, Arg278, Arg281, Leu300, Gln303 and Tyr304). Residues of RseB-D1 are mostly located on loops connecting β_8 and β_9, β_{10} and β_{11}, as well as β_7 and α_3 (Figure 18). On domain RseB-D2 all four loops pointing towards RseB-D1 are involved in interface stabilization. They mediate attachment to the unclosed barrel wall of RseB-D1, more precisely, to loops connecting β_8 and β_9, β_{10} and β_{11}. Furthermore, a highly conserved loop of RseB-D2 of invariant residues (Asp256, Gly257, Leu258 and Phe259, see also alignment in Figure 13C) promotes interaction to a loop of RseB-D1 which fills the unclosed barrel.

2.2.5. Conserved Patches on the Surface of RseB

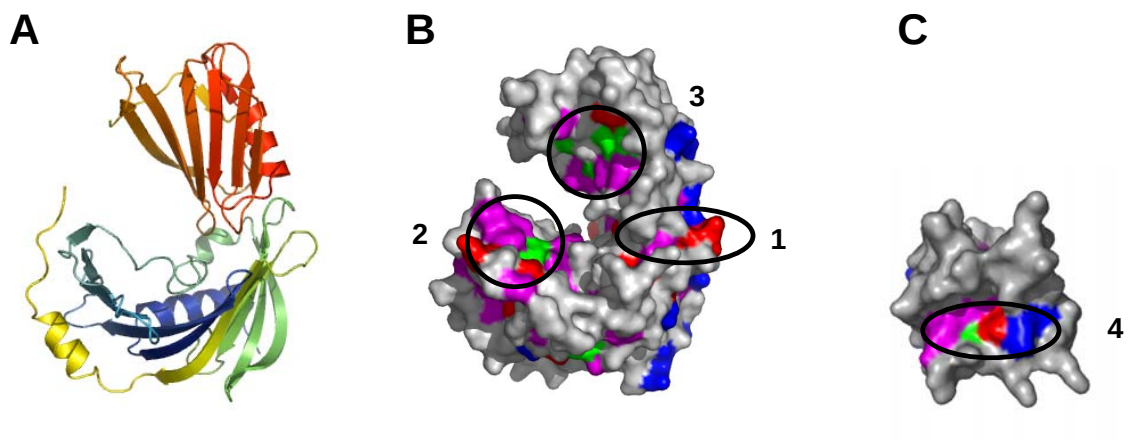

Figure 19. Conserved residues on the surface of RseB. (A) Ribbon representation of RseB colored in rainbow from blue (N-terminus) to red (C-terminus). **(B)** and **(C)** are surface representations with highly conserved residues colored according to their chemical properties (hydrophobic: purple, basic: blue, acidic: red and polar: green). Four patches of highly conserved residues are located on the surface of RseB. Patch 1 includes conserved residues involved in contacts of the D1/D2 interface. Patch 2 is located near the unclosed barrel of RseB-D1. Patch 3 as well as patch 4 **(C)** are putative binding sites on RseB-D2. Figure **(B)** is in same orientation as **(A)**; and **(C)** is viewed from the top, relative to orientation in **(A)** and **(B)**. For clarity, only the small domain is shown in **(C)**.

Patches of conserved residues of a certain protein throughout different organisms often indicate regions that are of biological relevance. Conserved amino acids were kept stable during the evolutionary process as they carry out key functions (Zvelebil et al., 1987). From this point of view it is possible to detect e.g. residues that compose the active site of a protein, regions that play a basic role in structural maintenance or patches of residues that are important for oligomerization or interaction to binding partners. Whereas highly conserved residues involved in stabilization of the fold are mostly located inside the protein, highly conserved residues important for interaction are frequently located in conserved patches on the surface of a protein (Lichtarge et al., 1996).

In order to identify regions on RseB that are potential interaction interfaces, highly conserved residues were colored on the surface according to their chemical properties (Figure 19 and sequence alignment in Figure 13C). Four patches containing accumulations of highly conserved residues are exposed on the surface of RseB (Figure 19B and C). Patch 1 of the small domain was found to account for the attachment to the large domain (see Chapter 2.2.4.). Two other patches are located at the top (patch 4, Figure 19C) and on the flat side (patch 3, Figure 19B) of the small domain, and could highlight potential interaction interfaces. Patch 2 is located on the large domain in close proximity to the hydrophobic half barrel.

2.2.6. Oligomeric Assemblies of RseB in the Crystal Lattice

For investigation of putative oligomeric forms of RseB, the crystal lattice was analyzed for all possible contacts between monomers of RseB. The crystal lattice is a regular arrangement of molecules that is stabilized by intermolecular contacts. Two different contact types can be distinguished (Janin, 1997; Janin and Rodier, 1995). First, there are crystal contacts that are characterized by only a few interactions and a small interface area. Those contacts mostly evolve during the crystallization process to mediate periodic protein-protein contacts. Second, there are crystal contacts with larger interaction surfaces that involve a set of often conserved residues (Valdar and Thornton, 2001). Such contacts are generally real oligomeric interfaces in terms of biological relevance.

2.2.6.1. Large Oligomeric Assemblies in the Crystal

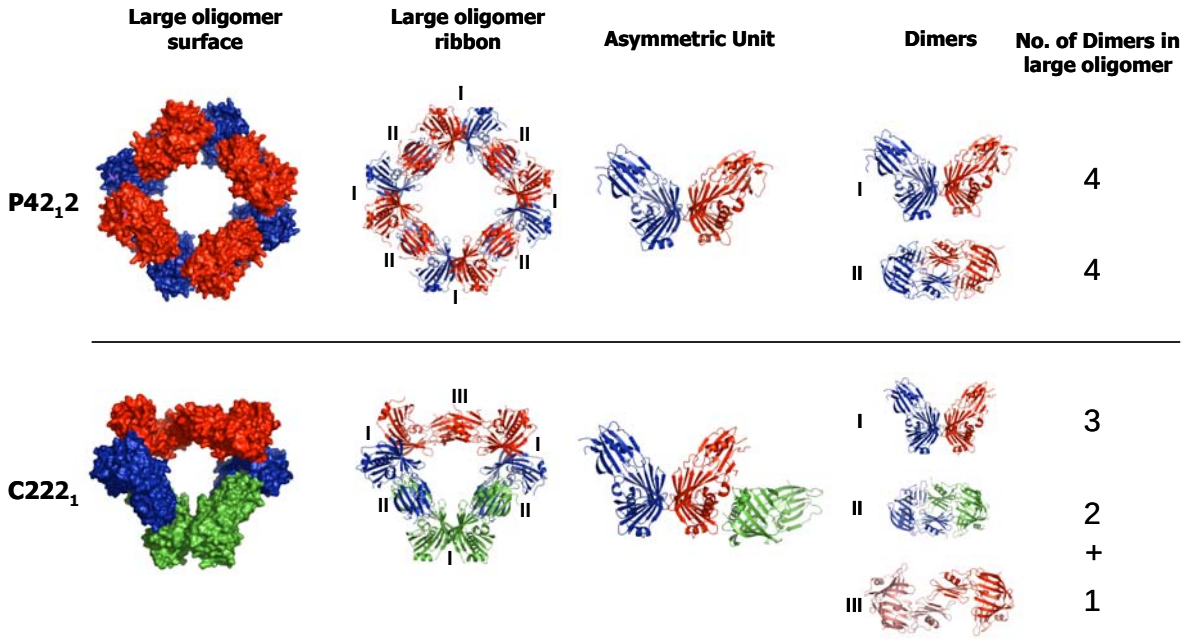

Figure 20. Large oligomeric assemblies in the crystal. Octameric and hexameric ring structures can be found in the tetragonal (P42$_1$2) and orthorhombic (C222$_1$) crystal form of RseB, respectively. For both crystal forms, the asymmetric unit is depicted which comprises two or three RseB molecules. The number of dimers necessary for ring formation is specified on the right. Monomers A and B are colored in red and blue, respectively. Monomer C of the orthorhombic asymmetric unit is colored in green. Three different contact types can be distinguished – an open (I), a close (II) and a semi-close contact (III).

The analysis of the tetragonal crystal lattice revealed large octameric rings as metastructure (Figure 20). The octamer forms a pore with a diameter of 53 Å and has a size of

approximately 150 Å in diagonal axis and a width of 128 Å. An oligomer like this would have a molecular weight of 270 kDa. It is composed of four asymmetric units and is a four-fold symmetric object.

In crystal form II, three monomers compose the asymmetric unit which then assembles to a hexameric ring. The hexameric ring has a pore of approximately 38 Å and an overall dimension of 130 x 108 Å. A hexameric assembly of RseB would have a molecular weight of 205 kDa. It is composed of two asymmetric units and has a two-fold symmetry (Figure 20).

In order to analyze to biologic relevance of these oligomeric rings, the protein contacts were analyzed in both the hexameric and the octameric assemblies (Figure 20).

Two predominant contacts were observed, termed 'open' and 'close' according to their respective dimer architecture. Whereas both domains, RseB-D1 and RseB-D2, contribute to dimer formation of the closed type, only RseB-D1 (large domain) is involved in the open form (Figure 20). The octameric ring can be formed upon an assembly of four open as well as four closed dimers and can be as such regarded as a tetramer of dimers.

The hexameric ring can be assembled by three open dimers but not by three closed dimers. The three fold symmetry is hampered by a unique contact which is formed by a small interface area with just a small number of residues involved. This type of contact was termed semi-close, as it resembles the closed contact but is less extended and only mediated by the small domain of RseB. The occurrence of different contacts and the possibilities for constitution to octamers and hexamers is explained in Figure 20.

2.2.6.2. Contacts in the Crystal

Three different types of contacts were observed in the crystal lattice. To elucidate the biological relevance, the contacts were analyzed according to interface area, number of observed contacts, degree of conservation of residues involved and relative abundance in the two crystal forms.

The Open Contact

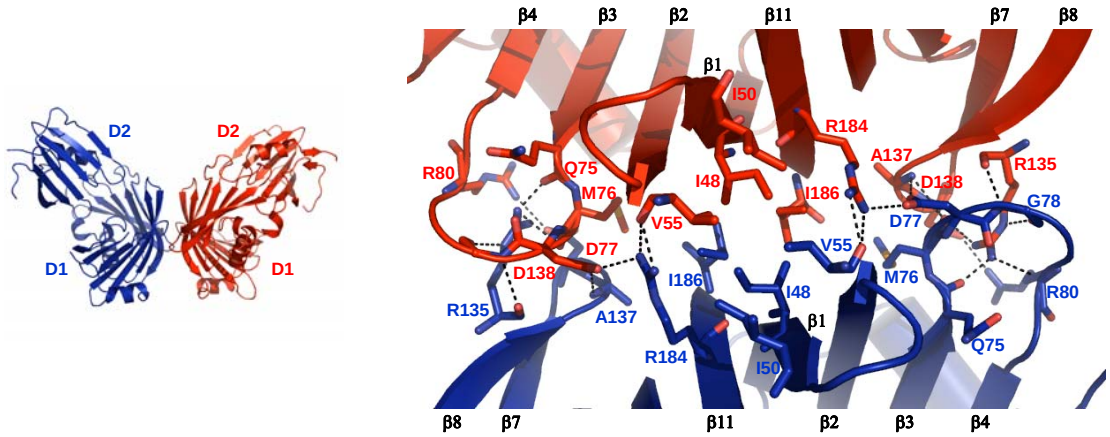

Figure 21. Open contact of crystal form I. On the left, D1 and D2 indicate the positions of the large and small domains of the two monomers P1 (red) and P2 (blue) of RseB. On the right, close-up view of the dimerization interfaces. In the open dimer residues **Ile48**, Ile50, *Val55*, Gln75, **Met76**, *Asp77*, **Gly78**, Arg80, **Arg135**, Ala137, *Asp138*, Arg184, *Ile186* are involved; (bold for highly conserved and italic for conserved). Residues **Ile48**, Ile50, *Val55* and *Ile186* form a small hydrophobic core. Names of secondary elements are indicated. In orthorhombic crystal lattice the open contact is conserved.

The open contact observed in both crystal lattices is mediated only by residues of the large domain of RseB. As shown in Figure 21, this interface is stabilized by 20 hydrogen bonds and four salt bridges in the tetragonal crystal. The interface area covers 874 $Å^2$, representing 6% of the total accessible surface area and includes a small hydrophobic core. 13 residues were found to be involved in interchain contacts, with four residues being highly and additional four residues being conserved (see also Table 2). This high level of conservation is an indication for biological relevance.

The residues of the large domain contributing to open dimer formation are predominantly located on the extended loops linking β_3 to β_4 (Gln75, Arg80, Met76, Asp77 and Gly78) and

β_7 to β_8 (Ala137, Asp138 and Arg135). Residues additionally involved in the open contact are found on β_{11}, β_2 and β_1 forming a small hydrophobic core.

The analysis of the open contact in the orthorhombic crystal revealed this contact as conserved in all monomers (see Table 3).

The Close Contact

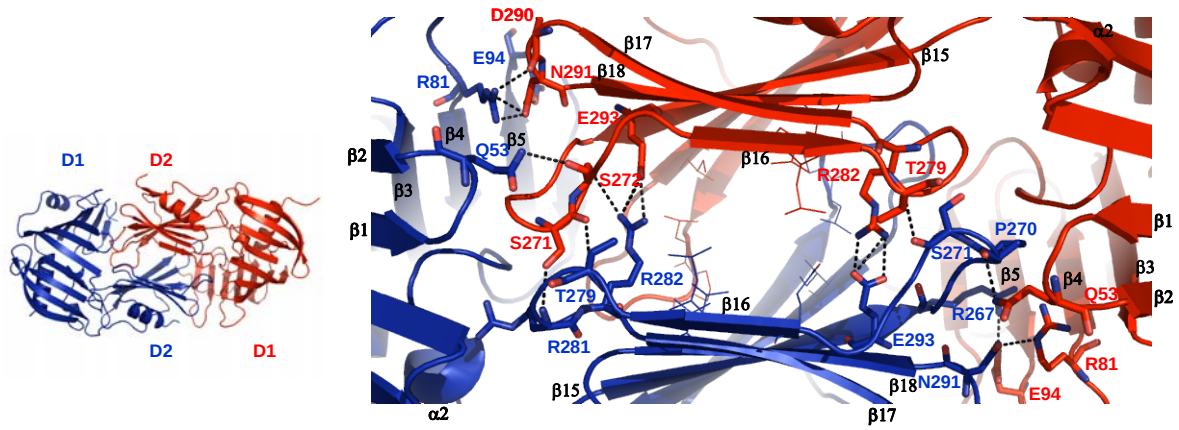

Figure 22. Close contact of crystal form I. In the close dimer residues Gln53, Arg81, **Glu94**, Arg267, Pro270, Ser271, Ser272, Thr279, Arg281, *Arg282*, Asn291 and Glu293 are involved. Residues **Leu240**, Pro242, Ile249, *Leu277*, **Val284** and Val297 form a hydrophobic core (depicted as lines, for clarity not specified; bold for highly conserved and italic for conserved). Names of secondary elements are indicated. In orthorhombic crystal lattice, the closed contact is not conserved due to an increased distance between the two small domains.

The close contact of the tetragonal crystal is mediated by residues of the large as well as of the small domain. As illustrated in Figure 22, contact stabilization is governed by 12 hydrogen bonds and 7 salt bridges. Besides, a relatively large hydrophobic area is buried upon dimerization, yielding a large interface area of 2083 $Å^2$ (14.3% of total surface area). Although this size suggests biological relevance, the bond forming residues are not well conserved (only one residue is highly and another is conserved, see also Table 2). A higher degree of conservation is found in the hydrophobic core that includes two highly conserved residues and one residue with lower conservation.

When investigating the closed contact in crystal form II, high differences concerning bond-forming residues were encountered. Here, the stabilization of the interface is mediated by solely one salt bridge and without any additional hydrogen bond (Table 3). These findings suggest that the closed contact is of high flexibility which is in contrast to the open dimer.

Furthermore, nearby loops could not be built due to bad electron density, which is also an implication for enhanced flexibility. The reason for this could be that the closed dimer interface is stabilized mainly by hydrophobic interactions. A superposition of the C2/C3 dimer and P1/P2 dimer explains the observed differences in both crystal forms: the distance of the small domains of C2/C3 was found to be 0.5-0.7 Å larger than observed for the tetragonal interfaces.

Table 2 lists bond forming residues observed in the two interfaces of crystal form I.

Table 2. Overview of bond-forming residues stabilizing the open and the close contact[a].

open			close		
P2	**distance (Å)**	**P1**	**P2**	**distance (Å)**	**P1**
Val 55B O	2.78	Arg 184A NH1	Gln 53B NE2	3.61	Ser 272A O
Val 55B O	2.87	Arg 184A NH2	Arg 81B NH2	3.05	Asp 290A O
Gln 75B O	3.17	**Arg 135A NH1**	Arg 81B NH1	2.43	Asn 291A OD1
Gln 75B O	2.37	**Arg 135A NH2**	Arg 81B NE	3.09	Asn 291A OD1
Met 76B O	3.47	**Arg 135A NH1**	**Glu 94B OE1**	2.41	Asn 291A ND2
Met 76B O	2.73	*Asp 138A N*	Arg 267B NH1	2.79	GluA 94 OE2
Met 76B O	3.19	Ala 137A N	Arg 267B NH2	3.06	Arg 81A NH2
Asp 77B OD1	2.90	Ala 137A N	Pro 270B O	2.96	Gln 53A NE2
Asp 77B OD2	3.30	Arg 184A NH1	Ser 271B O	3.12	Thr 279A OG1
Gly 78B N	2.66	**Arg 135A O**	Thr 279B OG1	3.13	Ser 271A O
Gly 78B O	2.97	**Arg 135A NE**	Arg 281B N	3.13	Ser 271A OG
Pro 79B O	3.33	**Arg 135A NH2**	*Arg 282B NH1*	3.02	Glu 293A OE2
Arg 80B NH1	3.08	*Asp 138A OD1*	*Arg 282B NH2*	3.22	Glu 293A OE1
Arg 135B NE	3.13	**Gly 78A O**	*Arg 282B NH2*	3.27	Glu 293A OE2
Arg 135B NH2	2.37	Gln 75A O	*Arg 282B NH2*	3.40	Ser 272A OG
Arg 135B NH2	3.28	**Met 76A O**	Asn 291B ND2	2.70	**Glu 94A OE2**
Arg 135B O	3.14	**Gly 78A N**	Glu 293 OE1	3.00	*Arg 282A NH2*
Ala 137B N	3.02	*Asp 77A OD1*	Glu 293 OE1	3.42	Arg 81A NE
Ala 137B N	3.51	**Met 76A O**	Glu 293 OE2	2.76	*Arg 282A NH1*
Asp 138B N	3.09	**Met 76A O**			
Asp 138B OD1	3.21	Arg 80A NH1			
Arg 184B NH1	2.77	*Val 55A O*			
Arg 184B NH2	3.10	*Val 55A O*			
Arg 184B NH2	3.21	*Asp 77A OD2*			

[a]Shown are observed contacts in the tetragonal crystals from open and close dimer. Hydrogen bonds (black), salt bridges (red) with highly conserved residues bold and conserved italic. The open contact is conserved in the orthorhombic crystal lattice, whereas for the open contact only a single contact was found (green).

The Semi-Close Contact

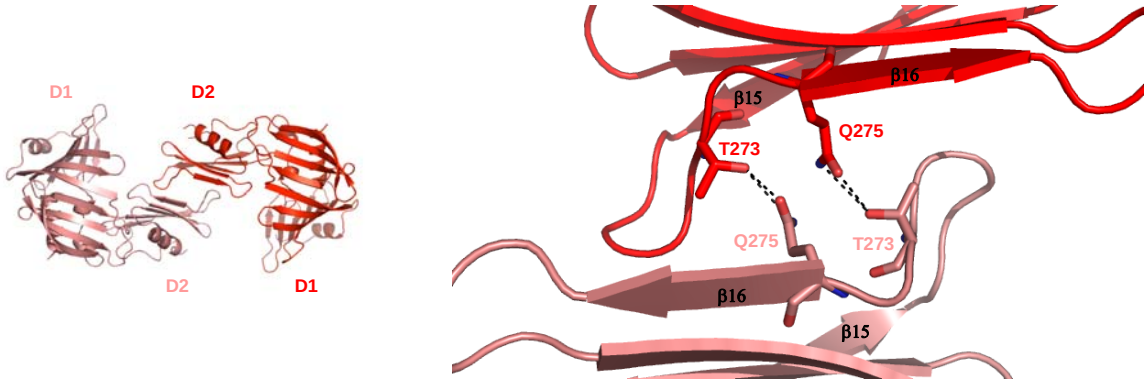

Figure 23. Semi-close contact of crystal form II. The semi-closed contact, unique for orthorhombic crystal lattice, is only stabilized by two unconserved residues Thr273 and Glu275. Names of secondary elements and positions of the large (D1) and small (D2) domains are indicated. Monomer A and monomer A' of an adjacent unit cell are colored in red and pink, respectively.

From the overall arrangement, the semi-closed contact is similar to the closed contact, but less compact. It is stabilized by only two non-conserved residues of the small domain of RseB which are involved in making four hydrogen bonds (Figure 23). With a very small interface area of 335 Å^2, this contact is probably not stable in free solution.

As the hexamer demands the semi-closed contact, further analysis of oligomeric states of RseB were intended to elucidate whether the hexamer and as such the semi-close contact has biological function.

A summary of analyzed interfaces in both crystal forms is given in Table 3.

Table 3. Contacts of observed interfaces in crystal forms I and II.[a]

	open			close		semi-close
Crystal form	$P42_12$	$C222_1$	$C222_1$	$P42_12$	$C222_1$	$C222_1$
Monomers	P1/P2	C3/C3*	C1/C2	P1/P2*	C2/C3*	C1/C1*
Area [Å²]	874.5	867.9	882.6	2083.0	1503.7	353.1
H-bonds	20	21	23	12	0	4
Salt-bridges	4	3	2	7	1	0
	conserved			flexible		small

[a]Listed are interface area and number of involved hydrogen bonds and salt bridges that stabilize the interface. The open contact that is mediated only by the large domain is more conserved than the closed contact. The interface area of the closed contact is more extended as the interface of the open contact, but is less conserved. In $C222_1$ only one salt bridge could be found in the closed form. Another contact, called semi-closed, found exclusively in the orthorhombic crystal has a very small interfacial area and only two residues were found to contribute to stabilizing contact formation. The asterix marks monomers of a crystallographic neighbor.

2.2.6.3. Co-Crystallization of RseB with Detergent

The large domain of RseB is structurally similar to proteins which are capable of binding lipophilic compounds. With respect of this functional background of homologous proteins, crystals with bound lipids or detergents were tried to obtain. One crystal, grown in 0.1 M Tris-HCl pH 8, 0.2 M magnesium chloride, 25% (w/v) polyethylene glycol 3350 and 0.5% dodecyl maltoside (DDM), was of orthorhombic space group $C222_1$ (a = 98.3 Å, b = 207.6 Å, c = 110.4 Å and α = 90°) and diffracted to 2.75 Å. It was solved by molecular replacement with the model of crystal form II. The structure was refined until the quality of the model allowed to trace additional density.

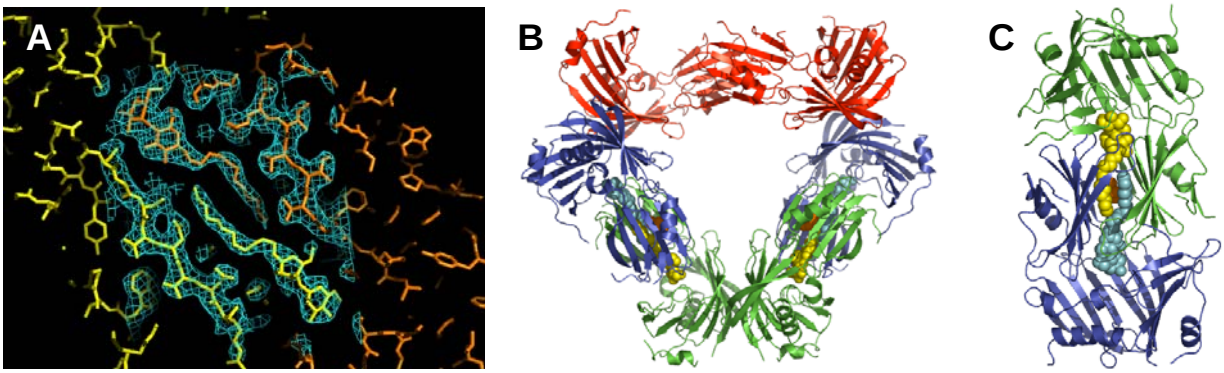

Figure 24. RseB crystallized with dodecyl maltoside (DDM). (A) Part of the electron density from RseB co-crystallized with DDM with monomer A and B drawn as yellow and orange sticks. **(B)** Illustration of two assymtetric units, containing each three monomers of RseB (colored in green, blue and red). **(C)** Closed dimer of crystal form III shows the embedment of two molecules of DDM and one glycerol in its interface. In **(B)** and **(C)** DDM is colored in cyan and yellow, whereas glycerol is depicted in orange.

This crystal, termed crystal form III, had an architecture as crystal form II and no obvious conformational variations were observed. However, as shown in Figure 24, additional density, which evolves from two molecules of DDM in the asymmetric unit, were detected. Surprisingly, these hydrophobic compounds were not located in the unclosed barrel of the large domains, but between the interfaces of the close contacts.

This indicates that the close dimeric assembly might have the property to accommodate hydrophobic compounds in between the small domains.

2.3. Biochemical Analysis of RseB

A set of experiments were performed to explore the precise function of RseB. Four main questions were posed: (1) which oligomeric states exist in solution; (2) which is/are the biological relevant oligomer(s) that interact with RseA; (3) do observed contacts play a role in oligomerization and (4) what is the function of the small and the large domain of RseB?

2.3.1. Oligomeric State of RseB in Solution

Previous reports described RseB to behave as a monomeric protein (Missiakas et al., 1997). To test the oligomeric state of RseB used for crystallization, a sample of purified RseB was analyzed by size exclusion chromatography.

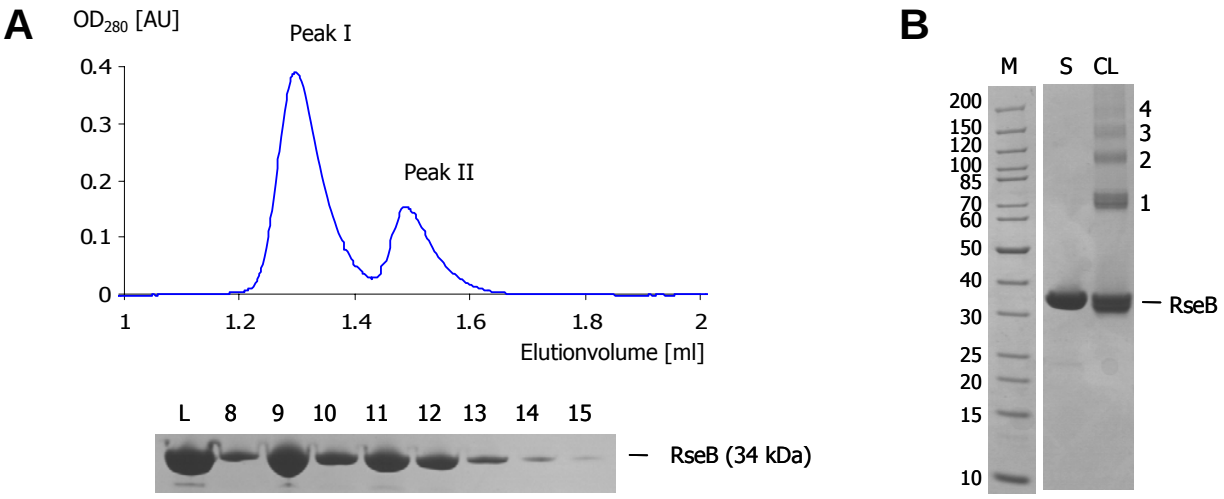

Figure 25. Size exclusion chromatography and chemical cross-linking of RseB. The chromatogram of the size exclusion experiment with corresponding fractions analyzed by SDS-PAGE is depicted in **(A)**. L corresponds to the sample loaded onto the column. RseB elutes in two peaks (Peak I, 1.28 ml; Peak II, 1.46 ml) of apparent molecular weights of ~220 kDa and 65 kDa, respectively. **(B)** Cross-linked RseB (CL) is analyzed by SDS-PAGE together with non cross-linked sample (S) for comparison. Cross-linking results in the formation of an additional faster migrating band due to intramolecular cross-link. Furthermore, cross-links of dimers (1), trimers (2), tetramers (3) and pentamers (4) were observed. The molecular weights of the protein standard (M) are indicated.

Figure 25A illustrates the elution profile of RseB and shows that it is characterized by two peaks. The presence of two peaks implies that RseB can exist in two different oligomeric forms. With the use of molecular weight standards the apparent molecular weights of RseB

oligomers were determined. The peak at lower elution volumes (peak I) corresponds to an apparent molecular weight of approximately ~220 kDa. Peak II has an apparent molecular weight of 65 kDa. With a molecular weight of 34 kDa, peak I is likely to include RseB in a hexameric or larger oligomeric assemblies (6 x 34 = 204), whereas peak II is formed of dimeric specimen of RseB (2 x 34 = 68). Thus, RseB is unlikely to be a monomeric protein, but rather exists as a dimer and in higher oligomeric assemblies.

To further characterize the oligomeric properties, cross-linking experiments using glutaraldehyde were performed. Glutaraldehyde is a bifunctional agent that is commonly used for cross-linking proteins and for tissue fixation. The reaction is based on the formation of Schiff bases and results in inter- and intramolecular cross-links of proteins. Mainly free amino groups especially that of lysines (Bowes and Cater, 1968), but also tyrosines and histidines have been shown to react with glutaraldehyde (Habeeb and Hiramoto, 1968). For comparison, samples of cross-linked and non-cross-linked RseB were analyzed by SDS-Page, as shown in Figure 25B.

Cross-linked RseB runs as an additional faster-migrating band, possibly due to intramolecular cross-linking of the small (RseB-D2) and the large domain (RseB-D1). The oligomeric forms observed correspond to a dimer (68 kDa), trimer (102 kDa), tetramer (136 kDa) and pentamer (170 kDa). The dimer is the most prominent oligomer. Interestingly no hexameric or octameric specimen could be detected.

These results indicate that RseB forms dimers in solution and has the potential to self associate into higher oligomeric structures.

2.3.1.1. Analytical Ultracentrifugation of RseB

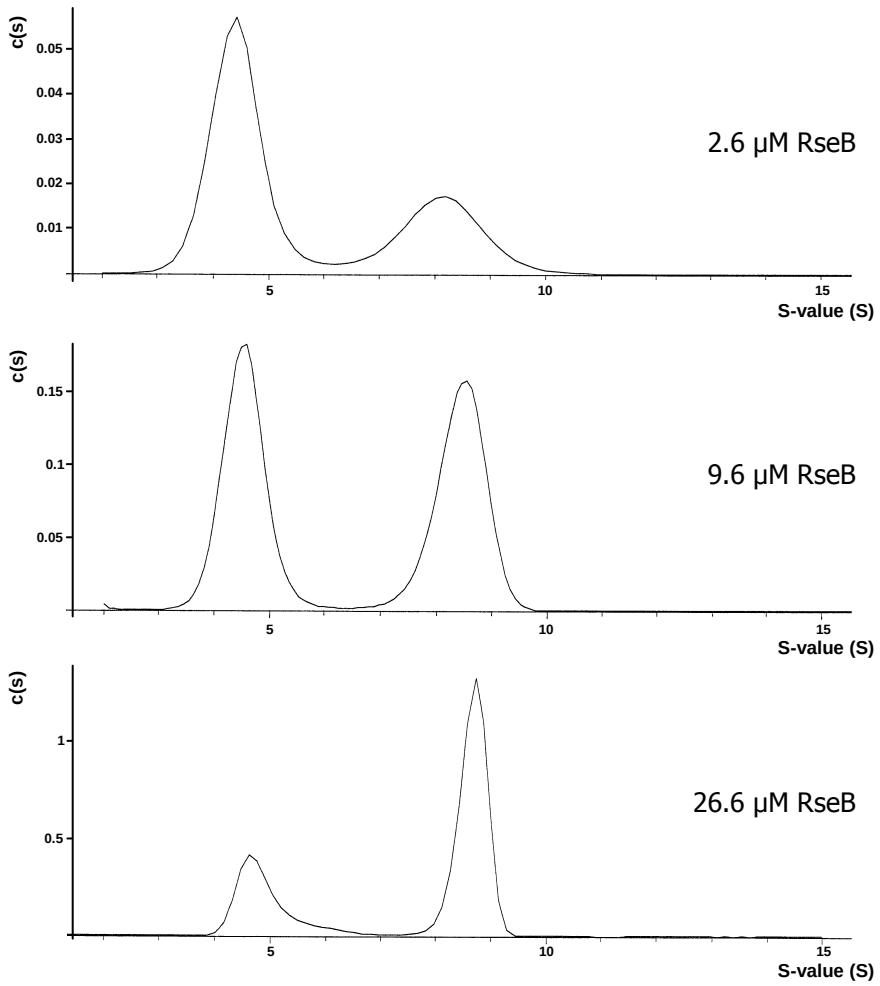

Figure 26. Sedimentation coefficient distribution of RseB. Illustration of sedimentation coefficient distribution of analytical centrifugation experiments with RseB concentrations of 2.6 µM (top), 9.6 µM (middle) and 26.6 µM (bottom). In all concentrations, oligomers with S-values of ~4.7 S and 8.6 S were found. Formation of oligomer with higher S-values is dependent on the protein concentration.

Analytical ultracentrifugation (AUC) was performed to analyze the oligomeric behaviour of RseB in more detail. Initial sedimentation velocity experiments with RseB showed that the RseB solution is heterogenic. This heterogeneity was due to the presence of two different oligomeric states of RseB with sedimentation coefficients of approximately 4.7 S and 8.6 S.

The formation of two discrete peaks in sedimentation velocity experiments suggests that the interconversion to the two oligomeric species is not changing rapidly.

In all tested concentrations of RseB two oligomeric types were existent. However, when comparing the sedimentation coefficient distributions from different concentrations varying

ratios of the oligomeric forms were observed (Figure 26). At low concentration predominantly smaller oligomers was present, whereas at the highest protein concentration assemblies with higher sedimentation coefficient were prevalent. This suggests that the formation of larger oligomer is favoured at enhanced protein concentration.

At a concentration of 9.6 µM RseB, almost equal amounts of the two oligomeric forms were present, indicating that the K_D for an equilibrium mixture of the smaller oligomer and higher oligomer is at similar concentrations. The peak with 4.7 S is likely to include the dimeric specimen. The oligomer with higher sedimentation coefficient was not analyzed for molecular weight estimations yet. To sum up in line with size exclusion experiments, RseB seems to exist as a dimer in solution and higher multimerization occurs at elevated concentrations.

2.3.1.2. Small Angle X-ray Scattering (SAXS) of RseB

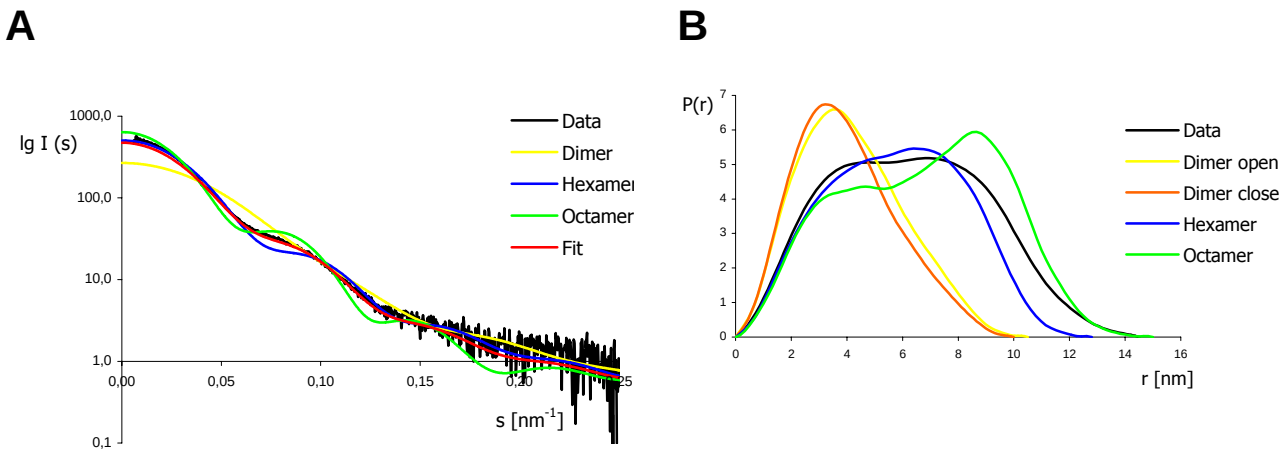

Figure 27. SAXS analysis of RseB. Small angle X-ray scattering (SAXS) was performed for determining the oligomeric states in a solution of RseB at a concentration of 5 mg/ml. **(A)** Buffer-subtracted scattering profiles of experimental data (black) and calculated pattern of different oligomeric forms of RseB observed in the crystal lattice. The curve of the best fit is given in red. **(B)** Electron pair distribution computed from experimental data and calculated for different oligomeric forms. SAXS data suggest that RseB in solution is composed of a mixture of dimeric, hexameric and octameric assemblies.

Small angle X-ray scattering (SAXS; Tsutakawa et al., 2006) was performed for determining the oligomeric states of RseB in solution. The processed X-ray scattering pattern of RseB relative to calculated patterns from different oligomeric models of RseB are shown in Figure 27A. As the experimental curve does not match any of the calculated ones, data suggest that RseB is polydisperse in solution. Fitting the experimental pattern with only two different

oligomeric species wasn't successful. The best fit was achieved with a mixture of 0.6% open dimer, 38% octamer and 56% hexamer. This indicates that most of RseB at a concentration of 5 mg/ml is assembled to large oligomers of hexameric and octameric nature.

Similar results were obtained by the electron pair distribution plots of RseB. The resulting p(r) function, illustrated in Figure 27B, indicates that RseB in solution has a maximum diameter of 145 Å.

The theoretical calculated curves from pdb files of an open and a closed dimeric assembly revealed to be very similar to each other but different from the experimental curve. Both have a calculated single peak at 35 Å and a maximal diameter of only 100 Å; hence, being about one third too small. This suggests that the dimer is not the prominent oligomeric form of RseB in solution under these conditions.

The maximal diameter of the octameric ring (150 Å) is similar to the observed maximal diameter (145 Å). This indicates that the octameric assembly observed in the tetragonal crystal lattice is likely to occur also in solution under the tested protein concentration. However, when comparing the curve progression of the experimental data and the theoretical data for octameric species, differences were observed.

The hexamer has a maximal diameter of 125 Å. As the plot derived from hexameric model shows most similarity in overall curvature, it is likely that a mixture of hexameric and octameric assemblies of RseB is present in solution. Moreover, as the experimental curve has a peak similar to the calculated functions of the dimer models it is to suggest that at least some dimeric specimen had been present in the sample.

In sum, these experiments indicate that (1) the octameric ring is likely to occur in solution as its calculated curve and the experimental curve have similar maximal diameter, (2) the hexamer is a predominant assembly in solution and (3) a rather small portion of dimers exist in solution in the tested condition (5 mg/ml).

2.3.1.3. Electron Microscopy of RseB

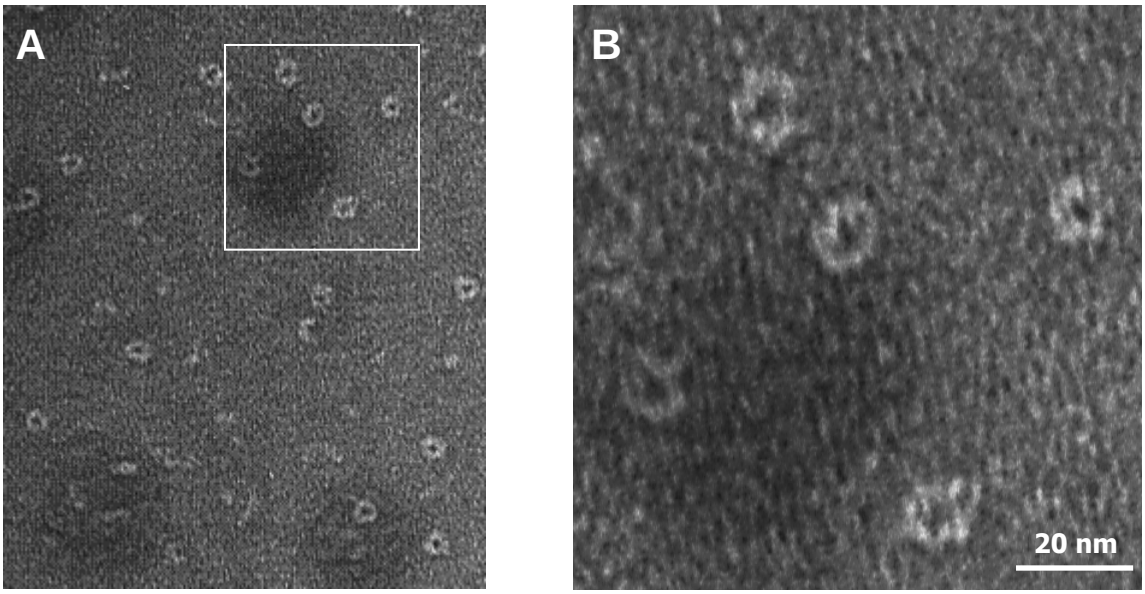

Figure 28. Negatively stained electron micrographs of RseB. (A) Electron micrographs, showing fields of negatively stained molecules of RseB. Large oligomeric assemblies with ring-like structures are visualized. Part of **(A)** indicated by a square is enlarged in **(B)**. A scale bar is given in **(B)**.

As there were indications from AUC, SAXS and gel filtration experiments for the existence of higher oligomeric states of RseB in solution, it is to be asked whether observed hexameric or octameric assemblies could be visualized in electron micrographs. For this, fractions from peak I of gel filtration studies (Chapter 2.3.1.) were analyzed by electron microscopy methods.

Pictures obtained from negatively stained electron micrographs show the presence of ring-like structures (Figure 28A and B). The approximate size of observed particles was estimated to vary between 126 and 146 Å with pore dimensions of 30 to 40 Å. This implies that RseB is able to form high oligomeric assemblies similar to those that were observed in the crystal lattice and were predicted by size-sensitive methods. Whether these observed rings are octameric or hexameric assemblies or both is not clear to date.

2.3.2. Interaction of RseB and RseA-PP

Previous findings from literature report on a direct interaction of RseB and the periplasmic domain of the anti-sigma factor RseA (De Las Penas et al., 1997b; Missiakas et al., 1997). In order to elucidate more clearly the binding behavior of RseA and RseB, the periplasmic domain of the monotopic transmembrane anti-sigma factor (RseA-PP) was cloned, expressed and purified and a peptide was synthesized including a region of RseA of predicted helical structure.

2.3.2.1. Cloning, Purification and Biochemical Analysis of RseA-PP

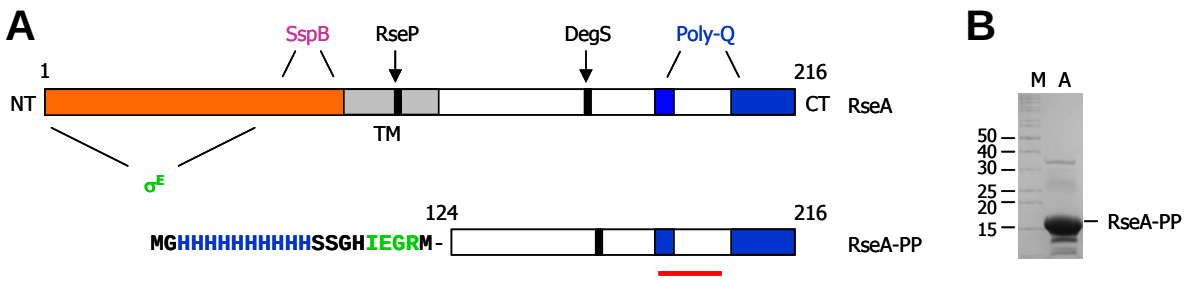

Figure 29. Features of the anti-sigma factor RseA and cloning and purification of RseA-PP. (A) The upper panel depicts important areas of RseA. The cytoplasmic domain (orange) of RseA inhabits binding sites for σ^E and SspB as well as cleavage sites (black) of RseP and DegS. Transmembrane helix is colored in grey and the two poly-Q stretches near the C-terminus are shown in blue. The lower panel shows the periplasmic domain of RseA that was cloned and expressed. The His-tag (blue) needed for purification is cleavable as a Factor Xa cleavage site was included in cloning (green). The red bar indicates the region that was chosen for peptide synthesis. **(B)** Purified periplasmic domain of RseA (RseA-PP) is loaded in lane A, marker protein of the standard in lane M.

The anti-sigma factor RseA, as the key player of the σ^E stress response pathway, exhibits numerous important features (Figure 29A). The N-terminal cytoplasmic domain harbours the interaction site of σ^E as well as a binding site for SspB that is required for degradation by the ClpXP protease (Campbell et al., 2003; Flynn et al., 2004; Levchenko et al., 2005). RseP cleaves RseA within the membrane spanning helix, whereas DegS cleaves RseA in the periplasmic domain (Ades et al., 1999; Alba et al., 2002; Alba et al., 2001; Walsh et al., 2003). Besides the cleavage site of DegS, this domain also contains two glutamine rich stretches that are believed to be important for a regulated degradation.

As RseB is known to bind the periplasmic domain of RseA, the periplasmic part of RseA (RseA-PP: residues 124-216, Figure 29 A and B) was cloned, expressed and purified as described in Materials and Methods.

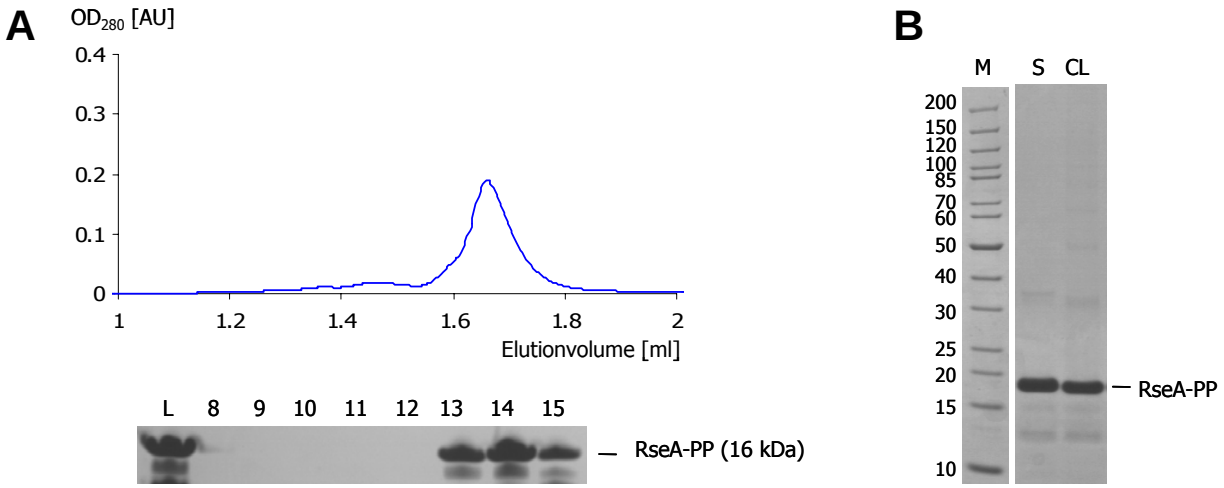

Figure 30. Size exclusion chromatography and chemical cross-linking of RseA-PP. The chromatogram of the size exclusion experiment of RseA-PP (peak 1.66 ml) with corresponding fractions analyzed by SDS-PAGE is shown in **(A)**. L corresponds to the load used for this experiment. **(B)** Cross-linked RseA-PP (CL) is analyzed by SDS-PAGE together with non-cross-linked sample (S). RseA-PP is not able to produce cross-linked products. The molecular weights of the protein standard (M) are indicated.

Size exclusion experiments were performed for initial characterization of RseA-PP. As illustrated in Figure 30A, RseA-PP eluted in a single peak with an apparent molecular weight of 20 kDa and likely to correspond to monomeric specimen (16 kDa). As RseA-PP contains no tryptophans, the absorption properties are rather low.

Similar results were obtained in cross-linking experiments using glutaraldehyde as a cross-linker, where RseA was not able to form cross-linked multimers (Figure 30B). This indicates that RseA-PP behaves as a monomeric protein.

2.3.2.2. Direct Interaction of Dimeric RseB and RseA-PP

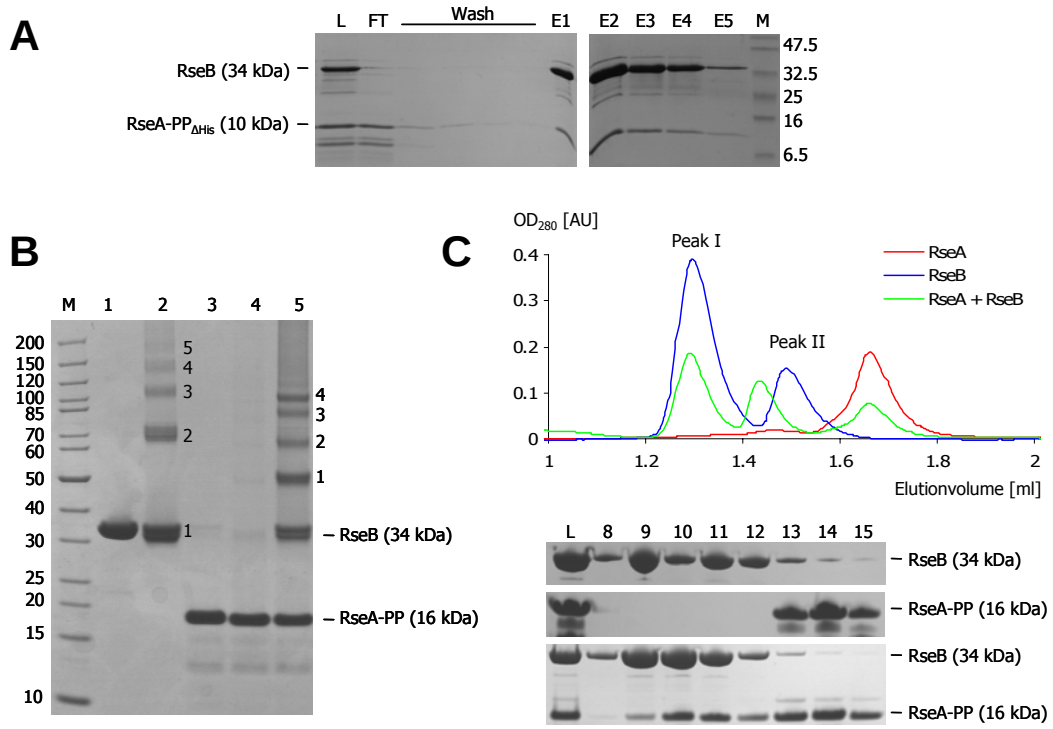

Figure 31. Interaction of RseA-PP and RseB. (A) Co-immobilization of RseB with untagged RseA to test direct interaction. The His-tag of RseA was removed by Factor Xa protease. Cleaved RseA-PP (RseA-PP$_{\Delta His}$) was incubated with C-terminally His-tagged RseB and loaded on a Ni-chelating column. Both proteins co-elute from the column, which indicates a direct interaction of RseA and RseB. The molecular weights of protein standard are indicated (M). **(B)** SDS-PAGE of proteins, cross-linked with glutaraldehyde. Non cross-linked proteins were loaded on lane 1 (RseB) and lane 3 (RseA-PP). Cross-linked RseB (lane 2) leads to the generation of an additional faster migrating band (1), possibly due to intramolecularly cross-linking the small (D2) and the large domain (D1). Observed oligomeric forms are dimers (68 kDa) (2), trimers (102 kDa) (3), tetramers (136 kDa) (4) and pentamers (170 kDa) (5). The dimer is the most prominent oligomer. RseA-PP cannot cross-link by itself (lane 4). Cross-links of RseB and RseA-PP lead to the formation of four additional products (lane 5): a dominant 50 kDa band (1) (RseB and RseA-PP), a weak 66 kDa band (2) (RseB and two RseA-PP), a weak 84 kDa band (3) (two RseB and RseA-PP) and a dominant 100 kDa band (4) (two RseB and two RseA-PP). The molecular weights of protein standard are indicated (M). **(C)** Fractions from size exclusion chromatography were analyzed by SDS-PAGE. RseB (top; elution peaks 1.28 and 1.46 ml) interacts with RseA-PP (middle; elution peak 1.66 ml) as both proteins co-elute in fraction 10 (bottom; elution peak 1.40 ml). This indicates an interaction of RseA-PP with dimeric RseB and not with higher oligomeric form of RseB. L corresponds to sample applied onto the column and numbering of lanes corresponds to fractions collected.

For evaluation of the reported interaction of RseB with the periplasmic domain of RseA, initial binding studies were performed using a co-elution approach. For this, the cleavable His-tag of RseA-PP was removed by Factor Xa treatment and cleaved RseA-PP (RseA-PP$_{\Delta His}$) was incubated with His-tagged RseB. Both proteins were loaded on a Ni-chelating column to specifically immobilize RseB by its His-tag. As shown in Figure 31A, RseB as well as RseA-PP$_{\Delta His}$ co-eluted, whereas RseA-PP$_{\Delta His}$ on its own was unable to bind to the column. This affirms a direct interaction of RseB and RseA-PP.

To further investigate the interaction of RseB and RseA-PP, both proteins were subjected to size exclusion chromatography. The elution profile of both proteins was analyzed before (see also Figures 25A and 30A). As depicted in Figure 31C, application of both proteins yielded co-elution of RseA-PP in Peak II of RseB but not in peak I, suggesting that RseA-PP only interacts with dimeric RseB. Additionally, peak II was shifted to lower elution volumes in the presence of RseA-PP. This indicates that all dimeric RseB is complexed with RseA-PP which suggests a strong binding between the two proteins.

These findings were further supported by cross-linking studies. When cross-linking both proteins, four additional bands were observed that correspond to complexes of RseB and RseA-PP (Figure 31B, lane 5). The two prominent bands correspond to RseB monomer/RseA-PP monomer (Figure 31B, lane 5, band 1) and RseB dimer/RseA-PP dimer interaction (Figure 31B, lane 5, band 4), indicating an interaction of the proteins in a 1:1 stoichiometry. Interestingly, all RseB-only cross-links (Figure 31B, lane 2) were missing in the presence of RseA-PP.

2.3.2.3. RseB Binds RseA$_{162\text{-}186}$

```
            124                                                                                                                                                                                                                                                                                                                                                                                                                                                                                                                                                                                                                                                                                                                                                                                                                                                                                                                                                                                                                                                                                                                                                                                                                                                                                                                                                                                                                                                                                                                                                                                                                                                                                                                                                                                                                                                                                                                                                                                                                                                                                                                                                                                                                                                                                                                                                                                                                                                                                                                                                                                                                                                                                                                                                                                                                                                                                                                                                                                                                                                                                                                                                                                                                                                                                                                                                                                                                                                                                                                                                                                                                                                                                                                                                                                                                                                                                                                                                                                                                                                                                                                                                                                                                                                                                                                                                                                                                                                                                                                                                                                                                                                                                                                                                                                                                                                                                                                                                                                                                                                                                                                                                                                                                                                                                                                                                                                                                                                                                                                                                                                                                                                                                                                                                                                                                                                                                                                                                                                                                                                                                                                                                                                                                                                                                                                                                                                                                                                                                                                                                                                                                                                                                                                                                                                                                                                                                                                                                                                                                                                                                                                                                                                                                                                                                                                                                                                                                                                                                                                                                                                                                                                                                                                                                                                                                                                                                                                                                                                                                                                                                                                                                                                                                                                                                                                                                                                                                                                                                                
rsea_ecoli  SETSQQPETPVFNTLPMMGKASPVSLGVPSEATANNGQQQQVQEQRRRINAMLQDYELQRRLHSEQLQFEQAQTQQAAVQVPGIQTLGTQSQ
rsea_haein  NDASNLPETPVLQTLPFNNAVQEVSYNAPSKDTLTS---DQLEKKSRRIGAMLQNYELQRRMHSDAL-------------------------
PROF_sec              EEE          EE             HHHHHHHHHHHHHHHHHHHHHHHH                EE
                                                  /                       \
                                                 QQQQVQEQRRRINAMLQDYELQRRL
                                                 162                     186
```

Figure 32. Synthetic RseA peptide. The protein sequence of the periplasmic domain of RseA of *E. coli* is shown in the first row, including N- and C-terminal residue numbers. RseA from *Haemophilus influenzae* has 40% homology and was chosen as a representative for evaluating the conserved residues that are colored in red. The result of secondary structure prediction (PredictProtein, Rost et al., 2004) is shown below with predicted sheet regions (E) and helical regions (H). As the periplasmic domain of RseA harbours relatively few structured regions, the only long stretch with predicted secondary structure is suggested to bind RseB. Residues 162 to 186 were therefore chosen for generation of a synthetic peptide which was used for binding studies with RseB. The distribution of acidic (red) and basic (blue) amino acids is indicated.

To locate the interaction site of RseB on RseA, the periplasmic part of the anti-sigma factor was examined with secondary structure prediction tools. As shown in Figure 32, just a few stretches of the periplasmic domain of RseA were predicted to be structured.

One of these comprises the cleavage site of DegS which is located between Ser151 and Leu152. Besides this, a region of highly conserved residues (162-186) was observed, which is predicted to form a long helix. Moreover, this stretch includes one of the poly-Gln regions which are suggested to be important for regulated degradation of RseA. As this helix is speculated to be the interaction site for RseB, a peptide was synthesized, comprising residues 162-186 (RseA$_{162\text{-}186}$), and was used to test for a specific binding to RseB.

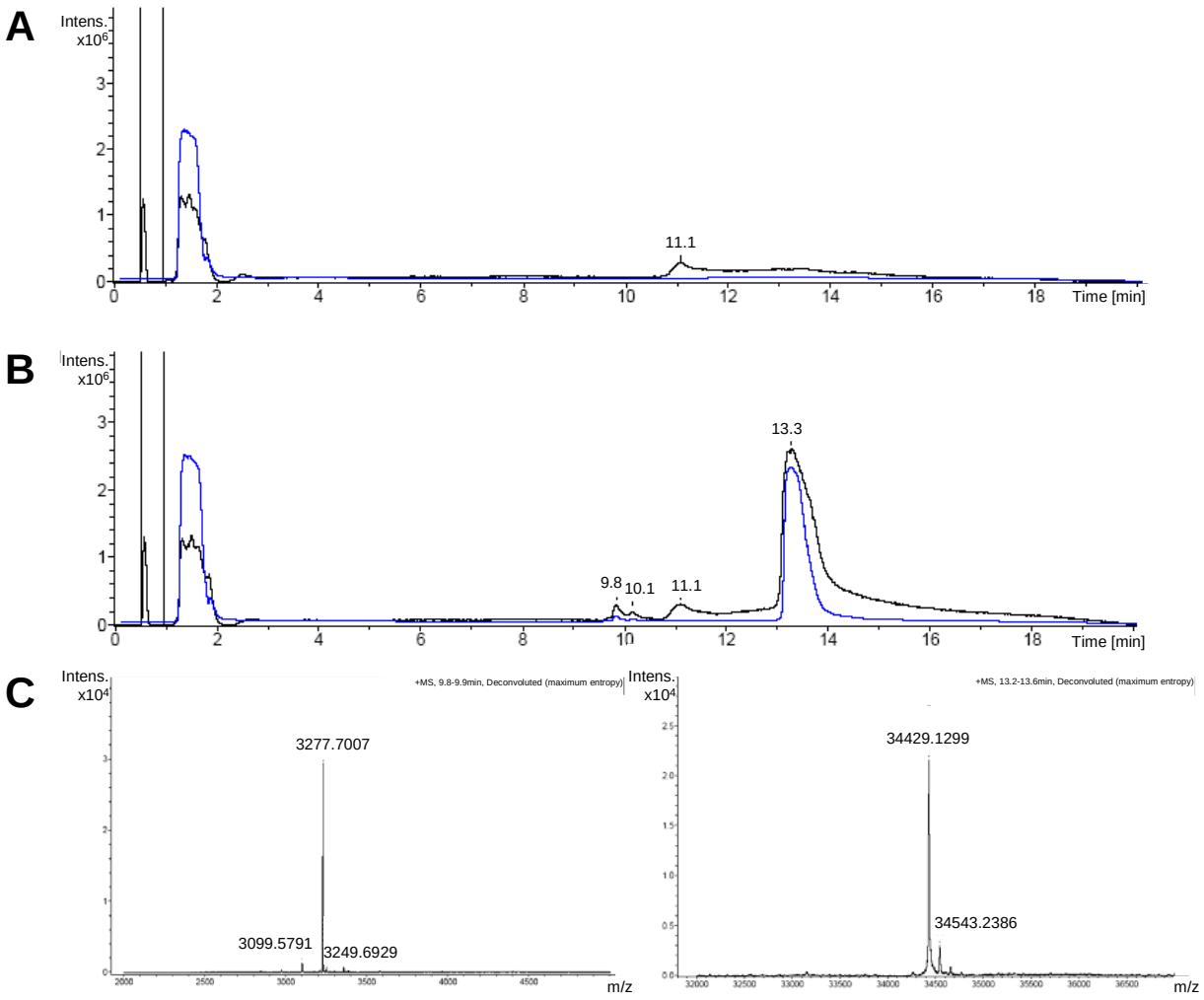

Figure 33. Binding of RseA$_{162-186}$ to RseB. The peptide RseA$_{162-186}$ was tested for specific interaction to RseB. For this, RseA$_{162-186}$ was applied to a Ni-chelating column with **(B)** or without **(A)** His-tagged RseB. The eluate was analyzed by HPLC/ESI-MS to verify the existence of the peptide. **(C)** The peptide mass (3277.7 Da) could only be detected by mass analysis when RseB was present which indicates that RseB was able to fish RseA$_{162-186}$.

RseA$_{162-186}$ was found to specifically bind to a Ni-NTA column only in the presence of C-terminally His-tagged RseB. The elution of the peptide was confirmed by HPLC/ESI-MS analysis, as illustrated in Figure 33. This indicates that RseA$_{162-186}$ is sufficient for interaction to RseB and that the long helix of RseA is likely to be the interaction site for RseB.

2.3.3. Biochemical Properties of the Large and Small Domains of RseB

The structure of RseB presented above revealed that the protein consists of two domains D1 and D2. These two domains were cloned, expressed and purified separately for biochemical analysis (see Materials and Methods). Both domains were analyzed by size exclusion techniques and cross-linking experiments for investigation of their oligomeric behaviour. Furthermore, the experiments were repeated in the presence of RseA-PP to identify the domain(s) interacting with the anti-sigma factor RseA.

2.3.3.1. Cloning and Purification of the Large and Small Domain of RseB

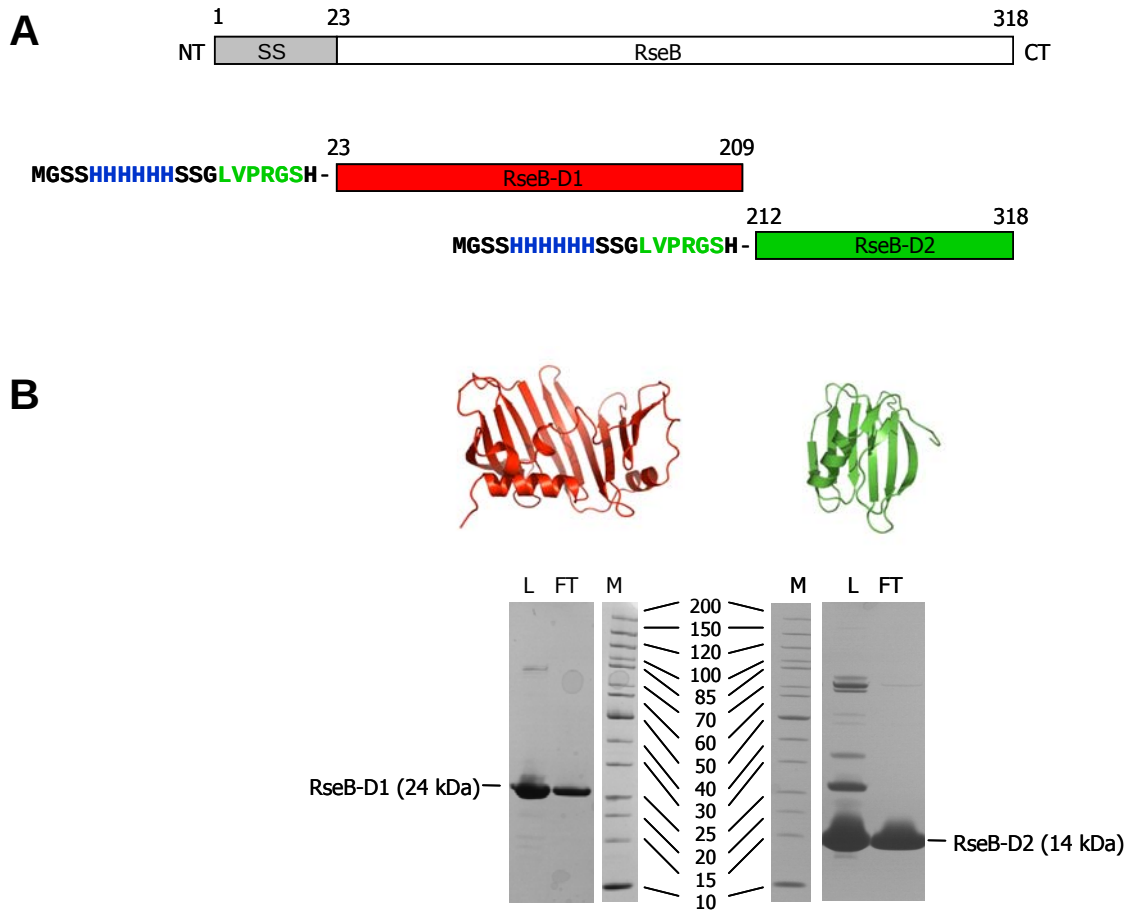

Figure 34. RseB small (RseB-D2) and large domain (RseB-D1) constructs and purification. (A) Schematic representation of the large (residues 23-209, red) and the small domain (residues 212-318, green) of RseB in comparison to full length RseB. Additional sequences like the His-tag (blue) and a thrombin cleavage site (green) are indicated. **(B)** Last step of purification of RseB-D1 and RseB-D2. Sample containing the protein of interest was loaded (L) on an anion exchange chromatographic column. Both proteins appeared in the flow through (FT) with high purity. Molecular weights are indicated (M). Structures of the large (red) and the small (green) domains are illustrated.

For designing the fragments suitable for expression of the large and the small domains, the structure of full length RseB was analyzed to define optimal domain boarders. The large and the small domains are connected by a flexible long loop. To obtain the domains separately, the flexible loop was omitted for enhanced stability of the domains. The large domain includes residues 23 to 209, whereas residues 212 to 318 were chosen for the small domain (Figure 34A). The appropriate fragments were cloned, expressed and purified as described in Materials and Methods (Figure 34B).

2.3.3.2. Large Domain of RseB Forms Multiple Oligomers

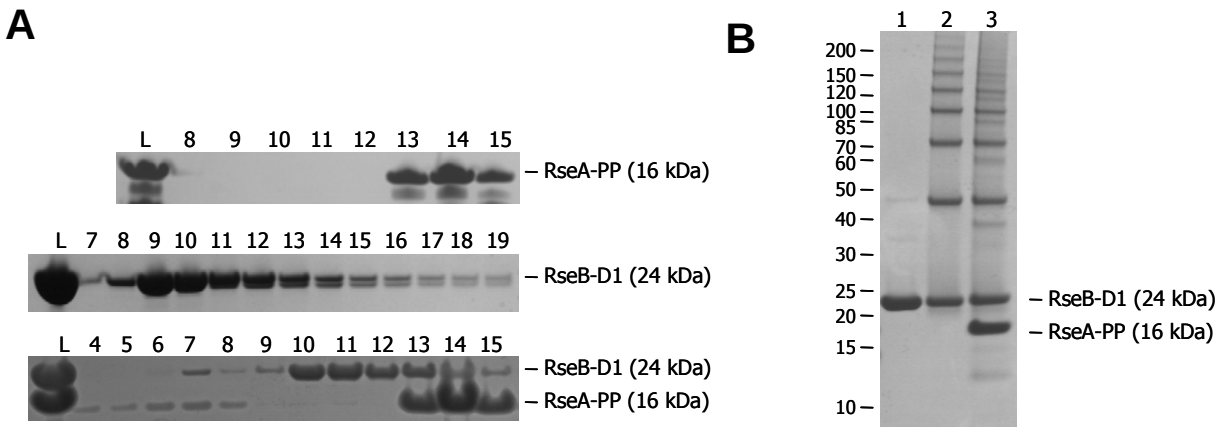

Figure 35. Size exclusion chromatography and chemical cross-linking of RseB-D1. (A) Fractions from size exclusion chromatography were analyzed by SDS-PAGE. RseB-D1 shows a high tendency to build up diverse oligomeric assemblies (middle; elution peaks 1.29; 1.5 and 1.61 ml), but cannot form a high-affinity complex with RseA-PP (bottom). L corresponds to sample applied onto the column and numbering of lanes corresponds to fractions collected. **(B)** SDS-PAGE of proteins, cross-linked with glutaraldehyde. Untreated RseB-D1 was loaded onto lane 1. RseB-D1 shows a strong tendency to form multimers (lane 2) with dimeric (48 kDa), trimeric (72 kDa), tetrameric (96 kDa), pentameric (120 kDa), hexameric (144 kDa), heptameric (168 kDa) and octameric (220 kDa) assemblies that exist also in the presence of RseA-PP (lane 3). Addition of RseA-PP results in formation of faintly visible additional bands corresponding to 40 kDa (RseB-D1 monomer and RseA-PP monomer), 60 kDa (RseB-D1 dimer and RseA-PP monomer) and 85 kDa (RseB-D1 dimer and RseA-PP dimer). Molecular mass is indicated by bands of definite protein mass.

Purified large domain of RseB was loaded on a size exclusion column to analyze its oligomeric properties (Figure 35A). The elution profile is characterized by multiple peaks indicating unspecific complexation or aggregation. Similarly, in cross-linking experiments RseB-D1 shows the tendency to form multiple oligomers (up to octameric assemblies) that remained similar in frequency and intensity upon addition of RseA-PP (Figure 35B, lane 2, 3 and Figure 35A, middle). These experiments suggest that RseB-D1 tends to form multiple oligomeric assemblies.

Although RseA-PP and RseB-D1 was found to cross-link in faintly visible bands (Figure 35B, lane 3), size exclusion experiments revealed no specific interaction of RseA-PP and RseB-D1 (Figure 35A, bottom). Only a small portion of RseA-PP was shifted to very low elution volumes, but most RseA-PP remained to elute as a monomeric specimen. These results suggest that RseA-PP and RseB-D1 do not interact specifically.

2.3.3.3. Small Domain of RseB Interacts with RseA-PP

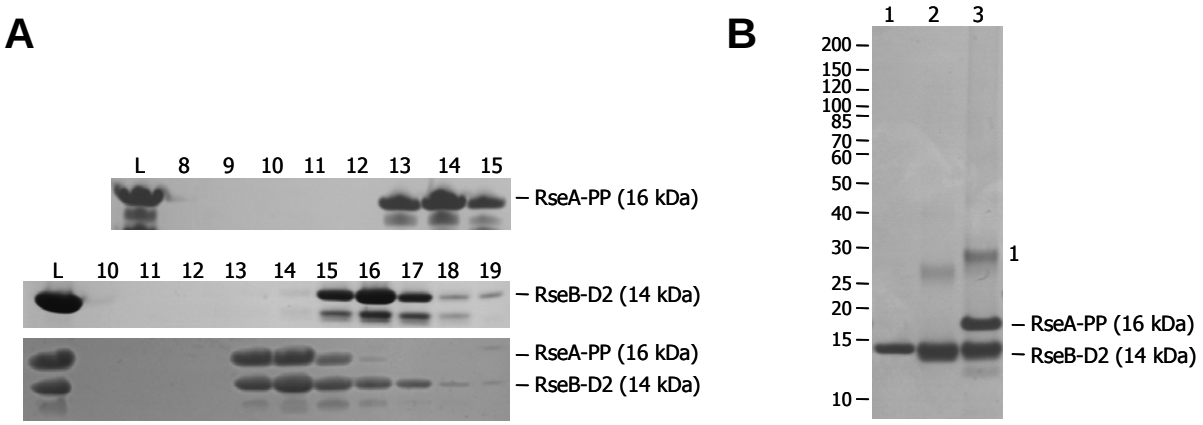

Figure 36. Size exclusion chromatography and chemical cross-linking of RseB-D2. **(A)** Fractions from size exclusion chromatography were analyzed by SDS-PAGE. RseB-D2 (top; elution peak 1.82 ml) and RseA-PP co-elute in fractions 13/14 (bottom; elution peak 1.64 ml), indicating binding of RseA to the RseB small domain. L corresponds to sample applied onto the column and numbering of lanes corresponds to fractions collected. **(B)** SDS-PAGE of proteins, cross-linked with glutaraldehyde. Untreated RseB-D2 was loaded onto lane 1. RseB-D2 shows weak tendency for dimerization (28 kDa; lane 2), whereas a distinct complex of 29 kDa is formed in the presence of RseA-PP (lane 3, (1)). Molecular mass is indicated by bands of definite protein mass.

In contrast to the large domain, the small domain (RseB-D2), exhibits only a weak tendency to cross-link with itself (Figure 36B, lane 2). It eluted in a single peak from the gel filtration column with an apparent molecular weight of 14 kDa corresponding to monomeric specimen (Figure 36A, middle). Both results suggest that RseB-D2 does not have the property for oligomerization.

In the presence of RseA-PP, RseB-D2 elution was shifted to earlier elution volumes leading to co-elution with RseA-PP, as shown in Figure 36A, bottom. This strongly indicates that the small domain of RseB is responsible for interaction to RseA-PP. Formation of a distinct cross-linked product containing both, RseB-D2 and RseA-PP, was confirmed by mass analysis (Figure 36B, lane 3, (1)).

3. Discussion

3.1. RseB Binding Site on RseA

RseB interaction with RseA is reported to exert an inhibitory effect on RseP cleavage efficiency and thus negatively regulates the σ^E activity. Two models are proposed for this inhibition: (1) RseB sterically restricts RseP from cleaving RseA; (2) RseB has a stabilizing effect on RseA. Both models refer to the fact that RseB interacts with the periplasmic domain of RseA.

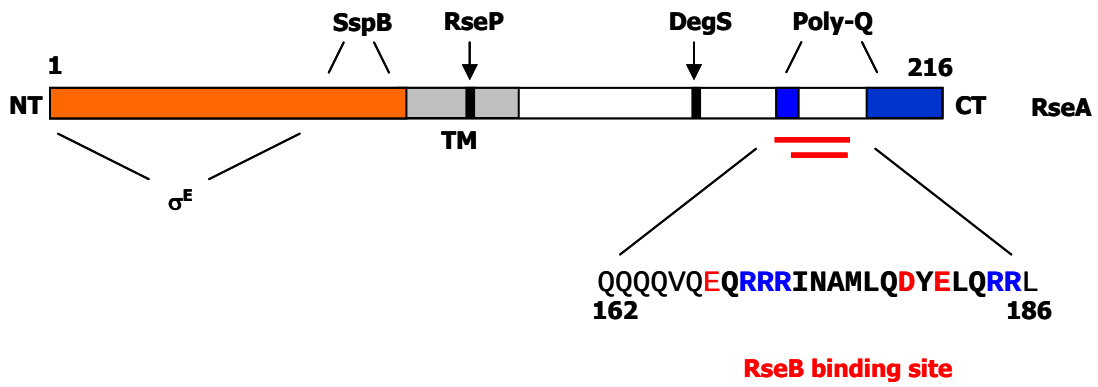

Figure 37. RseB binding site on RseA. Results obtained from binding studies of RseB and a synthetic peptide of RseA revealed that residues 162-186 comprise the putative binding site for RseB (upper red bar). Comparing these results with recently published data (Cezairliyan and Sauer, 2007; Kim et al., 2007) the minimal RseB binding region is suggested to be a predicted helix spanning residues 169-185 (bottom red bar). Sequence details of RseB binding site is given below, with acidic and basic residues shown in blue and red, respectively and with the putative minimal binding site in bold.

Results described in Chapter 2.3.2. confirm the interaction of the periplasmic part of RseA to RseB, as reported in literature (De Las Penas et al., 1997b; Missiakas et al., 1997). Secondary structure predictions revealed that most of the periplasmic part of RseA is not well structured (see Chapter 2.3.2.3.). One of the few structured regions was chosen for peptide synthesis (residues 162-186). The binding of $RseA_{162-186}$ to RseB could encircle the interaction site on RseA. This part of RseA, constituted by several highly conserved charged residues (Glu168, Arg170, Arg171, Arg172, Glu181 and Arg185) is likely to form a long helix. Dynamic interaction between RseB and RseA could occur through the formation of charged interfaces as reported for protein-protein interactions (Cherfils et al., 1991; Novotny and Sharp, 1992; Warshel and Russel, 1984; Xu et al., 1997).

During the preparation of this thesis two publications on RseB were released that both are in accordance with these results. In one contribution, residues 160 to 189 of RseA were found to be sufficient for binding to RseB (Cezairliyan and Sauer, 2007), in the other a fragment of residues 169 to 186 with Arg172 and Arg185 as the key residues were stated to promote binding to RseB (Kim et al., 2007). Both results are consistent with observed data and suggest that the region 169 to 185 of RseA, forming a putative helix, comprises the minimal interaction site for RseB.

3.2. RseA Binding Site on the small domain of RseB

X-ray structural analysis revealed that RseB is a two-domain protein (see Chapter 2.2.1.). Experiments analyzing individual domains for RseA interaction indicate that only the small domain (RseB-D2) specifically interacts with the periplasmic part of RseA (see Chapters 2.3.3.2. and 2.3.3.3.) and propose that binding to RseA is a function of the small domain of RseB. This suggestion is in full agreement with unpublished results of C. Gross, stated in a recent paper (Kim et al., 2007), where residues 245 to 250 of the small domain of RseB are believed to mediate interaction to RseA. By analysis of conserved patches on the surface of RseB (see Chapter 2.2.5.), two putative interaction sites (patch 3 and 4) were identified on the small domain (Figure 38 and also Figure 19).

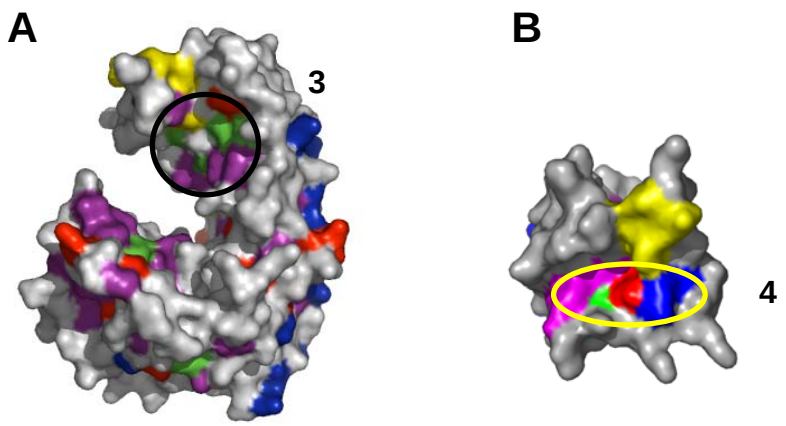

Figure 38. Potential RseA interaction sites on RseB. Patches 3 **(A)** and 4 **(B)** on RseB were identified to be potential interaction sites for RseA. Residues are colored according Figure 19; residues 245-250, which are reported to be involved in interaction to RseA, are colored in yellow (Kim et al., 2007). Patch 4 is suggested to mediate interaction to RseA.

Analysis of the position of residues 245 to 250 in the structure, revealed that this area is mostly surface exposed and in close proximity to patch 4. Patch 4 is constituted of six highly conserved residues including two charged amino acids (Trp222, Arg238, Glu250, Val265, Ile294 and Phe214) and is located on the top of the small domain forming a small groove for putative binding of the RseA helix ($RseA_{169-185}$). Binding of RseA to this region of RseB would be consistent with the suggestion that the RseA-RseB interaction is governed mainly by ionic interactions as discussed in Chapter 3.1.

3.3. Function of the Large Domain of RseB

Crystallographic studies demonstrate that the large domain of RseB (RseB-D1) is structurally remarkably similar to lipid binding proteins (see Chapter 2.2.3.2.). Two structural homologues were shown to be LolA and LolB. Both proteins are involved in the targeting process of outer membrane lipoproteins and are as RseB located in the periplasm of *E. coli*. Lipoprotein precursors are translocated by the Sec apparatus across the inner membrane (Sugai and Wu, 1992), where the attachment of the lipid moiety takes place (Sankaran and Wu, 1994). Lipoproteins, destined for the outer membrane, cross the periplasm in complex with LolA which is thought to protect the lipophilic part of the lipoprotein from the aqueous medium. LolB, a lipoprotein by itself, accepts and anchors the delivered lipoprotein into the outer membrane (Narita et al., 2004; Tokuda and Matsuyama, 2004).
Another structural homologue turned out to be LppX from *Mycobacterium tuberculosis*. LppX has a role in transporting a for this species specific lipid, phthiocerol dimycocerosate (DIM), which is important for bacterial virulence and assumed to influence the cell envelope permeability (Camacho et al., 2001; Daffe and Laneelle, 1988).

All structural homologs share a deep hydrophobic pocket that is formed by an unclosed barrel. For investigating the degree of similarity and as such the possibility for RseB-D1 to adopt similar functions, the unclosed barrels of all four proteins were examined in more detail.

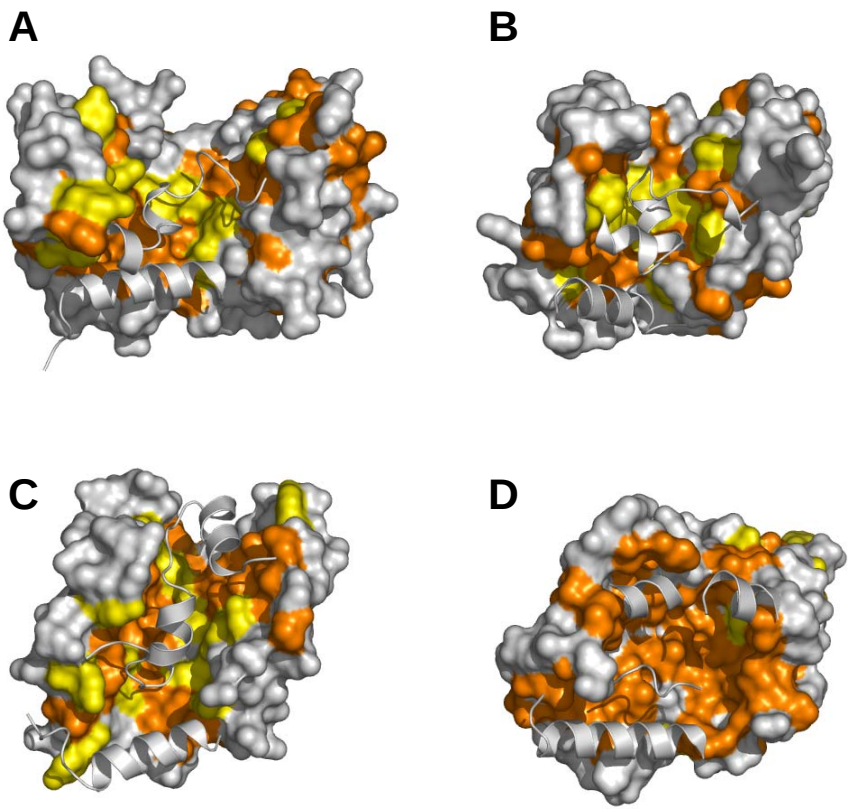

Figure 39. Hydrophobic residues lining the unclosed barrel. Pictures show surface representation of the large domain of RseB **(A)** in comparison to LolA **(B)**, LolB **(C)** and LppX **(D)** to illustrate the distribution of hydrophobic aliphatic (orange) and aromatic (yellow) residues lining the unclosed barrel. Whereas RseB, LolA and LolB comprise a mixture of hydrophobic aliphatic and aromatic residues, the barrel of LppX is equipped almost solely with non-aromatic residues. Internal loops and helices are drawn as ribbons.

As shown in Figure 39, the hydrophobic cavities of LolA, LolB and RseB are equipped with a mixture of hydrophobic, aliphatic and aromatic residues, while the barrel of LppX is – with one exception – solely composed of non-aromatic hydrophobic residues.
Although RseB-D1 and LppX share a similar topology, a DIM binding function of RseB is unlikely: (1) DIM is a lipid that is unique to *Mycobacteria* (Daffe and Laneelle, 1988) and does not exist in *E. coli*. (2) The composition of hydrophobic residues lining the unclosed barrel is different.

Both, RseB and LolA have a central accumulation of aromatic residues; most of them are structurally conserved. In contrast, the cavity of LolB is decorated with fewer aromatic residues. This has been suggested to account for LolB's higher affinity towards lipoproteins which is important for unidirectional transport (Takeda et al., 2003; Taniguchi et al., 2005).

Due to the high structural similarity of RseB-D1 and LolA, the most likely function of the large domain of RseB might be the binding of lipoproteins.

To deduce the property of RseB-D1 to accommodate lipophilic compounds, hydrophobic residues of the unclosed barrel were analyzed for their degree of conservation (Figure 40A). Within RseB homologs, seven aromatic residues are conserved, five of which were invariant in the sequence alignment (Tyr43, Tyr60, Tyr92, Tyr126 and Tyr156), and two of which were exchanged by other aromatic residues (Phe47 and Phe183) (for alignment see Figure 13C). Eleven additional aliphatic residues surrounding the barrel show conservation as well, but to a minor extent compared to the aromatic residues. Hydrophobic residues of the N-terminal helix are also well conserved and form the bottom of the putative binding site of a lipophilic ligand. This accumulation of highly conserved residues inside the RseB cavity supports a possible function of RseB-D1 in binding lipophilic compounds.

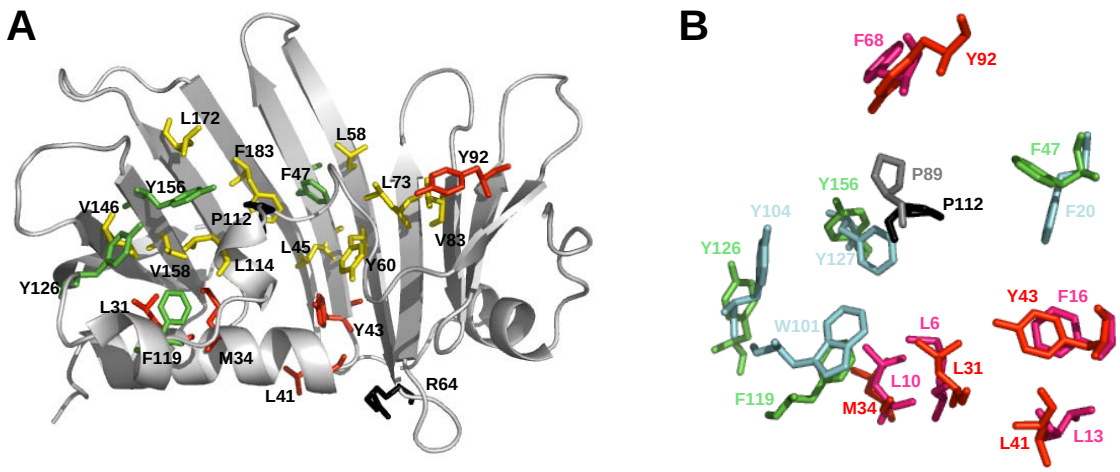

Figure 40. Hydrophobic unclosed barrel of RseB and structural comparison with LolA. Picture **(A)** illustrates the large domain of RseB forming the unclosed barrel. Hydrophobic residues that are conserved in LolA and RseB are colored in green and red, other hydrophobic residues conserved in RseB that line the cavity are shown in yellow. The hydrophobic cavity hosts a putative binding site for the tail of lipoproteins. A lid, composed of residues Gly104 to Asp118, including the two small helices α_2 and α_3, plugs this area and has to be moved upon ligand binding. The highly conserved Pro112 (depicted in black) is structurally conserved in LolA and LolB and could function as a hinge to open and close the lid. Arg64 (black) which is important for lid closing in LolA (Arg43) is indeed equally positioned in RseB but does not seem to have the same function. **(B)** Pairs of structurally conserved residues of RseB and LolA are colored in red and magenta, respectively. Residues with important functionality in LolA (cyan) are colored in green for RseB. The conserved proline is depicted in black for RseB and in grey for LolA.

To further elucidate the likeliness of RseB to have similar function as LolA, RseB-D1 and LolA were structurally compared in detail. The analysis of structurally conserved residues of LolA and RseB-D1 revealed that 9 hydrophobic residues of RseB-D1 have equivalent residues in LolA (Figure 40A and B). Moreover, four of these structurally conserved residues are important for LolA function (Phe20, Trp101, Phe127 and Tyr104 from LolA match Phe47,

Phe119, Tyr156 and Tyr126 in RseB respectively, Figure 40B). Mutation of two residues resulted in an enhanced periplasmic accumulation of LolA-lipoprotein complexes, either by increased affinity for lipoproteins or by impaired transfer to LolB (Watanabe et al., 2006). Thus, these residues seem to be directly involved in lipoprotein binding. Structural similarities are also observed for the N-terminal helix and the internal loop. (1) Three hydrophobic residues of α_1 facing the hydrophobic cavity match positions in LolA (Leu6, Leu10 and Val13 in LolA to Leu31, Met34 and Leu41 in RseB). (2) A proline of the internal loop in RseB (Pro112) is equally positioned in LolA (Pro89) (as well in LolB (Pro110) (Figure 41)). This loop, filling the unclosed barrel, was proposed to function as a lid for LolA and LolB opening and closing the binding site for lipophilic compounds. A similar function could be envisioned for the internal loop of RseB (lid RseB: Gly104-Asp118). Observed high B-factor values in this part of the protein are consistent with this hypothesis as they indicate flexibility as expected from a lid (see Chapter 2.2.2. and Figure 14C).

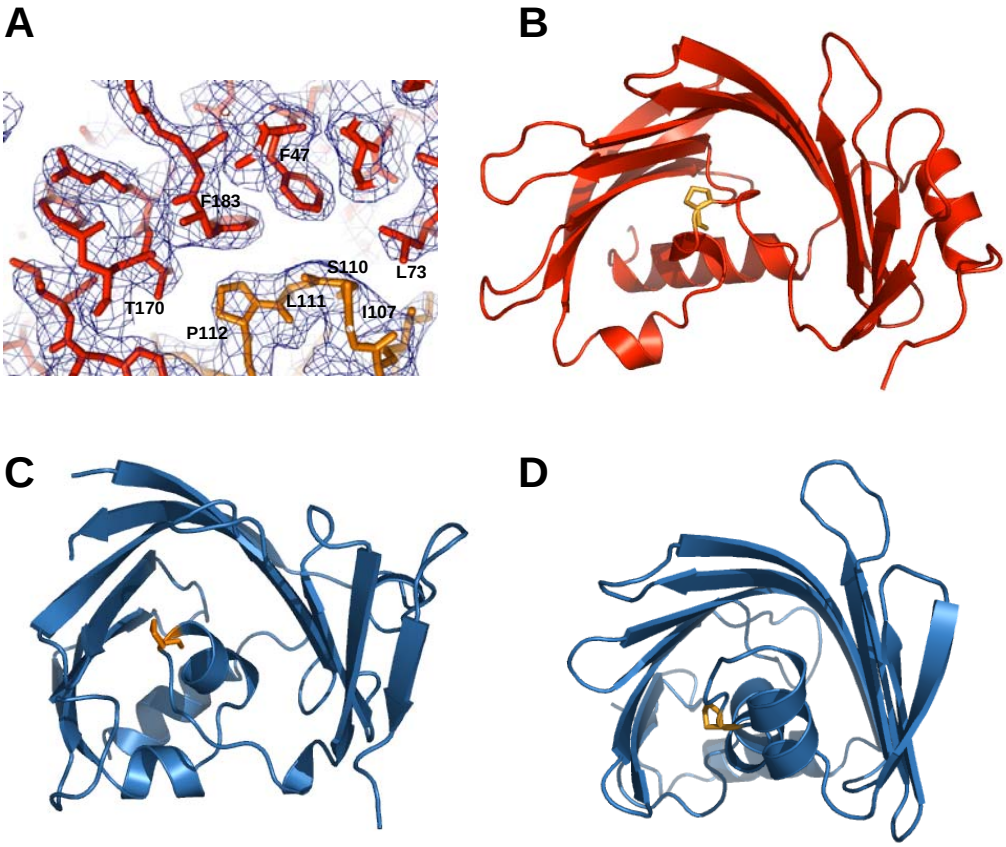

Figure 41. Electron density of the lid region and top view of RseB-D1 and its structural homologs. **(A)** Electron density of the lid region (orange), showing Pro112 and hydrophobic residues of the barrel wall. **(B)** A highly conserved proline in the internal loop is colored in orange which may function as a hinge (LolA: Pro 89 **(C)**; LolB: Pro110 **(D)**; RseB: Pro112 **(B)**).

To sum up, it seems that the large domain adopts similar properties as LolA. Thus, it is to assume that the large domain is able to bind lipophilic tails of lipoproteins. The putative binding site is highly conserved in the hydrophobic cavity as well as on the surface, which could provide an entry site for a lipoprotein (patch 2, see Chapter 2.2.5.).

3.3.1. Lipoproteins as Signals for RseB?

In the classical periplasmic stress response scenario, initiation of the signal cascade is dependent on DegS to act as a site-1 protease after being activated by unfolded OMPs. When DegS cleaves the C-terminal part of RseA (including bound RseB), RseP is enabled to function as a site-2 protease. Previous reports proposed that besides DegS, also RseB acts as a sensor for periplasmic stress. RseB is believed to either stabilize RseA or inhibit RseP by binding to RseA. In literature, it is speculated that RseB might be titrated away by an unknown signal, which results in direct RseP activation.

The fold of the large domain as an unclosed barrel suggests binding of lipophilic compounds. From our structural data, lipophilic compounds like lipids or LPS can thus not be excluded from being bound by RseB. However, structural comparisons of RseB, LolA and LolB suggest that RseB should be able to bind lipoproteins.

Lipoproteins are periplasmic proteins that have three acyl chains covalently attached to their N-terminal cysteine (Sankaran and Wu, 1994). By this, they can either be inserted in the inner or the outer membrane. Outer membrane lipoproteins that have to cross the periplasm are loaded onto LolA by the ABC transporter LolCDE located in the inner membrane (Narita et al., 2002; Yakushi et al., 2000). Complexed by LolA, ensures shielding of the lipoproteins' acyl chains from the aqueous surrounding. LolA delivers the lipoprotein to LolB that is involved in the insertion process of the lipoproteins into the outer membrane (Matsuyama et al., 1997; Taniguchi et al., 2005).

In a stressful situation, the envelope suffers from the unfavorable environment. This can affect the membrane integrity and can cause any protein to aggregate and to turn nonfunctional. If periplasmic stress affects a part of the lipoprotein targeting mechanism, the pathway might be ineffective or disabled. This or damaged membrane integrity could result in accumulation of mistargeted outer membrane lipoproteins to the inner membrane or the periplasmic space.

Lpp, also known as the Braun's lipoprotein, with approximately 7.5 x 10^5 per cell is one of the most abundant proteins of *E. coli* (Braun et al., 1970; Inouye et al., 1972). It is essential for fixation of the mureinsacculus to the outer membrane by a covalent linkage which confers enhanced rigidity to the bacterial cell wall (Braun and Rehn, 1969; Yakushi et al., 1997). A mislocation to the inner membrane was reported to be lethal for the cell as the murein sacculus was shown to be covalently misattached to the inner membrane (Yakushi et al., 1997). Therefore, the periplasmic stress response would gain functionality when besides being sensitive for misfolded OMPs (*via* DegS as a sensor), mislocation of the most abundant lipoprotein could be sensed as well (*via* RseB as a sensor). As OMPs do, also mislocalized lipoproteins could indicate the existence of stress in the envelope.

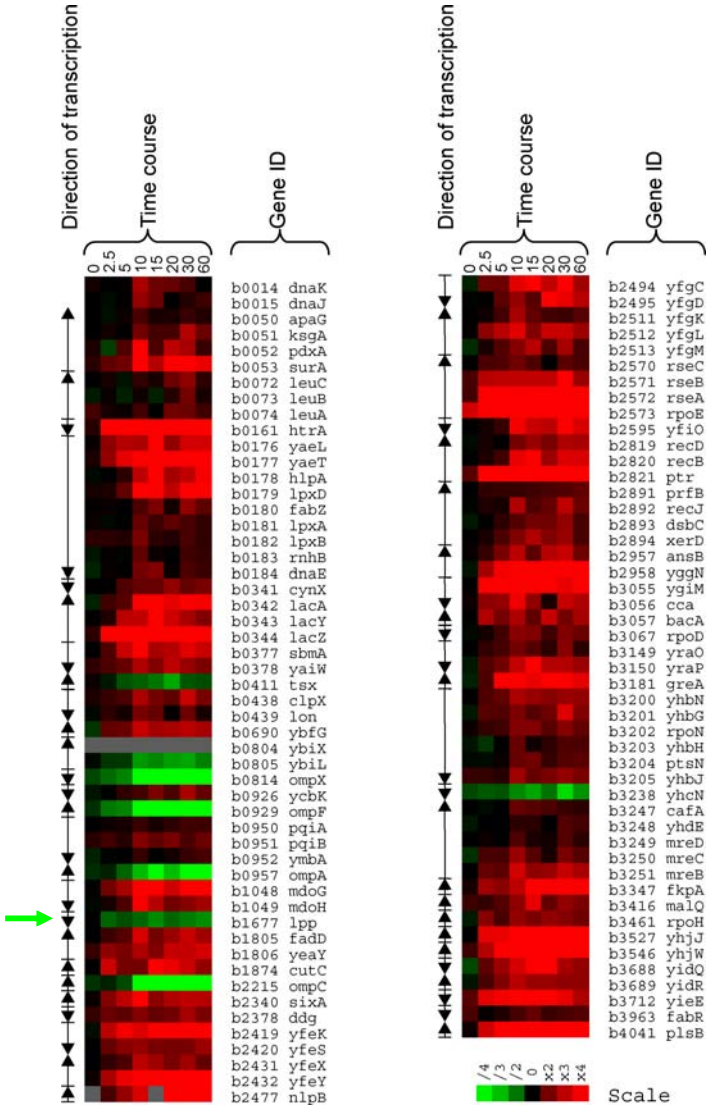

Figure 42. Expression profile of σ^E regulated genes. σ^E regulated genes identified in comparing *rpoE* overexpressed versus wild-type transcription. Red denotes induced; green denotes repressed genes. Only eight genes were shown to be repressed by σ^E, including the gene coding for the most abundant lipoprotein Lpp, marked by a green arrow (illustration modified from Rhodius et al., 2006).

Recently, the expression profile of members of the σ^E regulon was analyzed and 100 genes were reported to be regulated by σ^E (Rhodius et al., 2006). Whereas the transcription of all genes belonging to this regulon was found to be induced by σ^E, only eight genes were found to be repressed (Figure 42). These eight genes include *tsx* and four *omp* genes that encode the most prominent β-barrel proteins of the outer membrane, as well as *lpp* encoding the most abundant lipoprotein in *E. coli*. One protein family (OMPs) acts as an activation signal for DegS when not properly folded. Thus, down-regulation of *omp* genes prevents from further accumulation of unassembled OMPs (Johansen et al., 2006; Rhodius et al., 2006). The transcription of *lpp* might be down-regulated for similar reasons. Under stressful conditions, Lpp is presumably not properly inserted into the outer membrane and accumulates in the periplasm and thereby could be sensed by RseB. Mislocalization of Lpp could be a result of damaged membrane integrity or of defective targeting *via* LolB and LolA. In contrast to small lipophilic compounds, lipoproteins should not be able to form a micellar-like state if unassembled and should expose their lipophilic tails to the environment.
Moreover, six liproteins (YfiO, NlpB, YraP, YgfL, YeaY and YfeY) are part of the σ^E regulon and upregulated when σ^E is activated upon stress (Onufryk et al., 2005). Three of them (YfiO, NlpB and YfgL) are involved in the assembly of OMPs and therefore required for restoring the outer membrane integrity (Malinverni et al., 2006). As under stressful situations these six lipoproteins seem to be needed, the shutdown of Lpp enables the Lol proteins to focus on the targeting of the lipoproteins demanded.

3.3.2. Model for RseB Binding to RseA and Lipoprotein

The structure of RseB revealed that the interface of the large and the small domain is composed of highly conserved residues. Most striking is a loop (β_{14}-β_{15}) from the small domain that consists of four invariant residues (see Chapter 2.2.4.). To draw conclusions about the function of this loop, the interface was inspected in detail. The loop is in very close proximity to the internal loop (lid) of the large domain. In fact, an interaction was observed between Thr117, located on the lid of RseB-D1 and the highly conserved loop of RseB-D2. It seems as this loop is positioned to push the lid (with α_2 and α_3) into the unclosed barrel, occupying the potential binding site (Figure 43). Arg43, essential for fixing the lid in LolA (Taniguchi et al., 2005), is conserved in RseB (Arg64, located in RseB-D1); however, not

involved in crucial contacts. It can be deduced that lid fixation in RseB is rather mediated by the invariant loop of RseB-D2 than by Arg64.

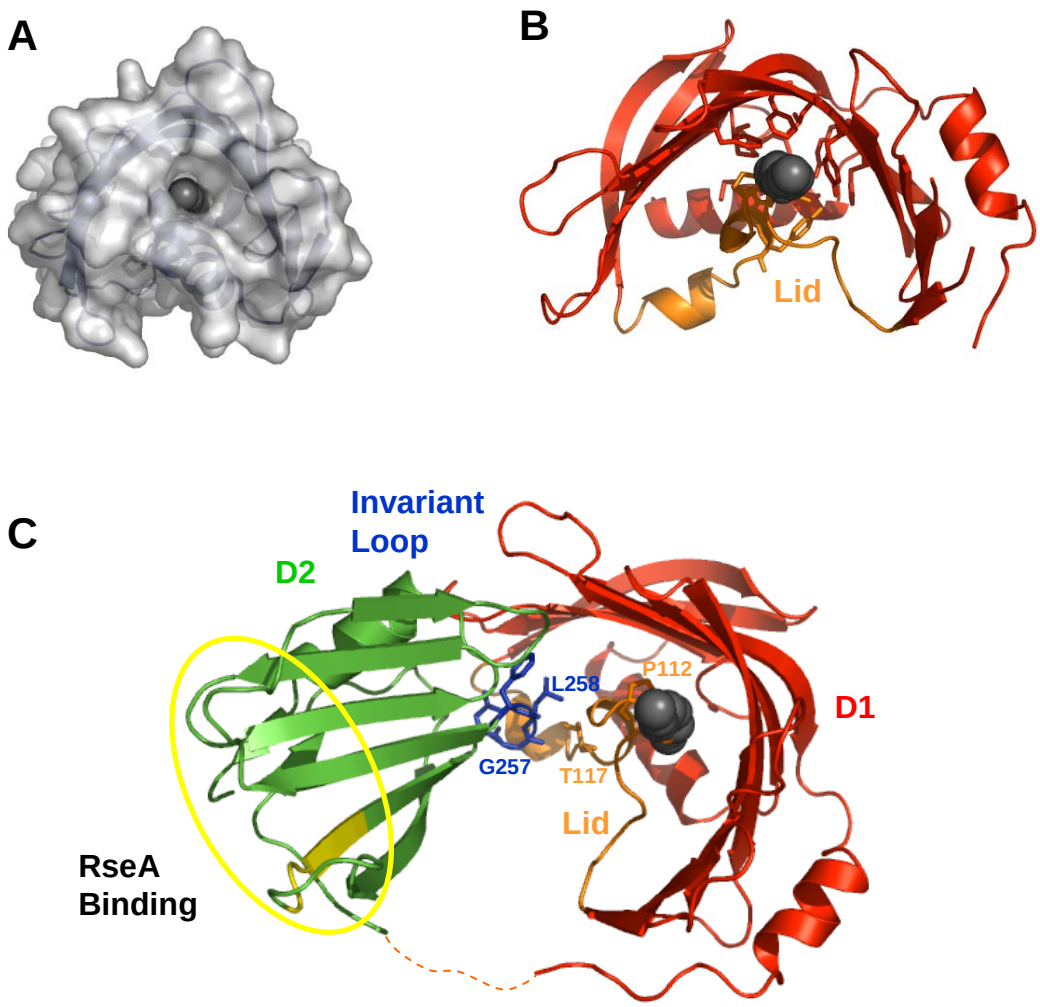

Figure 43. Superposition of LolB ligand onto RseB-D1 and model of signal binding and transduction. (A) LolB, a structural homolog of RseB, crystallized with PEGMME2000 (dark grey spheres) which could mimic an acyl chain of a lipoprotein (Takeda et al., 2003). **(B)** PEGMME2000 from LolB was superposed on the RseB structure and clashes with the lid including Pro112, colored in orange. This indicates that binding of a putative lipophilic compound, causes a movement of the lid. **(C)** The interface links the two domains RseB-D1 and RseB-D2. It links a binding event on the large domain (RseB-D1, red) *via* the highly conserved loop (blue) to the small domain (RseB-D2, green). This could result in a diminished affinity for RseA in RseB-D2 (RseA binding region indicated in yellow) and could promote σ^E activation

As mentioned above, the lid of RseB shares the conserved proline with the Lol proteins (Figure 41). One of the structural homologs of RseB, LolB, was crystallized in complex with PEGMME2000 (Figure 43) (Takeda et al., 2003). This compound was found bound inside the hydrophobic cavity of the protein and the authors suggested that PEGMME2000 could mimic an acyl chain of a lipoprotein. When superposing the ligand onto the structure of RseB-D1, it matches the hydrophobic cavity of RseB, but clashes with the lid including the conserved proline (Figure 43).

Besides well documented cis-trans isomerization of prolines (Dugave and Demange, 2003) as rate-limiting steps during protein folding (Brandts et al., 1975), other functions are assigned to prolines residues as well. For example, the neurotransmitter-gated ion channel (5-HT3) is suggested to open its pore upon ligand binding by a cis-trans isomerization of a highly conserved proline, which links ligand binding on one domain to conformational rearrangements in the other domain (Lummis, 2005).

Structural data of RseB suggest that only a minimal rearrangement of the lid releases steric restriction from the putative binding site of a lipophilic compound. A key residue in such a conformational change might be the proline, acting as a hinge to open and close the lid. Binding of a ligand to RseB-D1 could thus cause a structural rearrangement of the lid which is subsequently transduced to RseB-D2 by the invariant loop. This could in turn trigger a structural change in RseB-D2 which releases interaction of RseA and RseB-D2. This would be in accordance with the proposed function of RseB, which is the withdrawal from RseA by stress signals.

These findings lead to a hypothetic model of RseB sensing function, abstracted in Figure 44A and B.

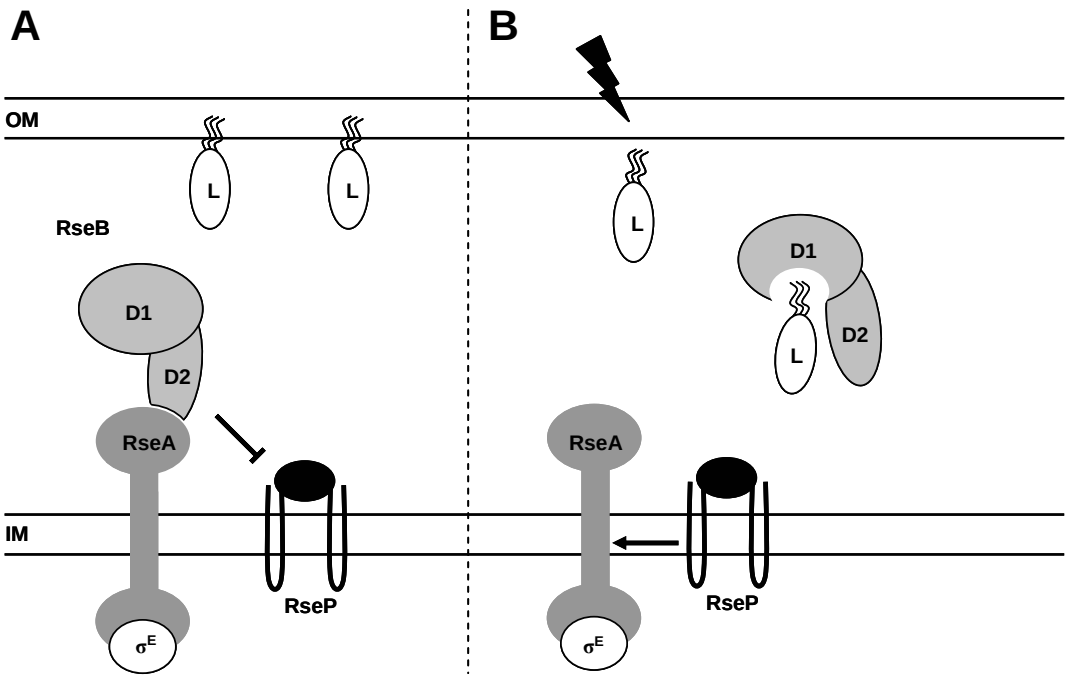

Figure 44. Model of RseB function. (A) RseB binds RseA by its small domain, thereby shielding RseA from being degraded by RseP. **(B)** In the presence of stress that affects the outer membrane integrity, mislocalized outer membrane lipoproteins (L) accumulate in the periplasm and are sensed by the large domain of RseB. Binding of lipoproteins triggers a conformational change in the large domain (RseB-D1) that is transduced by the interface of the two domains to the small RseA-binding domain RseB-D2. By this RseB-RseA interaction is diminished and allows RseA degradation by RseP. Finally σ^E is activated to induce genes that regenerate the integrity of the outer membrane and reduce the transcription of the most abundant outer membrane proteins to prevent further build up of already damaged compounds (OM: outer membrane; IM: inner membrane).

3.4. Oligomeric Forms of RseB

In biochemical experiments including size exclusion chromatography, cross-linking, analytical ultracentrifugation (AUC) and small angle X-ray scattering (SAXS), RseB was determined to exist in different oligomeric forms. In gel filtration experiments RseB eluted in two separated peaks with apparent molecular weights of 65 and ~220 kDa (Chapter 2.3.1.). AUC data similarly revealed the co-existence of RseB dimer and higher oligomer. This equilibrium was shown to be dependent on the concentration of the protein (Chapter 2.3.1.1.). In SAXS experiments the experimental curve of RseB solution revealed to be different from theoretical electron pair distributions of oligomers found in the crystal (Chapter 2.3.1.2.). Preliminary fitting of the functions suggests that RseB in solution contains a mixture of different oligomeric forms, including dimeric, hexameric and octameric assemblies. In the crystal lattice hexameric and octameric rings were observed that can be constituted by three different forms of interfaces (Chapter 2.2.6.). Furthermore electron micrographs clearly visualized the existence of ring-like assemblies similar to those observed in the crystal lattices (Chapter 2.3.1.3.).

To sum up, in contrast to previous reports that suggested RseB to be monomeric (Missiakas et al., 1997), none of our experiments revealed RseB to be monomeric. It is rather to suggest that RseB is able to exist in dimeric and higher oligomeric assemblies.

3.4.1. Possible Role of the RseB Dimers

Data presented above demonstrated the existence of RseB dimers in solution. Furthermore, binding studies with the periplasmic domain of RseA revealed that the dimeric form of RseB, but not the higher oligomeric forms, interacts with RseA (Chapter 2.3.2.2.). This agrees with data, published recently (Cezairliyan and Sauer, 2007). Thus, dimeric RseB seems to be the active form binding the anti-sigma factor, which raises the question how such a dimeric assembly of RseB capable to bind RseA could look like. Three dimeric interfaces (close, open, semi-close; Chapter 2.2.6.2.) were found in the structure.

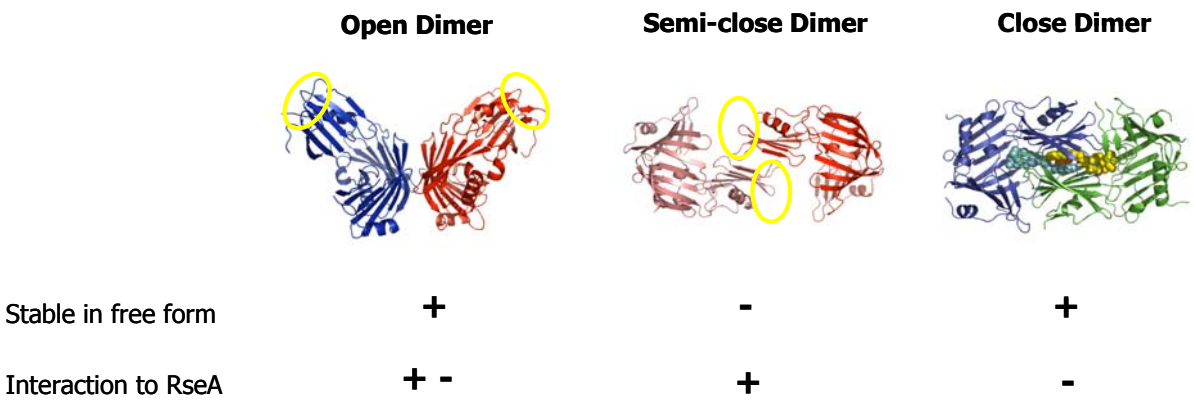

Figure 45. Overview of possible dimeric assemblies of RseB. Three dimeric assemblies of RseB were observed in the crystal lattice. The open and the close dimer are assumed to be stable in free form, whereas a dimer assembled by the semi-closed contact is very unlikely to exist in free form. The putative RseA-binding region is marked by a yellow circle. In the close dimer the RseA-binding region is not accessible, whereas it is accessible in the open and the semi-close dimer. Conclusions from cross-linking experiments suggest that the semi-close contact could be stabilized upon RseA-binding. The close dimer is able to enclose two detergent molecules.

The open contact is the only dimer that can be used to construct both crystal lattices. This dimeric assembly is stabilized by a conserved interface of medium size and involves mainly the same residues in both crystal lattice forms. It is mediated only by residues from the large domain. In gel filtration and cross-linking analysis of isolated large domains this domain was shown to build up multiple oligomers (Chapter 2.3.3.2.). This suggested that the open dimer has the propensity to exist in solution.

To elucidate the ability of the open dimer to interact with RseA, structural and biochemical data were evaluated. Cross-linking experiments revealed that RseB-only dimers were totally missing in the presence of RseA (see Chapter 2.3.2.2.). If the open dimer would be the dimer to interact with RseA, at least some cross-linked RseB dimers should have been formed in this experiment. Furthermore, cross-linked products were observed with molecular weights corresponding to one RseB in complex with two RseA. If RseA binds to the top portion of the small domain of RseB (as concluded in Chapter 3.2) it is not possible to form a specific cross-link with these stoichiometries. This suggests that although the open dimer should be stable in solution and even when it is the most abundant dimer found in the crystals, it is unlikely that it represents the RseA interacting conformation (Figure 45).

The semi-closed contact is only present in one crystal form and totally missing in the other. The interface is of very small size and only stabilized by 4 hydrogen bonds. These observations imply that the semi-closed dimer is not favored in solution.

However, this dimer could gain stability when bound to RseA. Indeed, the Kim group postulates that the RseA-helix is bound in a groove formed between the small domain of one

RseB and the large domain of the other RseB in the semi-closed dimer (Figure 45) (Kim et al., 2007). These clefts seem to be large enough to each accommodate one helix of 16 Å widths representing the conserved RseA helix. This arrangement would be consistent with cross-linking studies (Chapter 2.3.2.2.). Here, the interaction between the RseB dimer is very small which probably didn't result in formation of cross-linked products. Furthermore, cross-links of RseB/2 RseA as well as 2 RseB/RseA are possible.
Nevertheless, such an interaction would only be in accordance with biochemical results, if the interaction to RseA is mainly stabilized by the small domain of RseB as only the small domain was observed to directly interact with RseA. Additionally it has to be mentioned, that the interface of the semi-closed dimer is not well conserved.

The third interface observed in the structure is the closed contact which is mediated mainly by residues of the small domain and some residues of the large domain. It was shown to be of flexible nature, as the number of residues, involved in stabilizing the contact, was highly variable in both crystal forms (see Chapter 2.2.6.2.). This was observed to be the result varying angles of inclination of the large and the small domains (see Chapter 2.2.2.). The small domains of crystal from II ($C222_1$) were shown to be less tilted than in crystal form I ($P42_12$) monomers, leading to an increased interdomain distance of the small domains in the close contacts. This flexible character could enable the closed dimer to accommodate ligands.
In fact the close dimer was found to bury a large hydrophobic interface, able to bind two detergent molecules like dodecyl maltoside (crystal form III, $C222_1$, see Chapter 2.2.6.3.). Similar results were obtained from the Kim group, as they crystallized RseB in the presence of octyl glycoside (OG) (Kim et al., 2007), with one molecule of OG bound in the interface between the close dimer at similar position as observed for DDM. Both closed dimers including detergent molecules can be overlaid with an RMSD of 0.69 Å, suggesting these structures to be very similar (Figure 46A). As RseB was independently crystallized twice with detergent molecules, it is to speculate that the observed enclosure of detergent molecules (Figure 46B) might represent a binding site for hydrophobic substances.
Although the bond-forming residues of the closed contact are less conserved than observed for the open contact, the buried area comprises conserved hydrophobic residues (patch 3, Figure 19B), that could be the main determinants in mediating this dimeric interaction. However, as indicated from cross-linking studies of isolated small domains, the small domain alone seems to be impaired to multimerize. Thus, a stable close contact demands the large domain and/or an additional compound like hydrophobic detergents.

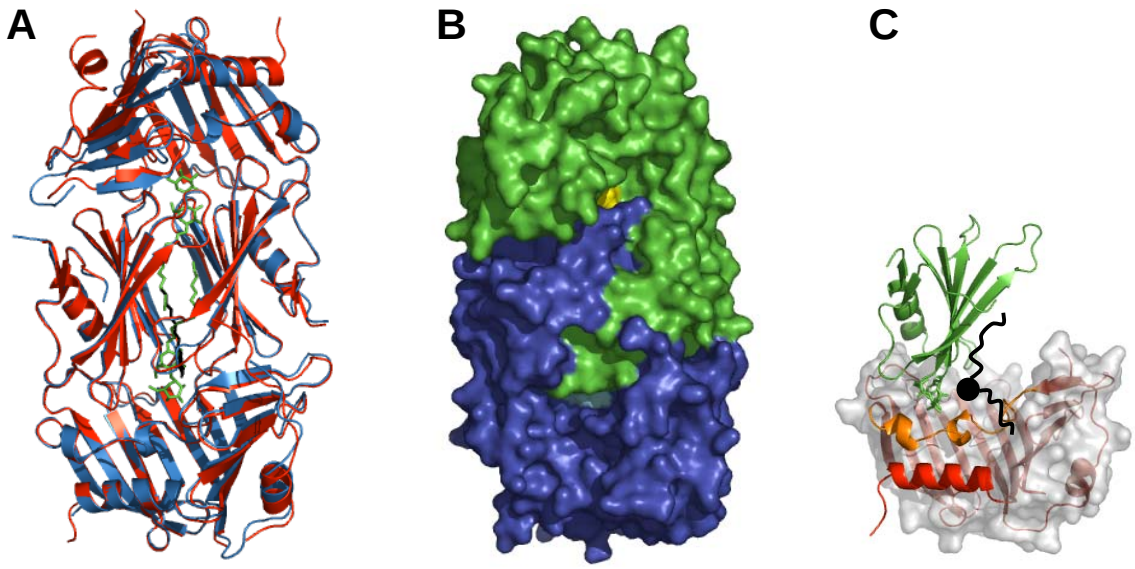

Figure 46. Binding of detergents to close RseB dimer and supposed binding mode of lipoprotein's acyl chains. (A) Superposition of two RseB structures ($RseB_{DDM}$ red, $RseB_{Kim}$ blue) crystallized with detergents OG (black) (Kim et al., 2007) and DDM (green) (RMSD 0.67 Å). **(B)** Surface representation of the RseB close dimer (monomer B in blue and C in green) completely encloses bound hydrophobic compounds (DDM). **(C)** Two binding sites for lipophilic compounds (indicated in black) are proposed. One binding site resides in the hydrophobic unclosed barrel of the large domain and the second could be formed by the small domains upon dimerization of two RseB molecules in the close type.

Hence, the addition of detergents or lipids, which are chemically similar, could be the driving force to shift the equilibrium to close dimers. These conclusions are in contrast to what was expected from the analysis of the large domain of RseB which was supposed to bind lipophilic ligands.

However, when considering that lipoproteins have three acyl chains, RseB with two putative binding sites for hydrophobic compounds would be a very potent binder of mislocalized lipoproteins. RseB could then accommodate acyl chains in the large domain and as well as in the interface of the small domains of the close dimer, as abstracted in Figure 46C.

To sum up, all dimeric forms might be of physiological interest. For unbound RseB, the open dimer is favored, as its contacts are conserved in both crystal lattices and its stabilization is mediated by many contacts of conserved residues. The semi-closed contact could be stabilized upon interaction with RseA. Although the interface is not well conserved this model fits best to our biochemical data. The close dimer could preferably exist in a ligand bound

state as this conformation allows embedment of further acyl chains in the interface of the small domains.

Keeping in mind that the crystal did not contain any RseA, the RseB dimer interacting with RseA could be different from those dimeric forms observed in the crystal. For a clear determination of dimeric assemblies of RseB, mutational studies are a promising task in the near future.

3.4.2. Possible Role of the Large Oligomeric Forms of RseB

Data imply that RseB is able to form large oligomers. This is in full agreement with results obtained from Cezairliyan and Sauer (2007), where RseB was also found to elute in two peaks in size exclusion chromatography. However, results from the Kim group are not consistent, as RseB is reported to only exist as a dimer, although the same type of column was used (Kim et al., 2007).

Several attempts were done to analyze the hexameric and octameric rings observed in the structure for likeliness to occur in solution. However, it was difficult to clearly distinguish whether both or only one of them occurs in solution. A summary of observed large oligomeric forms and their characteristics is given in Table 4.

Table 4. Characteristics and experimental data of RseB hexamers and octamers.

	Hexamer	Octamer	Experimental Data
MW (kDa)	205	270	
Symmetry	2-fold	4-fold	
overall dimensions (Å)	125 x 108	145 x 150	
pore diameter (Å)	38	53	
SAXS maximal overall dimension (Å)		+	145
EM approximate diameter (Å)	+	+	126-146
EM pore diameter (Å)	+		30-40
Gel filtration peak I (kDa)	±	±	220

SAXS analysis revealed that oligomeric forms with a maximal diameter similar to octameric assemblies are existent in solution (Chapter 2.3.1.2.). These data are consistent with SAXS data published recently (Kim et al., 2007). Comparing distance distribution functions of RseB

from experimental data, clearly reveal, that RseB behaved similar in both experiments (Figure 47A and B). The only difference in data is that the maximal diameter from the Kim experiment is ~ 25 Å larger. However, the authors propose that the semi-close dimer is the most probable oligomeric from to exist in solution, as they state, that its calculated function is most similar to experimental function (Figure 47B). This is in contrast to observations that octameric and hexameric functions mostly agree with experimental curve progression (Figure 47A).

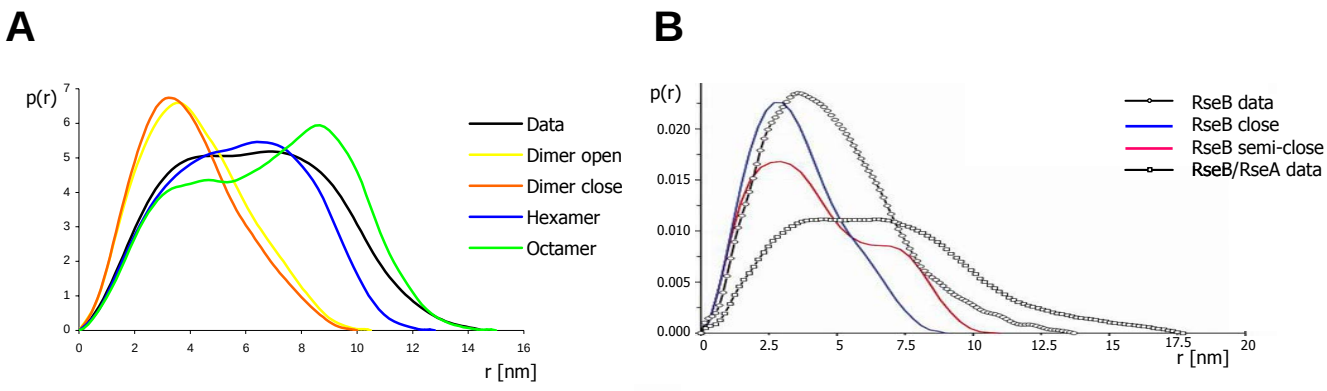

Figure 47. Comparison of SAXS data. (A) Illustration of distance distribution functions of RseB. **(B)** Distance distribution functions of RseB and RseB/RseA (modified from Kim et al., 2007).

Interestingly, experimental electron pair distribution of RseB/RseA complexes reported by Kim resembles the theoretical dimeric distributions (Kim et al., 2007). This is in agreement with the finding that RseA only interacts with dimeric RseB (Chapter 2.3.2.2.).

Electron micrographs clearly demonstrated the existence of ring-like structures (see Chapter 2.3.1.3.). Thus, the higher oligomers observed are likely to be ring-like structures of hexameric or octameric nature similar those seen in the crystal lattice. Approximate size estimation of the ring-like structures in EM micrographs resulted in dimensions fitting both the hexameric and the octameric dimensions (see Table 4). However, the observed pore diameter better suits the pore diameter of the hexamer. A clear determination of the nature of the oligomeric rings awaits EM image averaging or calculation of *ab initio* models of SAXS data from monodisperse solutions which could not be done yet.

Ring-like assemblies are commonly observed for multi-homo-oligomeric proteins (e.g. AAA-proteases (reviewed by Vale, 2000)). The clear visualization of ring-like structures in both

electron micrographs and the crystal lattice is unlikely to be a coincidence. Hence, it is reasonable to assume, that the ring-like assemblies of RseB are not an artifact. The only experiment not supporting this idea is the missing detection of hexameric or octameric cross-links, which could have been an effect of the resolution limit of the gel.
Moreover it is unclear whether both the hexameric and the octameric rings coexist at all. In size exclusion experiments only two peaks – one peak containing dimeric, the other higher oligomeric specimen – were detectable. Similarly AUC experiments just gave two oligomeric specimens. Therefore, it has to be asked if both of the large oligomeric assemblies or only one of them is existent.

Biochemical experiments could demonstrate that the higher oligomeric states are RseB conformations that do not bind to RseA. Therefore hexamers or octamers might represent free RseB or RseB bound to other compounds. The hexamer was shown, as stated above, to be able to enclose in its closed contact hydrophobic ligands, and might thereby be stabilized. Therefore, it is possible that the hexameric state is favored when lipophilic compounds are bound.
The octamer is stabilized by open and closed contacts. Here, the closed contact seems to be more compact which could render the octamer to be a stable form in solution. Like the hexamer, also the octamer was not shown to interact with RseA-PP. As the closed contact of crystal form I is more compact, it is unlikely to represent a lipoprotein bound form and it its tempting to speculate that it represents the completely unbound form. Therefore, a role for the octameric state could be to prevent RseB interaction with lipophilic ligands in an RseA-unbound state by hiding all potential binding-sites.

All experiments performed to explore oligomeric states of RseB were done in the absence of additional molecules. In AUC it was shown that the number of higher oligomeric form increases with enhanced protein concentration. The association constant was estimated to be 9.6 µM (Chapter 2.3.1.2.). Recent suggestion that the higher oligomeric states of RseB are a result of protein aging could be shown to be incorrect (Cezairliyan and Sauer, 2007), as higher oligomerization occurred at a critical protein concentration and is thus rather a function of the protein concentration.
The intracellular concentration of RseB is believed to be rather low. As all experiments were performed at higher concentrations one should consider whether the higher oligomeric forms are of physiological relevance. However, it is known that the special character of the bacterial periplasm can lead to the formation of microenvironments due to highly decreased protein mobility (Brass et al., 1986). As a result, a spatial restricted area could contain higher

RseB concentration in some cases. E.g. when DegS cleaves off the domain of RseA with bound RseB, an enhanced free pool of RseB could be generated; which similarly can be envisioned during expression of RseB.

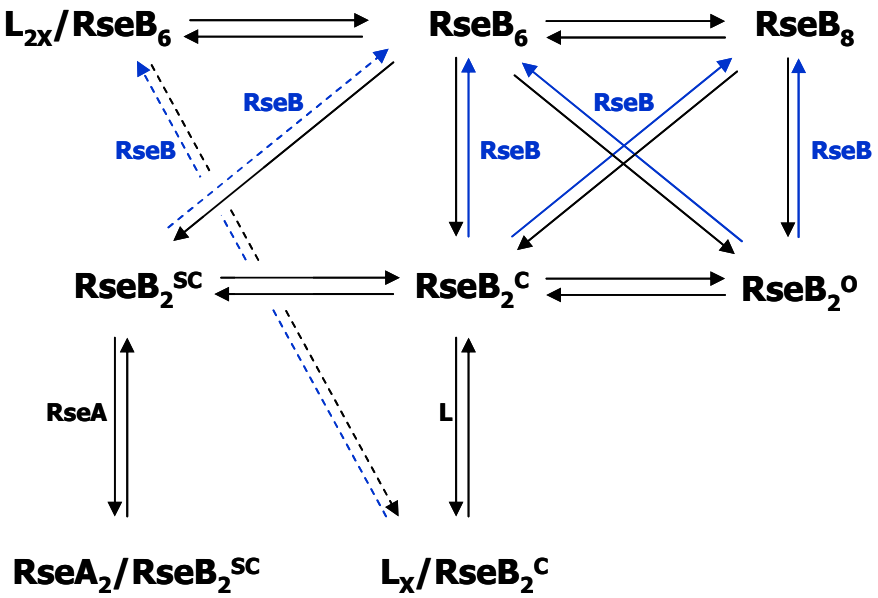

Figure 48. Model for oligomeric states of RseB. A possible equilibrium state is shown which is influenced by binding partners of RseB to shift the equilibrium towards favored conformations. This equilibrium is suggested to be changed by high concentrations of RseB (indicated in blue) favoring larger oligomeric assemblies (hexamers: $RseB_6$ and octamers $RseB_8$). The open dimer of RseB ($RseB_2^O$), as well as the octamer ($RseB_8$) are likely to be stable in unbound form. The closed form of RseB ($RseB_2^C$) is presumably favored by lipoproteins, binding to the large domain as well as to the interface of two small domains. This could also lead to a stabilization of the hexameric state ($L_{2x}/RseB_6$). The semi-closed dimer ($RseB_2^{SC}$) is unlikely to be stable in free form, but could be stabilized by binding to two RseA.

In Figure 48, a model for the interplay of all potential oligomeric states of RseB is abstracted. Various oligomeric states might exist in solution. The relative distributions is changed and influenced by the concentration of binding partners like RseA and lipoproteins.

For a clear evaluation of the function of the oligomers, analysis of oligomeric distribution in the presence or absence of RseA and/or lipophilic compounds is a challenging project.

4. Summary

An elegant network of signal transduction has evolved in the bacterial cell envelope to respond to environmental stress. The σ^E stress response pathway is initiated by sensing unfavourable and harmful changes in the periplasm. The stress signal is transmitted by a controlled three-step proteolysis (DegS – RseP – ClpXP) of the transmembrane anti-sigma factor RseA that leads to the activation of the alternative sigma factor σ^E. The periplasmic protein RseB exerts a crucial role in modulating the stability of RseA. It is speculated that an unknown signal titrates RseB away from RseA, leading to activation of σ^E.

RseB from *Escherichia coli* has been crystallized and crystal structures were determined at 2.4 Å and at 2.8 Å resolution. The structure of cytoplasmic expressed RseB revealed that it consists of two domains; an N-terminal large and a C-terminal small domain. The large domain resembles an unclosed β-barrel that is structurally remarkably similar to a protein family (LolA, LolB) capable of binding the lipid anchor of lipoproteins. Detailed structural comparison of RseB and LolA led to the hypothesis that RseB might be a sensor for mislocalized lipoproteins. The small C-terminal domain, connected to the large domain by a partially unstructured loop, was identified to mediate interaction with RseA. A peptide comprised of a putative helix of RseA was shown to constitute the binding site for RseB.

Structural investigations showed that the interface of the large and the small domain is stabilized by highly conserved residues. This interface is proposed to have a role in linking a signal-binding event in the large domain to the small domain, which subsequently destabilizes RseA interaction with RseB, hence making RseA prone for degradation.

Several experiments determined that RseB exists as a dimer and as higher oligomers (hexameric or octameric ring-like assemblies) in solution. The equilibrium of oligomers was shown to be dependent on the protein concentration. Biochemical data revealed that RseA interacts only with dimeric RseB, suggesting dimeric RseB to be the active conformation. As the crystal structure provided different modes of dimeric assemblies (*via* open, close, semi-close interfaces), biochemical data in combination with structural data were explored for putative functions of the observed dimers. The most abundant open dimer is suggested to be stable in solution, whereas the close and semi-close dimers may be favoured in the presence of lipoproteins and RseA, respectively. The precise role of the hexameric and

octameric rings, unable to interact with RseA, is not clearly understood but will be a challenging task for further evaluation.

Structure based results presented in this thesis indicate a new role of RseB in acting as a sensor for periplasmic stress: it detects mislocalized lipoproteins in the periplasm and propagates the signal to induce σ^E-response.

5. Materials and Methods

5.1. Material

5.1.1. Bacterial Strains

For all cloning and plasmid maintenance purposes, *Escherichia coli* strain DH5α (Gibco BRL) was used. For high level expression of protein, BL21(DE3) (Stratagene), BL21-gold(DE3) (Stratagene) or BL21-star(DE3) (Invitrogen) was used.

DH5α (Gibco BRL)
F^-, endA1, glnV44, thi-1, recA1, gyrA96, deoR, nupG, Φ80dlacZΔM15, Δ(lacZYA-argF)U169, hsdR17(rK^-, mK^+), λ^-

BL21(DE3) (Stratagene)
F^-, ompT, hsdSB(rB^- mB^-), dcm^+, galλ(DE3)

BL21-gold(DE3) (Stratagene)
F^-, ompT, hsdSB(rB^- mB^-), dcm^+, galλ(DE3) Tet^r endA Hte

BL21-star(DE3) (Invitrogen) one shot chemical competent cells
F^-, ompT, hsdSB(rB^- mB^-) gal dcm rne131 (DE3)

5.1.2. Chemicals

Table 5. Chemicals.

Chemical	Distributor
Acryl amide	Biorad
Protogel	National Diagnostics
Agarose	Seakem
Bromphenyl blue	Serva
Coomassie Brilliant Blue R-250	Serva

IPTG	Gerbu
Gel filtration Calibration Kit LWM	Amersham Biosciences
Sodium dodecylsulfate	Carl Roth GmbH
Polyethyleneglycol 3350	Fluka
Molecular Weight Standard M6	Pharmacia
Prestained Molecular Weight Marker	New England Biolabs
PageRuler unstained Protein ladder	Fermentas
Ni-NTA Nickel Chelating Material	Amersham Biosciences
Ni-NTA superflow	Qiagen
Ethidium bromide	Boehringer
Deoxyribonuceotides (dNTPs)	Pharamcia
DNA-Ladder	New England Biolabs
Glutaraldehyde	Sigma
ABI BigDye 3.1	Applied Biosystems
PCR Mastermix	Roche

5.1.3. Enzymes and Proteins

Table 6. Enzymes and Proteins.

Name	Distributor
Pfu DNA polymerase	Promega
Expand™ polymerase	Boehringer
Taq polymerase	Promega
DNA ligase (T4)	New England Biolabs
Restriction Enzymes	New England Biolabs
Ribonuclease A	Sigma
Shrimp alkaline phosphatase (SAP)	Roche
Antarctic phosphatase	New England Biolabs
Factor Xa	Qiagen

5.1.4. Plasmids

Table 7. Plasmids.

Name	Resistence	Origin/Remark
pET22b	Amp^R	Novagen Expression of C-terminally His_6-tagged proteins
pET16b	Amp^R	Novagen Expression of N-terminally His_{10}-tagged proteins, tag cleavable with Factor Xa protease
pET15b	Amp^R	Novagen Expression of N-terminally His_6-tagged proteins, tag cleavable with thrombin protease
pET22-rseb	Amp^R	*RSEB* gene amplified from genomic DNA of *E. coli* was cloned *via* NdeI/XhoI sites (M. Grininger, unpublished)
pET22-rsea	Amp^R	*RSEA* gene amplified from genomic DNA of *E. coli* was cloned *via* NdeI/XhoI sites (M. Grininger, unpublished)
pET22-rseb-ss	Amp^R	this work Cloned from pET22-rseb using primers *rseB-SS* and *rseB-CT*. PCR product was digested with NdeI and XhoI and ligated into pET22b
pET15-rseb-d1	Amp^R	this work Cloned from pET22-rseb-ss using primers *rseB-SS* and *rseB-D1rev*. PCR product was digested with NdeI and XhoI and ligated into pET15b
pET15-rseb-d2	Amp^R	this work Cloned from pET22-rseb-ss using primers *rseB-D2forw* and *rseB-CT*. PCR product was digested with NdeI and XhoI and ligated into pET15b
pET16-rsea-PP	Amp^R	this work Cloned from pET22-rseb using primers *rseA-PPforw* and *rseA-PPrev*. PCR product was digested with NdeI and XhoI and ligated into pET16b

5.1.5. Oligonucleotides

All oligonucleotides were purchased from Metabion, purification grade 'desalted'.

rseB-SS	GCG CGC ATA TGG CCA CTC CCG CGT CCG
rseB-CT	CGC GGC CAC GAG TCA TTG CGC TGC CCC GAA C
rseB-D1rev	CGC GCC TCG CGT CAA ACA GAA AGC AAC GGC GGC AA
rseB-D2forw	GCG CGC ATA TGG AAA AAG CTA AAT TCA GCT GGA CGC
rseA-PPforw	GCG CGC ATA TGT CTG AAA CGT CCC AGC AGC CC
rseA-PPrev	CGC GCC TCG AGT TAC TGC GAT TGC GTT CCT AAA GTT TGA ATT C

5.1.6. Instruments and Devices

5.1.6.1. Centrifuges

Eppendorf Centrifuge 5417R with rotor F 45-30-11; Beckman Avanti J-25 centrifuge with rotor JA-25.50; Beckman Avanti J-20XP centrifuge with rotors JA-25.50 and JLA-8.1000; Sigma 4K15 swing-out rotor; Hettich Rotixa/KS centrifuge with rotor 5094-684 and Beckman Optima LE-80K ultracentrifuge with rotors 45Ti and 60Ti.

5.1.6.2. Devices for X-ray Data Collection

X-ray structural data were recorded at the Swiss Light Source (SLS, Zürich) and at the European Synchrotron Radiation Facility (ESRF, Grenoble).

5.1.6.3. Software

All figures illustrating structural work were prepared with PYMOL (www.pymol.org). Other figures were created in Corel Draw or Power Point. Protein sequence alignment was done using ClustalW (Thompson et al., 1994); for DNA sequences, Bioedit was used. Secondary structure predictions were performed with PredictProtein (Rost et al., 2004).

5.1.6.4. Consumables

Table 8. Consumables.

Consumable	Distributor
Crystallization material	Hampton Research
Centrifugal filter devices	Millipore Amicon
Cellulose membrane dialysis tubing	Biorad
NuPAGE Gel System	Invitrogen
Concentrator, Centrifugal filter device	Millipore Amicon
QIAquick PCR Purification Kit	Qiagen
QIAquick Gel Extraction Kit	Qiagen
QIAprep Spin Miniprep Kit	Qiagen

5.1.6.5. Additional Instruments and Devices

Table 9. Additional instruments and devices.

Instrument/Device	Distributor
Agarose Gel Electrophoresis System	manufactured in house
DNA Thermal Cycler	Perkin Elmer
DNA Sequencer ABI Prism 377	Applied Biosystems
Shaking incubator Multitron AJ20	Infors-HT AG
French Pressure Cell Press	Polytec GmbH, Aminco SLM Instruments
Spectrophotometer, ND-1000	NanoDrop Technologies Inc.
UV-VIS spectrometer, Ultrospec II	LKB Biochrom
Gene Pulser	Biorad
Hg-High Pressure Lamp	Leica
Multiple Gel Caster	manufactured in house
Power Supply EPS 300 (SDS-PAGE, blot)	Pharmacia
Power Supply (agarose gel-electrophoresis)	Carl Roth GmbH
Gel-Electrophoresis System SE215 Mighty Small II	Hoefer/Pharmacia Biotech
XCell SureLock Electrophoresis Cell (Novex Minin-Cell)	Invitrogen
Pre-Cast Gel NuPAGE Bis-Tris	Invitrogen
Varioklav	H + P Labortechnik
Gene Amp 5700 Sequence Detection System	Applied Biosystems
Optical Power Meter HT-90	Hi-Top

5.1.7. Media and Stock Solutions

5.1.7.1. *E. coli* Media

Media used for growth of *E. coli* cells were autoclaved at 120 °C (2 bar) for 20 min. Antibiotics, used for selection, were added at a temperature of 60 °C. Agar plates were prepared using LB-medium enriched with 15 g bacto-agar per liter.

LB-Medium	1% (w/v) bacto tryptone 0.5% (w/v) bacto-yeast extract 1% (w/v) NaCl (171 mM) pH 7.0, adjusted with NaOH
TB-medium (Terrific broth medium):	1.2% (w/v) bacto tryptone 2.4% (w/v) bacto-yeast extract 0.4% (w/v) glycerol pH 7.5, adjusted with 100 mM KH_2PO_4/K_2HPO_4-buffer

5.1.7.2. Stock Solutions

Ampicillin
100 g/l (0.25 M); sterile filtered; 1000-fold stock

IPTG (isopropyl-ß-D-thiogalactopyranoside)
238 g/l (1 M); sterile filtered; 1000-fold stock

5.2. Methods

5.2.1. Molecular Biological Methods

5.2.1.1. Polymerase Chain Reaction

For DNA amplification Pfu polymerase was used. The reaction was mixed on ice to prevent the generation of unspecific products. Optimal temperature conditions of the standard protocol were adjusted for individual primers.

Standard Mix:	Primer 1 (10 µM)	1 µl
	Primer 2 (10 µM)	1 µl
	dNTPs (25 mM each)	1 µl
	10 x buffer	5 µl
	DMSO	2.5 µl
	Pfu Polymerase	0.75 µl

Standard protocol:

Initial denaturation	95 °C	4 min	
Denaturation	95 °C	1 min	30 cycles
Annealing	55 °C	1 min	
Elongation	72 °C	1.5 min	
Final Elongation	72 °C	7 min	

5.2.1.2. Digestion of DNA

For digestion of DNA, restriction enzymes belonging to type II endonucleases were used in appropriate buffers. The standard protocol was as follows:

0.5 – 1 µg DNA
50 – 100 µg BSA (if required)
10 U restriction enzyme
ad 20 µl reaction buffer

The reaction was incubated for 1 h at 37 °C and analyzed by agarose gelelectrophoresis.

5.2.1.3. Dephosphorylation of linear DNA Fragments

To prevent religation of vectors in the ligation process, linearized vectors were treated with phosphatases which catalyze the removal of 5' phosphate groups from DNA. 28 µl DNA extracted from preparative gels was incubated with 3 µl shrimp alkaline phosphatase (SAP) or antarctic phosphatase in corresponding buffer in a total volume of 40 µl. After 1 hour of incubation at 37 °C, SAP was inactivated by incubation at 60 °C for 20 minutes. Reactions containing antartic phosphatase were incubated at 37 °C for 30 minutes. Heat inactivation of antartic phosphatase was achieved by incubation at 65 °C for 5 minutes.

5.2.1.4. DNA Ligation

For ligation of linearized vector and PCR-derived inserts with compatible cohesive ends T4 DNA ligase was used. The ratio of the linearized vector and insert was approximately 1:3. In a typical reaction 1 U of T4 ligase and 100 ng of linearized vector was mixed in a total volume of 10 µl and incubated either at room temperature for 2 h or over night.

5.2.1.5. DNA Sequencing

DNA sequencing was performed with the chain-termination method using fluorescence labeled 2', 3'-dideoxy nucleotides. The sequencing reaction was composed of 100-500 ng DNA, 2 µl primer (20 pmol), 3 µl ABI Prism BigDye-kit (BigDye Terminator Cycle Sequencing Ready Reaction Kit, Perkin Elmer Applied Biosystems), 2 µl betaine and was added to a final volume of 15 µl with H_2O_{bidest}. The reaction was cycled using the following program:

Initial denaturation	95 °C	1 min	
Denaturation	95 °C	30 sec	30 cycles
Annealing	50 °C	20 sec	
Elongation	60 °C	4 min	
Final Elongation	60 °C	7 min	

Purification of the PCR samples was achieved with Micro-Spin G-50 columns (Pharmacia) according to the manufacturer's protocol. Amplified products were analyzed in an ABI Prism 377 DNA sequencer.

5.2.1.6. DNA Electrophoresis

For analytical and preparative separations of DNA agarose DNA electrophoresis was used. The gels were prepared in dissolving 0.8 – 1.2% agarose and 0.5 µg/ml ethidium bromide in TBE buffer (1 M Tris-HCl, 0.83 M boric acid, 10 mM EDTA). The gel was placed in a gel tank and covered with TBE buffer. DNA samples were mixed with loading buffer (0.2% (w/v) bromphenol blue, 30% glycerol) and loaded onto the gel. Gels were run at 5 V/cm until optimal separation was achieved. The DNA was visualized by transillumination with ultraviolet light and sizes were estimated by application of a DNA ladder as a size standard.
For isolation, DNA was excised from preparative gels and purified using the QIAquick gel extraction kit protocol as recommended by the manufacturer.

5.2.1.7. Cultivation of *E. coli*

For all cloning and plasmid maintenance purposes, *E. coli* were cultivated in 5 ml or 35 ml LB medium at 37 °C at 250 rpm. For high level expression of protein an *E. coli* overnight culture of 35 ml LB-medium was inoculated in 3 l of TB-medium and grown at 20 – 37 °C at 180 rpm.

5.2.1.8. Preparation and Transformation of electro-competent *E. coli*

For preparation of electro-competent *E. coli* cells, a fresh overnight culture was diluted 100-fold in LB medium and grown at 37 °C at 250 rpm for 3 to 4 hours to a final density of OD_{600} of 0.6 to 0.8. The culture was chilled to 0 °C and cells were harvested by centrifugation at 400 rpm for 20 min at 4 °C. Cell pellets were successively washed with 1, 0.5 and 0.25 l of a sterile 10% glycerol solution. After the final centrifugation step, the cell pellet was resuspended in 700 µl of 10% glycerol and portioned into 50 µl aliquots. These aliquots were frozen in liquid nitrogen and stored at -80 °C.
For transformation, aliquots were thawed on ice and mixed with 2 µl of ligation product or 0.5 µl of plasmid DNA. The cells were transferred to cold electroporation cuvettes (0.2 mm gap widths, BioRad) and placed into BioRad Gene Pulser System (25 µF, 1.5 kV, 800 Ω) and subjected to electroporation. Cells were regenerated in 2 ml LB medium at 37 °C for 60 min and plated on LB agar plates containing the appropriated antibiotic for selection of transformands.

5.2.1.9. Transformation of chemo-competent *E. coli*

For chemical transformation of DNA into purchased *E. coli* cells (Gibco BRL, Invitrogen), 2 µl DNA was mixed with 50 µl competent cells and incubated on ice for 30 min. Cells were subjected to heat shock for 40 sec using a water bath warmed to 42 °C and subsequently placed on ice for 2 min. For regeneration, cells were mixed with 1 ml warm LB medium and incubated at 37 °C for one hour. Selection of transformands was achieved by plating the cells onto selective LB agar plates.

5.2.1.10. Isolation of Plasmid DNA from *E. coli*

For plasmid DNA isolated single colonies were picked from LB agar plates and inoculated in 5 ml LB medium containing the desired antibiotic for selection. Cells were grown overnight and harvested by centrifugation at 5000 g for 5 min. The plasmid purification was performed with the QIAprep Miniprep (Qiagen) protocol as recommended by the manufacturer.

5.2.1.11. Determination of DNA Concentration

The concentration of DNA was estimated by comparing DNA of interest with DNA of known concentration after agarose gel electrophoresis. Moreover for more accurate determination of the DNA concentration, a solution of DNA was analyzed for its absorption at 260 and 280 nm using quartz cuvettes. At a wavelength of 260 nm and a path length of 1 cm, an OD_{260} value of 1 corresponds to a concentration of 50 µg/ml of double stranded DNA. A pure solution of double stranded DNA has an OD_{260}/OD_{280} ratio of 1.8.

5.2.2. Protein Biochemical Methods

5.2.2.1. SDS Polyacrylamide Gel Electrophoresis

SDS polyacrylamide gel electrophoresis was performed using a discontinuous buffer system under denaturating conditions. Gels with 13 or 17 % acrylamide (see below) were prepared in an in-house manufactured multiple gel caster. Solutions of the running gel and the stacking gel (see below) were poured between two glass plates separated by spacers. A well forming comb was inserted into the stacking gel. The polymerized gels were placed in a Mighty Small II apparatus (Amersham Biosciences) and covered with running buffer (see below). Protein samples to be separated on the gel were mixed with SDS sample buffer and heated for 10 min at 95 °C. Protein samples and protein molecular weight marker were loaded onto the gel and were separated using electrophoresis power supply (EPS 300, Pharmacia) at 180-200 V for one hour. For visualization of the protein bands, the gel was stained in staining solution (glacial acetic acid : methanol : water ratio of 10 : 45 : 45 and 0.1% Coomassie) for 2 hours and destained by incubation in destaining solution (glacial acetic acid : methanol : water ratio of 10 : 45 : 45).

4-fold running buffer:	**4-fold stacking buffer:**
0.5 M Tris-HCl, pH 8.8	1.5 M Tris-HCl, pH 6.8
0.5 mM EDTA	0.5 mM EDTA
0.4% (w/v) SDS	0.4% (w/v) SDS

SDS running gel:	**13%**	**17%**
30% Protogel	32.5 ml	42.5 ml
4-fold running buffer	18.75 ml	18.75 ml
10% Ammoniumpersulfate	250 µl	250 µl
TEMED	50 µl	50 µl
$H_2O_{bid.}$	23.75 ml	13.75 ml

SDS stacking gel:	
30% Protogel	13.1 ml
4-fold running buffer	13.1 ml
10% Ammoniumpersulfate	250 µl
TEMED	50 µl
$H_2O_{bid.}$	26.25 ml

5-fold SDS sample buffer:

0.5 M Tris-HCl, pH 6.8

10% Glycerol

2.3% (w/v) SDS

5% DTT

0.1% bromphenyl blue

Alternatively, pre-cast Bis-Tris NuPAGE gels were used according to the protocol of the manufacturer (Invitrogen).

5.2.2.2. Cloning and Purification of C-terminally His_6-tagged RseB

The signal sequence is important for proteins that are destined for secretion or that have to be transported across the inner membrane to reach their final destination like the membranes or the periplasmic space. After translocation *via* the SecY/E complex, signal peptidase I cleaves off the signal sequence (Breyton et al., 2002; Mitra et al., 2005; van den Berg et al., 2004) reviewed by (Driessen et al., 1998; Müller et al., 2001). As periplasmic expressed RseB was insufficient in amount, the signal sequence was deleted for purification from the cytoplasm.

The gene encoding the N-terminally truncated version of RseB missing the first 22 residues was amplified by PCR from a plasmid with full length *RSEB* (pET22-rseb, M. Grininger, unpublished results) using the primers *rseb-SS* (5′ CGGGCATATGTCATTAGTGACAGGTAGCC 3′) and *rseB_C-term* (5′ CGCGGCCACGAGTCATTGCGCTGCCCCGAAC 3′) and subcloned into the pET-22b(+) vector (Novagen). The recombinant plasmid (pET22-rseb-ss) was transformed into *E. coli* strain BL21(DE3) (Stratagene) and cells were selected on agar plates containing 100 µg/ml ampicillin. Single colonies were chosen for further inoculation first in Luria Bertani and later cultivated in terrific broth medium with 100 µg/ml ampicillin. Bacteria were grown at 37 °C to an OD_{600} of 0.7 and subsequently cooled to 20 °C for expression. Expression was induced by addition of 0.5 mM isopropyl β-D-thiogalactopyranoside (IPTG) and cells were allowed to grow for 4 hours. Cells of a 9-liter culture were harvested and resuspended in buffer A containing 20 mM Tris-HCl pH 7.4, 300 mM NaCl, 5 mM imidazole and 10% (v/v) glycerol and broken by french press. The solution was centrifuged at 40000 g

for 1 h at 4 °C to remove insoluble material and unbroken cells. The supernatant was batch-incubated by end-over-end-rotation with Ni-NTA-matrix (Ni-NTA Fastflow, Amersham Biosciences) for 30 min at room temperature. The matrix was extensively washed with buffer A and unspecific binders were eluted with a stepwise gradient of buffer A containing 10 mM, 15 mM, 20 mM and 32 mM imidazole. RseB was then eluted with buffer A containing 500 mM imidazole. The eluate was dialysed against buffer B (20 mM Tris-HCl pH 7 and 10% (v/v) glycerol, centrifuged at 40000 g for 30 minutes and applied to anion exchange chromatography (MonoQ HR5/5, Amersham Biosciences) using buffer B. Pure RseB protein appeared in the flowthrough and was concentrated to 1 or 5 mg/ml for crystallization trials.

5.2.2.3. Cloning and Purification of RseA-PP

The gene coding for the periplasmic domain of RseA (RseA-PP, residues 124-216) was amplified by PCR from a plasmid with full length *RSEA* (pET22-rsea, M. Grininger, unpublished results) using primers *rseA-PPforw* (GCGCGCATATGTCTGAAACGTCCCAGCAGCCC) and *rseA-PPrev* (CGCGCCTCGAGTTACTGCGATTGCGTTCCTAAAGTTTGAATTC) and subcloned into pET-16b(+) vector (Novagen). The recombinant plasmid (pET-16-rsea-PP) was transformed into *E. coli* strain BL21-gold(DE3) (Stratagene) and cells were selected on agar plates containing 100 µg/ml ampicillin. For N-terminally His_{10}-tagged RseA-PP, bacteria were grown at 37 °C to an OD_{600} of 0.7 and subsequently cooled to 20 °C for expression. Expression was induced by addition of 0.5 mM isopropyl β-D-thiogalactopyranoside (IPTG) and cells were allowed to grow for 4 hours. Cells of a 9-liter culture were harvested and resuspended in buffer A containing 20 mM Tris-HCl pH 8, 300 mM NaCl and 5 mM imidazole and disrupted by *french press*. The solution was centrifuged at 40000 g for 1 h at 4 °C to remove insoluble material and unbroken cells. The supernatant was batch-incubated by end-over-end-rotation with pre-equilibrated Ni-NTA-matrix (Ni-NTA Superflow, Qiagen) for 1 h at room temperature. The matrix was extensively washed with buffer A and unspecific binders were removed with buffer A containing 20 mM imidazole. For elution, a gradient from 20 mM to 500 mM imidazole in buffer A was applied using the ÄKTA system (Amersham Biosciences). For RseA-PP, fractions containing RseA-PP were pooled and dialysed against buffer C (20 mM Tris-HCl, pH 8) and applied to anion exchange chromatography (MonoQ HR5/5, Amersham Biosciences). A gradient using buffer C with 750 mM NaCl was applied and fractions containing pure RseA-PP were collected, concentrated to 10 mg/ml and stored at -80 °C.

5.2.2.4. Cloning and Purification of RseB-D1 and RseB-D2

pET22-rseb-ss (see Chapter 5.2.2.2.) was used as a template for cloning the large domain (RseB-D1, residues 23-209) and the small domain (RseB-D2, residues 212-318) of RseB. Primers used for subcloning into pET-15b(+) vector (Novagen) were *rseb_SS* (5′ GCGCGCATATGGCCACTCCCGCGTCCG 3′) and *rseb-D1_rev* (5′ CGCGCCTCGCGTCAAACAGAAAGCAACGGCGGCAA 3′) for RseB-D1 as well as *rseb-D2_forw* (5′ GCGCGCATATGGAAAAAGCTAAATTCAGCTGGACGC 3′) and *rseB_C-term* (5′ CGCGGCCACGAGTCATTGCGCTGCCCCGAAC 3′) (Metabion) for RseB-D2. The recombinant plasmids (pET15-rseb-d1 and pET15-rseb-d2) were transformed into *E. coli* strain BL21-star(DE3) (Invitrogen) and cells were selected on agar plates containing 100 µg/ml ampicillin. Single colonies were chosen for inoculation in Luria Bertani and further for cultivation in terrific broth medium with 100 µg/ml ampicillin. For N-terminally His_6-tagged RseB-D1/D2 bacteria were grown at 37 °C to an OD_{600} of 0.7 and subsequently cooled to 20 °C for expression. Expression was induced by addition of 0.5 mM isopropyl β-D-thiogalactopyranoside (IPTG) and cells were allowed to grow for 4 hours. Cells of a 9-liter culture were harvested and resuspended in buffer A containing 20 mM Tris-HCl pH 8, 300 mM NaCl and 5 mM imidazole and disrupted by french press. The solution was centrifuged at 40000 g for 1 h at 4 °C to remove insoluble material and unbroken cells. The supernatant was batch-incubated by end-over-end-rotation with pre-equilibrated Ni-NTA-matrix (Ni-NTA Superflow, Qiagen) for 1 h at room temperature. The matrix was extensively washed with buffer A and unspecific binders were removed with buffer A containing 20 mM imidazole. For elution, a gradient from 20 mM to 500 mM imidazole in buffer A was applied using the ÄKTA system (Amersham Biosciences). Fractions containing the protein of interest were collected and dialysed against buffer B (20 mM Tris-HCl pH 7), centrifuged at 40000 g for 30 minutes and applied to anion exchange chromatography (MonoQ HR5/5, Amersham Biosciences) using buffer B. Pure proteins appeared in the flow-through and were concentrated to 4 mg/ml and stored at -80 °C.

5.2.2.5. Determination of Protein Concentration

The concentration of proteins was determined by spectroscopic methods. The absorption of a protein solution was measured at 280 nm using UV-VIS spectrometer (Ultrospec II, LKB Biochrom) or spectrophotometer (ND-1000, NanoDrop Technologies Inc.). The concentration of the protein concentration was calculated in respect to the theoretical extinction coefficient of the tyrosines and tryptophans of the protein sequence.

5.2.2.6. N-terminal Sequencing of Proteins

Purified proteins and crystals were N-terminally sequenced by the Edman degradation, performed by an in-house service department.

5.2.2.7. Size Exclusion Chromatography

Size exclusion experiments were performed on the SMART system with a Superdex 200 PC3.2/30 column (Amersham Biosciences). Gel filtration was performed according to the protocol of the manufacturer. The column was equilibrated with 20 mM Tris-HCl pH 7, 150 mM NaCl. Proteins were loaded at concentrations of 4 mg/ml. The flow was 40 µl/min and fractions of 80 µl (injection at 200 µl) were collected and analyzed by SDS-PAGE. The column was calibrated with proteins of definite mass (LMW calibration kit, Amersham Biosciences).

5.2.2.8. Cross-Linking Proteins

For cross-linking, proteins were dialysed from Tris-HCl buffer to PBS buffer (137 mM NaCl, 2.68 mM KCl, 4.3 mM Na_2HPO_4, and 1.47 mM KH_2PO_4) to avoid quenching of the reaction with amines (Tris). The cross-linking reaction was carried out in a total volume of 100 µl with 10 µl of glutaraldehyde (0.25%) and protein concentrations of 0.4 mg/ml. Reactions were

incubated at 30 °C and samples were taken after 10 and 20 minutes for analysis by SDS-PAGE (4-12% NuPAGE Bis-Tris Gel, Invitrogen). Non cross-linked samples of each protein were taken for comparison. The hetero-oligomeric nature of cross-linked products was verified by mass analysis.

5.2.2.9. Binding Studies of RseA and RseB using Ni-chelating material

For analyzing the binding properties of RseB-His_6 to RseA-PP-His_{10}, RseA-PP was subjected to Factor Xa treatment to remove the His-tag. This was done by incubating 1,8 mg of RseA-PP-His_{10} in 20 mM Tris pH 8, 100 mM NaCl and 2 mM $CaCl_2$ with 20 Units of Factor Xa for 3 hours at 23 °C. For removal of intact RseA-PP-His_{10} (including His-tag), the reaction was batch incubated with Ni-NTA und cleaved RseA-PP, unable to bind the column was enriched in the supernatant. Cleaved RseA-PP (RseA-$PP_{\Delta His}$) was incubated with RseB-His_6 for 15 minutes and batch incubated with Ni-NTA for 15 minutes. For removal of Factor Xa protease and unbound proteins, Ni-NTA was extensively washed with buffer A (25 mM imidazole, 20 mM Tris-HCl pH 7.4, 300 mM NaCl and 10% glycerol). Buffer A containing 500 mM imidazole was used for elution of specifically bound proteins. Samples were analyzed by SDS-PAGE.

5.2.2.10. Binding of RseB to RseA-Peptide

$RseA_{162-186}$ was synthesized by an in-house service department. For investigating the binding property of RseB to synthetic $RseA_{162-186}$, RseB was immobilized (75 µl of 5 mg/ml in buffer: 20 mM Tris pH 8, 100 mM NaCl) on a Ni-chelating column. 20 µl of RseA-Peptide (10 mg/ml) was loaded on a column with or without preimmobilized RseB and incubated for 1 h. After extensively washing of the column with buffer A, RseB was eluted with buffer A containing 100 mM EDTA. Samples of eluate A (with RseB) and eluate B (without RseB) were analyzed by ESI-MS to verify specific binding of RseA-Peptide to RseB.

5.2.2.11. High Performance Liquid Chromatography/Mass Spectrometry

High Performance Liquid Chromatography/Mass Spectrometry (HPLC/MS) was used for identification of binding properties of RseA-Peptide to RseB. For gradient elution, the HPLC (Agilent 1100, DAD, 210 nm) was programmed as follows:

solvent A: 0.05% (v/v) TFA in water
solvent B: 0.05% (v/v) TFA in acetonitrile

equilibration at 5% solvent B
linear gradient: 0 min, 5% solvent B; 15 min: 90% solvent B

The peptide and the proteins were detected as protonated molecules in the positive electrospray ionization (ESI) mode (microTOF LC, Bruker Daltonics) as they elute from the Symmetry300 C4 (Waters) reversed-phase columns during the acetonitril/water gradient.
Mass analysis for peptide and protein was done separately at m/z-windows of 2000-5000 (ion source 4900 V, orifice 10 V) and 32000-37000 (ion source 5000V, orifice 30 V), respectively.

5.2.2.12. Analytical Ultracentrifugation (AUC)

Analytical ultracentrifugation (AUC) experiments were performed in an Optima XLI analytical ultracentrifuge (Beckman) using rotor of An-60 type with EPON centrepieces of 1.2 cm path length. Three different concentrations (2.6 µM, 9.6 µM and 26.6 µM) of RseB dialysed in 20mM Tris, pH 7.4 were tested in sedimentation velocity experiments. The experiment was performed at 38000 rpm for 6h and sedimentation curves were recorded by absorbance of 278 nm at 20°C. Data from sedimentation process were processed with SEDFIT (Schuck, 2000) to calculate the sedimentation coefficients.

5.2.3. Structure Based Methods

5.2.3.1. Small Angle X-ray Scattering (SAXS)

Small angle X-ray scattering allows determining the state of proteins in solutions at low resolution. Scattering pattern were collected by Gregor Witte and Sophia Hartung (Prof. Hopfner, Gene Center, Munich) from a RseB solution with a concentration of 5 mg/ml prepared in 20mM Tris pH 7, 10% Glycerol. As a control and for subtraction of the background a buffer sample was used. Small angle X-ray scattering data were collected at the X33 beamline (EMBL/DESY, Hamburg). Raw data were processed with PRIMUS (Konarev, 2003), gyration radii were determined with GUINIER and fourier transformation was performed with GNOM (Svergun, 1992). Similarly theoretical data of different dimeric and hexameric assemblies of RseB were generated and compared to the experimental curves (CRYSOL (Svergun, 1995)).

5.2.3.2. Negative Staining Electron Microscopy

Protein for electron microscopy was prepared by Reinhard Albrecht (Max Planck Institute of Developmental Biology, Tübingen) as follows: Purified RseB a concentration of 7.6 mg/ml was loaded on a size exclusion column (Superose 6 10/30). Gelfiltration was performed at a flow of 0.1 ml/min using a running buffer, containing 25 mM Tris pH 7.9 and 150 mM NaCl. RseB eluted in two peaks, containing different oligomeric species. Higher molucular weight fractions of peak I were pooled and used for electron microscopic analysis which was performed by Heinz Schwarz (Max Planck Institute of Developmental Biology, Tübingen). Protein was absorbed on freshly glow-discharged carbon-coated Pioloform support film mounted on grids and access liquid was removed by a filter paper. To remove buffer salts, grids were washed with H_2O and negatively stained with 1% aqueous uranyl acetate. Samples were analyzed at a primary magnification of 52 000x in a Philips CM10 transmission electron microscope at 60 kV acceleration voltage using a 30 µm objective aperture. EM negatives of 8.3 x 10,2 cm size (MACO EMS Film, Hans Mahn & Co, Stapelfeld/Hamburg) were scanned on Epson Pro 1600 at 2400 dpi with a pixel size of 2.04 Å (resulting in 50 MB image size).

5.2.3.3. Crystallization, Data Collection and Refinement

RseB used for crystallization trials was concentrated to 1 or 5 mg/ml. Crystallizations were performed by hanging drop vapour diffusion method against commercially available crystal screens from Hampton Research using 1.2 µl protein and 0.6 µl reservoir solutions. Drops were equilibrated against 500 µl reservoir solution and incubated at 18 °C.

Tetragonal crystals (form I) grew in a solution (1 mg/ml RseB) containing 2.4 M sodium malonate pH 7 and 0.3 M dimethylethylammonium propane sulfonate to final dimensions of 0.25 x 0.25 x 0.05 mm. Orthorhombic crystals (form II) were obtained from a solution containing 0.2 M magnesium chloride hexahydrate, 0.1 M Tris-HCl pH 8.5, 25% (w/v) polyethylene glycol 3350 and 10 mM L-cysteine after 3 weeks.

Tetragonal crystals belong to space group $P42_12$ with a=164.3 Å, c= 81.5 Å, α=90° and diffracted to 2.8 Å resolution with an R_{meas} of 8.7% and I/σ (I) of 18.8. Orthorhombic crystals diffracted to 2.4 Å resolution and belong to space group $C222_1$ with a=98.6 Å, b=200.7 Å, c=109.7 Å, α=90°, with R_{meas} of 11.1% and I/σ (I) of 12.64 (Table 1).

Prior to data collection RseB and derivative crystals were directly frozen in liquid nitrogen. Data were collected at beamline ID23-EH1 of the synchrotron radiation source ESRF (European Synchrotron Radiation Facility, Grenoble, France) and beamline PXII-X10SA at the SLS (Swiss Light Source, Villigen, Switzerland) at 100 K (see Table 1). Diffraction patterns were recorded on 225 mm MARCCD (PXII-X10SA) and ADSC Q315 detector (ID23-EH1). Diffraction intensities were integrated using XDS, and scaled and merged using XSCALE (Kabsch, 1988).

Derivative crystals were prepared using commercially available Pt-salts (Hampton Research). The best isomorphous phases resulted from labelling RseB tetragonal crystals soaked in reservoir solution containing 0.5 mM K_2PtCl_4, 0.5 mM $K_2Pt(SCN)_6$ or 0.5 mM $[Pt_2I_2(H_2NCH_2CH_2NH_2)_2](NO_3)_2$ with the derivative data collected at the Pt-edge. The heavy-atom substructure was identified and the structure was phased using the program package SOLVE/RESOLVE. Phases were determined at 3.2 Å using the program SOLVE (Terwilliger and Berendzen, 1999) and improved by solvent flattening using RESOLVE (Terwilliger, 2000). Manual model building based on the RESOLVE density and initial manual refinements of pdb files were done with COOT (Emsley and Cowtan, 2004) and O (Jones et al., 1991). The model of the native dataset was finally refined to 2.8 Å resolution using REFMAC5 (Murshudov et al., 1997). The structure of the orthorhombic crystal form was solved by molecular replacement using the first 200 residues of the tetragonal model and the program

MOLREP (Vagin and Teplyakov, 1997). After solvent flattening with RESOLVE, manual placement of the smaller domain into the solvent-flattened density was performed and we refined the structure to 2.4 Å resolution.

Tetragonal crystals contain two monomers (P1 and P2) per asymmetric unit (Matthews coefficient of 4, 69.3% solvent content). Orthorhombic crystals contain three monomers (C1, C2 and C3) per asymmetric unit at a solvent content of 53.1%.32 The Ramachandran plot shows that the structure has a good stereochemistry as 88.8% and 90.2% of all residues correspond to the core region in P1, P2 and C1, C2, C3, respectively (PROCHECK (Laskowski et al., 1993)).

In the structure presented, the N-terminal methionine residue and the eight C-terminal residues, including the His_6-tag, are missing. Additionally, four residues of the connecting loop (residues 212–215) were omitted, due to the poor quality of electron density in this region. As other monomers had more missing regions (P2, 94–99 and 209–218; C1, 208–221 and 234–251; C2, 208–220 and 241–246; C3, 192–195 and 204–219), structure graphs are all based on P1 (unless stated otherwise).

Figures were prepared using PyMOL (www.pymol.org), surface areas were calculated using AREAMOL (Lee and Richards, 1971), structural superpositions and RMSD calculations were done with CaspR (Claude et al., 2004).

6. References

Ades, S.E., Connolly, L.E., Alba, B.M., Gross, C.A. (1999). The *Escherichia coli* σ^E-dependent extracytoplasmic stress response is controlled by the regulated proteolysis of an anti-σ factor. *Genes & Development* **13**, 2449-2461.

Akiyama, Y., Kanehara, K., Ito, K. (2004). RseP (YaeL), an *Escherichia coli* RIP protease, cleaves transmembrane sequences. *EMBO Journal* **23**, 4434-4442.

Alba, B.M., Gross, C.A. (2004). Regulation of the *Escherichia coli* σ-dependent envelope stress response. *Molecular Microbiology* **52**, 613-619.

Alba, B.M., Leeds, J.A., Onufryk, C., Lu, C.Z., Gross, C.A. (2002). DegS and YaeL participate sequentially in the cleavage of RseA to activate the σ^E-dependent extracytoplasmic stress response. *Genes & Development* **16**, 2156-2168.

Alba, B.M., Zhong, H.J., Pelayo, J.C., Gross, C.A. (2001). *degS* (*hhoB*) is an essential *Escherichia coli* gene whose indispensable function is to provide σ^E activity. *Molecular Microbiology* **40**, 1323-1333.

Albin, R., Weber, R., Silverman, P.M. (1986). The Cpx proteins of *Escherichia coli* K12. Immunologic detection of the chromosomal *cpxA* gene product. *Journal of Biological Chemistry* **261**, 4698-4705.

Altschul, S.F., Gish, W., Miller, W., Myers, E.W., Lipman, D.J. (1990). Basic local alignment search tool. *Journal of Molecular Biology* **215**, 403-410.

Bardwell, J.C., Craig, E.A. (1987). Eukaryotic Mr 83,000 heat shock protein has a homologue in *Escherichia coli*. *Proceedings of the National Academy of Sciences of the United States of America* **84**, 5177-5181.

Bardwell, J.C., Tilly, K., Craig, E., King, J., Zylicz, M., Georgopoulos, C. (1986). The nucleotide sequence of the *Escherichia coli* K12 *dnaJ+* gene. A gene that encodes a heat shock protein. *Journal of Biological Chemistry* **261**, 1782-1785.

Bass, S., Gu, Q., Christen, A. (1996). Multicopy suppressors of *prc* mutant *Escherichia coli* include two HtrA (DegP) protease homologs (HhoAB), DksA, and a truncated R1pA. *Journal of Bacteriology* **178**, 1154-1161.

Berman, H.M., Westbrook, J., Feng, Z., Gilliland, G., Bhat, T.N., Weissig, H., Shindyalov, I.N., Bourne, P.E. (2000). The Protein Data Bank. *Nucleic Acids Research* **28**, 235-242.

Bernstein, F.C., Koetzle, T.F., Williams, G.J., Meyer, E.E., Brice, M.D., Rodgers, J.R., Kennard, O., Shimanouchi, T., Tasumi, M. (1977). The Protein Data Bank: a computer-based archival file for macromolecular structures. *Journal of Molecular Biology* **112**, 535-542.

Bond, C.S. (2003). TopDraw: a sketchpad for protein structure topology cartoons. *Bioinformatics* **19**, 311-312.

Bowes, J.H., Cater, C.W. (1968). The interaction of aldehyde with collagen. *Biochimica et Biophysica Acta* **168**, 341-352.

Brandts, J.F., Halvorson, H.R., Brennan, M. (1975). Consideration of the Possibility that the slow step in protein denaturation reactions is due to *cis-trans* isomerism of proline residues. *Biochemistry* **14**, 4953-4963.

Brass, J.M., Higgins, C.F., Foley, M., Rugman, P.A., Birmingham, J., Garland, P.B. (1986). Lateral diffusion of proteins in the periplasm of *Escherichia coli*. *Journal of Bacteriology* **165**, 787-795.

Braun, V., Rehn, K. (1969). Chemical characterization, spatial distribution and function of a lipoprotein (murein-lipoprotein) of the *E. coli* cell wall. The specific effect of trypsin on the membrane structure. *European Journal of Biochemistry* **10**, 426-438.

Braun, V., Rehn, K., Wolff, H. (1970). Supramolecular structure of the rigid layer of the cell wall of *Salmonella*, *Serratia*, *Proteus*, and *Pseudomonas fluorescens*. Number of lipoprotein molecules in a membrane layer. *Biochemistry* **9**, 5041-5049.

Breyton, C., Haase, W., Rapoport, T.A., Külbrandt, W., Collinson, I. (2002). Three-dimensional structure of the bacterial protein-translocation complex SecYEG. *Nature* **418**, 662-665.

Brown, M.S., Ye, J., Rawson, R.B., Goldstein, J.L. (2000). Regulated intramembrane proteolysis: a control mechanism conserved from bacteria to humans. *Cell* **100**, 391-398.

Buelow, D.R., Raivio, T.L. (2005). Cpx signal transduction is influenced by a conserved N-terminal domain in the novel inhibitor CpxP and the periplasmic protease DegP. *Journal of Bacteriology* **187**, 6622-6630.

Bukau, B. (1993). Regulation of the *Escherichia coli* heat-shock response. *Molecular Microbiology* **9**, 671-680.

Camacho, L.R., Constant, P., Raynaud, C., Laneelle, M.A., Triccas, J.A., Gicquel, B., Daffe, M., Guilhot, C. (2001). Analysis of the phthiocerol dimycocerosate locus of *Mycobacterium tuberculosis*. Evidence that this lipid is involved in the cell wall permeability barrier. *Journal of Biological Chemistry* **276**, 19845-19854.

Campbell, E.A., Tupy, J.L., Gruber, T.M., Wang, S., Sharp, M.M., Gross, C.A., Darst, S.A. (2003). Crystal structure of *Escherichia coli* σ^E with the cytoplasmic domain of its anti-σ RseA. *Molecular Cell* **11**, 1067-1078.

Cezairliyan, B.O., Sauer, R.T. (2007). Inhibition of regulated proteolysis by RseB. *PNAS* **104**, 3771-3776.

Chaba, R., Grigorova, I.L., Flynn, J.M., Baker, T.A., Gross, C.A. (2007). Design principles of the proteolytic cascade governing the σ^E-mediated envelope stress response in *Escherichia coli*: keys to graded, buffered, and rapid signal transduction. *Genes & Development* **21**, 124-136.

Cherfils, J., Duquerroy, S., Janin, J. (1991). Protein-protein recognition analyzed by docking simulation. *Proteins* **11**, 271-280.

Cho, K.O., Hunt, C.A., Kennedy, M.B. (1992). The rat brain postsynaptic density fraction contains a homolog of the Drosophila discs-large tumor suppressor protein. *Neuron* **9**, 929-942.

Claude, J.B., Suhre, K., Notredame, C., Claverie, J.M., Abergel, C. (2004). CaspR: a web server for automated molecular replacement using homology modelling. *Nucleic Acids Research* **32**, W606-609.

Collinet, B., Yuzawa, H., Chen, T., Herrera, C., Missiakas, D. (2000). RseB binding to the periplasmic domain of RseA modulates the RseA:σ^E interaction in the cytoplasm and the availability of σ^E·RNA polymerase. *Journal of Biological Chemistry* **275**, 33898-33904.

Connolly, L., De Las Penas, A., Alba, B.M., Gross, C.A. (1997). The response to extracytoplasmic stress in Escherichia coli is controlled by partially overlapping pathways. *Genes & Development* **11**, 2012-2021.

Daffe, M., Laneelle, M.A. (1988). Distribution of phthiocerol diester, phenolic mycosides and related compounds in mycobacteria. *Journal of General Microbiology* **134**, 2049-55.

Danese, P.N., Silhavy, T.J. (1997). The σ^E and the Cpx signal transduction systems control the synthesis of periplasmic protein-folding enzymes in *Escherichia coli*. *Genes & Development* **11**, 1183-1193.

Danese, P.N., Silhavy, T.J. (1998). CpxP, a stress-combative member of the Cpx regulon. *Journal of Bacteriology* **180**, 831-839.

Danese, P.N., Snyder, W.B., Cosma, C.L., Davis, L.J., Silhavy, T.J. (1995). The Cpx two-component signal transduction pathway of *Escherichia coli* regulates transcription of the gene specifying the stress-inducible periplasmic protease, DegP. *Genes & Development* **9**, 387-398.

Dartigalongue, C., Loferer, H., Raina, S. (2001a). EcfE, a new essential inner membrane protease: its role in the regulation of heat shock response in *Escherichia coli*. *EMBO Journal* **20**, 5908-5918.

Dartigalongue, C., Missiakas, D., Raina, S. (2001b). Characterization of the *Escherichia coli* σ^E regulon. *Journal of Biological Chemistry* **276**, 20866-20875.

Dartigalongue, C., Raina, S. (1998). A new heat-shock gene, *ppiD*, encodes a peptidyl-prolyl isomerase required for folding of outer membrane proteins in *Escherichia coli*. *EMBO Journal* **17**, 3968-3980.

De Las Penas, A., Connolly, L., Gross, C.A. (1997a). σ^E is an essential σ factor in *Escherichia coli*. *Journal of Bacteriology* **179**, 6862-6864.

De Las Penas, A., Connolly, L., Gross, C.A. (1997b). The σ^E-mediated response to extracytoplasmic stress in *Escherichia coli* is transduced by RseA and RseB, two negative regulators of σ^E. *Molecular Microbiology* **24**, 373-385.

Diederichs, K, Karplus, P.A. (1997). Omproved R-factors for diffraction data analysis in macromolecular crystallography. *Nature Structural Biology* **4**, 269-275.

DiGiuseppe, P.A., Silhavy, T.J. (2003). Signal detection and target gene induction by the CpxRA two-component system. *Journal of Bacteriology* **185**, 2432-2440.

Dong, J., Iuchi, S., Kwan, H.S., Lu, Z., Lin, E.C. (1993). The deduced amino-acid sequence of the cloned *cpxR* gene suggests the protein is the cognate regulator for the membrane sensor, CpxA, in a two-component signal transduction system of *Escherichia coli*. *Gene* **136**, 227-230.

Driessen, A.J., Fekkes, P., van der Wolk, J.P. (1998). The Sec system. *Current Opinion in Microbiology* **2**, 216-222.

Dugave, C., Demange, L. (2003). *Cis-trans* isomerization of organic molecules and biomolecules: implications and applications. *Chemical Reviews* **103**, 2475-2532.

Duguay, A.R., Silhavy, T.J. (2004). Quality control in the bacterial periplasm. *Biochimica et Biophysica Acta* **1694**, 121-134.

Emsley, P., Cowtan, K. (2004). Coot: model-building tools for molecular graphics. *Acta Crystallographica Section D-Biological Crystallography* **60**, 2126-2132.

Erickson, J.W., Gross, C.A. (1989). Identification of the σ^E subunit of *Escherichia coli* RNA polymerase: a second alternate σ factor involved in high-temperature gene expression. *Genes & Development* **3**, 1462-1471.

Erickson, J.W., Vaughn, V., Walter, W.A., Neidhardt, F.C., Gross, C.A. (1987). Regulation of the promoters and transcripts of *rpoH*, the *Escherichia coli* heat shock regulatory gene. *Genes & Development* **1**, 419-432.

Flynn, J.M., Levchenko, I., Sauer, R.T., Baker, T.A. (2004). Modulating substrate choice: the SspB adaptor delivers a regulator of the extracytoplasmic-stress response to the AAA+ protease ClpXP for degradation. *Genes & Development* **18**, 2292-2301.

Fraser, C.M., Gocayne, J.D., White, O., Adams, M.D., Clayton, R.A., Fleischmann, R.D., Bult, C.J., Kerlavage, A.R., Sutton, G., Kelley, J.M. *et al.* (1995). The minimal gene complement of *Mycoplasma genitalum*. *Science* **270**, 397-403.

Grigorova, I.L., Chaba, R., Zhong, H.J., Alba, B.M., Rhodius, V., Herman, C., Gross, C.A. (2004). Fine-tuning of the *Escherichia coli* σ^E envelope stress response relies on multiple mechanisms to inhibit signal-independent proteolysis of the transmembrane anti-σ factor, RseA. *Genes & Development* **18**, 2686-2697.

Grossman, A.D., Erickson, J.W., Gross, C.A. (1984). The *htpR* gene product of *E. coli* is a σ factor for heat-shock promoters. *Cell* **38**, 383-390.

Gupta, S.D., Lee, B.T., Camakaris, J., Wu, H.C. (1995). Identification of *cutC* and *cutF* (*nlpE*) genes involved in copper tolerance in *Escherichia coli*. *Journal of Bacteriology* **177**, 4207-4215.

Habeeb, A.J., Hiramoto, R. (1968). Reaction of proteins with glutaraldehyde. *Archives of Biochemistry and Biophysics* **126**, 16-26.

Harris, B.Z., Lim, W.A. (2001). Mechanism and role of PDZ domains in signaling complex assembly. *Journal of Cell Science* **114**, 3219-3231.

Hersch, G.L., Baker, T.A., Sauer, R.T. (2004). SspB delivery of substrates for ClpXP proteolysis probed by the design of improved degradation tags. *Proceedings of the National Academy of Sciences of the United States of America* **101**, 12136-12141.

Himmelreich, R., Hilbert, H., Plagens, H., Pirkl, E., Li, B.C., Herrmann, R. (1996). Complete sequence analysis of the genome of the bacterium *Mycoplasma pneumoniae*. *Nucleic Acids Research* **24**, 4420-4449.

Holm, L., Sander, C. (1995). Dali: a network tool for protein structure comparison. *Trends in Biochemical Sciences* **20**, 478-480.

Hung, D.L., Raivio, T.L., Jones, C.H., Silhavy, T.J., Hultgren, S.J. (2001). Cpx signaling pathway monitors biogenesis and affects assembly and expression of P pili. *EMBO Journal* **20**, 1508-1518.

Hutchings, M.I., Hoskisson, P.A., Chandra, G., Buttner, M.J. (2004). Sensing and responding to diverse extracellular signals? Analysis of the sensor kinases and response regulators of *Streptomyces coelicolor* A3. *Microbiology* **150**, 2795-2806.

Inouye, M., Shaw, J., Shen, C. (1972). The assembly of a structural lipoprotein in the envelope of *Escherichia coli*. *Journal of Biological Chemistry* **247**, 8154-8159.

Isaac, D.D., Pinkner, J.S., Hultgren, S.J., Silhavy, T.J. (2005). The extracytoplasmic adaptor protein CpxP is degraded with substrate by DegP. *Proceedings of the National Academy of Sciences of the United States of America* **102**, 17775-17779.

Janin, J. (1997). Specific *vs* non-specific contacts in protein crystals. *Nature Structural Biology* **4**, 973-974.

Janin, J., Rodier, F. (1995). Protein-protein interaction at crystal contacts. *Proteins: Structure Function and Genetics* **23**, 580-587.

Johansen, J., Rasmussen, A.A., Overgaard, M., Valentin-Hansen, P. (2006). Conserved small non-coding RNAs that belong to the σ^E regulon: Role in down-regulation of outer membrane proteins. *Journal of Molelcular Biology* **364**, 1-8.

Jones, T.A., Zou, J.Y., Cowan, S.W., Kjeldgaard, M. (1991). Improved methodes for building protein models in electron density maps and the location of errors in these models. *Acta Crystallographica Section A-Biological Crystallography* **47**, 110-119.

Kamio, Y., Nikaido, H. (1976). Outer membrane of *Salmonella typhimurium*: accessibility of phopholipid head groups to phospholipase c and canogen bromide activated dextran in the external medium. *Biochemistry* **15**, 2561-2570.

Kanehara, K., Akiyama, Y., Ito, K. (2001). Characterization of the *yaeL* gene product and its S2P-protease motifs in *Escherichia coli*. *Gene* **281**, 71-79.

Kanehara, K., Ito, K., Akiyama, Y. (2002). YaeL (EcfE) activates the σ^E pathway of stress response through a site-2 cleavage of anti-σ^E, RseA. *Genes & Development* **16**, 2147-2155.

Kanehara, K., Ito, K., Akiyama, Y. (2003). YaeL proteolysis of RseA is controlled by the PDZ domain of YaeL and a Gln-rich region of RseA. *EMBO Journal* **22**, 6389-6398.

Kim, D.Y., Jin, K.S., Kwon, E., Ree, M., Kim, K.K. (2007). Crystal structure of RseB and a model of its binding mode to RseA. *Proceedings of the National Academy of Sciences of the United States of America* **104**, 8779-8784.

Kim, E., Niethammer, M., Rothschild, A., Jan, Y.N., Sheng, M. (1995). Clustering of Shaker-type K+ channels by interaction with a family of membrane-associated guanylate kinases. *Nature* **378**, 85-88.

Koide, K., Maegawa, S., Ito, K., Akiyama, Y. (2007). Environment of the Active Site Region of RseP, an *Escherichia coli* Regulated Intramembrane Proteolysis Protease, Assessed by Site-directed Cysteine Alkylation. *Journal of Biological Chemistry* **282**, 4553-4560.

Konarev, P.V., Volkov, V.V., Sokolova, A.V., Koch, M.H.J., Svergun, D.I. (2003). *PRIMUS*: a Windows PC-based system for small angle scattering data analysis. *Journal of Applied Crystallography* **36**, 1277-1282.

Landick, R., Vaughn, V., Lau, E.T., VanBogelen, R.A., Erickson, J.W., Neidhardt, F.C. (1984). Nucleotide sequence of the heat shock regulatory gene of *E. coli* suggests its protein product may be a transcription factor. *Cell* **38**, 175-182.

Laskowski, R.A., MacArthur, M.W., Moss, D.S., Thornton, J.M. (1993). PROCHECK: a program to ckeck the stereochemical quality of protein structures. *Journal of Applied Crystallography* **26**, 283-291.

Lee, B., Richards, M. (1971). The interpretation of proteins structures: Estimation of static accessibility. *Journal of Molecular Biology* **55**, 370-400.

Levchenko, I., Grant, R.A., Flynn, J.M., Sauer, R.T., Baker, T.A. (2005). Versatile modes of peptide recognition by the AAA+ adaptor protein SspB. *Nature Structural & Molecular Biology* **12**, 520-525.

Lichtarge, O., Bourne, H.R., Cohen, F.E. (1996). An evolutionary trace method defines binding surfaces common to protein families. *Journal of Molecular Biology* **257**, 342-358.

Lipinska, B., Sharma, S., Georgopoulos, C. (1988). Sequence analysis and regulation of the *htrA* gene of *Escherichia coli*: a σ^{32}-independent mechanism of heat-inducible transcription. *Nucleic Acids Research* **16**, 10053-10067.

Lummis, S.C. (2005). *Cis-trans* isomerization at a proline opens the pore of a neurotransmitter-gated ion channel. *Nature* **438**, 248-252.

Malinverni, J.C., Werner, J., Kim, S., Sklar, J.G., Kahne, D., Misra, R., Silhavy, T.J. (2006). YfiO stabilizes the YaeT complex and is essential for outer membrane protein assembly in *Escherichia coli*. *Molecular Microbiology* **61**, 151-164.

Matsuyama, S., Tajima, T., Tokuda, H. (1995). A novel periplasmic carrier protein involved in the sorting and transport of *Escherichia coli* lipoproteins destined for the outer membrane. *EMBO Journal* **14**, 3365-3372.

Matsuyama, S., Yokota, N., Tokuda, H. (1997). A novel outer membrane lipoprotein, LolB (HemM), involved in the LolA (p20)-dependent localization of lipoproteins to the outer membrane of *Escherichia coli*. *EMBO Journal* **16**, 6947-6955.

Matthews, B.W. (1968). Solvent content of protein crystals. *Journal of Molecular Biology 33*, 491-497.

McEwen, J., Silverman, P. (1980). Mutations in genes *cpxA* and *cpxB* of *Escherichia coli* K-12 cause a defect in isoleucine and valine syntheses. *Journal of Bacteriology* **144**, 68-73.

Mecsas, J., Rouviere, P.E., Erickson, J.W., Donohue, T.J., Gross, C.A. (1993). The activity of σ^E, an *Escherichia coli* heat-inducible σ-factor, is modulated by expression of outer membrane proteins. *Genes & Development* **7**, 2618-2628.

Missiakas, D., Betton, J.M., Raina, S. (1996a). New components of protein folding in extracytoplasmic compartments of *Escherichia coli* SurA, FkpA and Skp/OmpH. *Molecular Microbiology* **21**, 871-884.

Missiakas, D., Mayer, M.P., Lemaire, M., Georgopoulos, C., Raina, S. (1997). Modulation of the *Escherichia coli* σ^E (RpoE) heat-shock transcription-factor activity by the RseA, RseB and RseC proteins. *Molecular Microbiology* **24**, 355-371.

Missiakas, D., Schwager, F., Betton, J.M., Georgopoulos, C., Raina, S. (1996b). Identification and characterization of HsIV HsIU (ClpQ ClpY) proteins involved in overall proteolysis of misfolded proteins in *Escherichia coli*. *EMBO Journal* **15**, 6899-6909.

Mitra, K., Schaffitzel, C., Shaikh, T., Tama, F., Jenni, S., Brooks, C.L.r., Ban, N., Frank, J. (2005). Structure fo the *E. coli* protein-conducting channel bound to a translating ribosome. *Nature* **438**, 318-324.

Mizuno, T. (1997). Compilation of all genes encoding two-component phosphotransfer signal transducers in the genome of *Escherichia coli*. *DNA Research* **4**, 161-168.

Mizuno, T. (1998). His-Asp phosphotransfer signal transduction. *Journal of Biochemistry* (Tokyo) **123**, 555-563.

Müller, M., Koch, H.G., Schäfer, U. (2001). Protein traffic in bacteria: multiple routes from the ribosome to and across the membrane. *Progess in Nucleic Acid Research and Molecular Biology* **66**, 107-157.

Murshudov, G.N., Vagin, A.A., Dodson, E.J. (1997). Refinement of macromolecular structures by the maximum-likelihood method. *Acta Crystallographica Section D-Biological Crystallography* **53**, 240-255.

Nakamoto, H., Bardwell, J.C. (2004). Catalysis of disulfide bond formation and isomerization in the *Escherichia coli* periplasm. *Biochimica et Biophysica Acta* **1694**, 111-119.

Narita, S., Matsuyama, S., Tokuda, H. (2004). Lipoprotein trafficking in *Escherichia coli*. *Archives of Microbiology* **182**, 1-6.

Narita, S., Tanaka, K., Matsuyama, S., Tokuda, H. (2002). Disruption of *lolCDE*, encoding an ATP-binding cassette transporter, is lethal for *Escherichia coli* and prevents release of lipoproteins from the inner membrane. *Journal of Bacteriology* **184**, 1417-1422.

Nevesinjac, A.Z., Raivio, T.L. (2005). The Cpx envelope stress response affects expression of the type IV bundle-forming pili of enteropathogenic *Escherichia coli*. *Journal of Bacteriology* **187**, 672-686.

Nikaido, H. (1996) Outer Membrane. In Neidhardt, F.C., Curtis III, R., Ingraham, J.L., Lin, E.C.C., Low, K.B., Magasanik, B., Reznikoff, W.S., Riley, M., Schaechter, M. and Umbarger, H.E., *Escherichia coli* and *Salmonella*: Cellular and Moleuclar Biology. ASM, Washington, DC, 29-47.

Nixon, B.T., Ronson, C.W., Ausubel, F.M. (1986). Two-component regulatory systems responsive to environmental stimuli share strongly conserved domains with the nitrogen assimilation regulatory genes *ntrB* and *ntrC*. *Proceedings of the National Academy of Sciences of the United States of America* **83**, 7850-7854.

Novotny, J., Sharp, K. (1992). Electrostatic fields in antibodies and antibody/antigen complexes. *Progress in Biophysics and Molecular Biology* **58**, 203-224.

Onufryk, C., Crouch, M.L., Fang, F.C., Gross, C.A. (2005). Characterization of six lipoproteins in the σ^E regulon. *Journal of Bacteriology* **187**, 4552-4561.

Otto, K., Silhavy, T.J. (2002). Surface sensing and adhesion of *Escherichia coli* controlled by the Cpx-signaling pathway. *Proceedings of the National Academy of Sciences of the United States of America* **99**, 2287-2292.

Pallen, M.J., Wren, B.W. (1997). The HtrA family of serine proteases. *Molecular Microbiology* **26**, 209-221.

Pogliano, J., Lynch, A.S., Belin, D., Lin, E.C., Beckwith, J. (1997). Regulation of *Escherichia coli* cell envelope proteins involved in protein folding and degradation by the Cpx two-component system. *Genes & Development* **11**, 1169-1182.

Raina, S., Missiakas, D., Georgopoulos, C. (1995). The *rpoE* gene encoding the σ^E (σ^{24}) heat shock σ factor of *Escherichia coli*. *EMBO Journal* **14**, 1043-1055.

Raivio, T.L. (2005). Envelope stress responses and Gram-negative bacterial pathogenesis. *Molecular Microbiology* **56**, 1119-1128.

Raivio, T.L., Silhavy, T.J. (1999). The σ^E and Cpx regulatory pathways: overlapping but distinct envelope stress responses. *Current Opinion in Microbiology* **2**, 159-165.

Raivio, T.L., Silhavy, T.J. (2001). Periplasmic stress and ECF σ factors. *Annual Review of Microbiology* **55**, 591-624.

Rezuchova, B., Miticka, H., Homerova, D., Roberts, M., Kormanec, J. (2003). New members of the *Escherichia coli* σ^E regulon identified by a two-plasmid system. *FEMS Microbiology Letters* **225**, 1-7.

Rhodius, V.A., Suh, W.C., Nonaka, G., West, J., Gross, C. (2006). Conserved and variable functions of the σ^E stress response in related genomes. *PloS Biology* **4**, 43-59.

Rost, B., Yachdav, G., Liu, J. (2004). The PredictProtein server. *Nucleic Acids Research (Web Server issue)* **32**, W321-W326.

Rouviere, P.E., De Las Penas, A., Mecsas, J., Lu, C.Z., Rudd, K.E., Gross, C.A. (1995). *rpoE*, the gene encoding the second heat-shock σ factor, σ^E, in *Escherichia coli*. *EMBO Journal* **14**, 1032-1042.

Rouviere, P.E., Gross, C.A. (1996). SurA, a periplasmic protein with peptidyl-prolyl isomerase activity, participates in the assembly of outer membrane porins. *Genes & Development* **10**, 3170-3182.

Rowley, G., Spector, M., Kormanec, J., Roberts, M. (2006). Pushing the envelope: extracytoplasmic stress responses in bacterial pathogens. *Nature Reviews*. *Microbiology* **4**, 383-394.

Ruiz, N., Silhavy, T.J. (2005). Sensing external stress: watchdogs of the *Escherichia coli* cell envelope. *Current Opinion in Microbiology* **8**, 122-126.

Sankaran, K., Wu, H.C. (1994). Lipid modification of bacterial prolipoprotein. Transfer of diacylglyceryl moiety from phosphatidylglycerol. *Journal of Biological Chemistry* **269**, 19701-19706.

Schuck, P. (2000). Size-distribution analysis of macromolecules by sedimentation velocity ultracentrifugation and lamm equation modeling. *Biophysical Journal* **78**, 1606-1619.

Seltmann, G., Holst, O. (2002) *The bacterial cell wall*. Springer-Verlag, Berlin Heidelberg.

Shuman, H.A., Panagiotidis, C.H. (1993). Tinkering with transporters: periplasmic binding protein-dependent maltose transport in *E. coli*. *Journal of Bioenergetics & Biomembranes* **25**, 613-620.

Snyder, W.B., Davis, L.J., Danese, P.N., Cosma, C.L., Silhavy, T.J. (1995). Overproduction of NlpE, a new outer membrane lipoprotein, suppresses the toxicity of periplasmic LacZ by activation of the Cpx signal transduction pathway. *Journal of Bacteriology* **177**, 4216-4223.

Straus, D., Walter, W., Gross, C.A. (1990). DnaK, DnaJ, and GrpE heat shock proteins negatively regulate heat shock gene expression by controlling the synthesis and stability of σ^{32}. *Genes & Development* **4**, 2202-2209.

Straus, D.B., Walter, W.A., Gross, C.A. (1987). The heat shock response of *E. coli* is regulated by changes in the concentration of σ^{32}. *Nature* **329**, 348-351.

Subbarao, G.V., van den Berg, B. (2006). Crystal structure of the monomeric porin OmpG. *Journal of Molecular Biology* **360**, 750-759.

Sugai, M., Wu, H.C. (1992). Export of the outer membrane lipoprotein is defective in *secD*, *secE*, and *secF* mutants of *Escherichia coli*. *Journal of Bacteriology* **174**, 2511-2516.

Sulzenbacher, G., Canaan, S., Bordat, Y., Neyrolles, O., Stadthagen, G., Roig-Zamboni, V., Rauzier, J., Maurin, D., Laval, F., Daffe, M. *et al.* (2006). LppX is a lipoprotein required for the translocation of phthiocerol dimycocerosates to the surface of *Mycobacterium tuberculosis*. *EMBO Journal* **25**, 1436-1444.

Svergun, D.I. (1992). Determination of the Regularization Parameter in Indirect-Transform Methods Using Perceptual Criteria. *Journal of Applied Crystallography* **25**, 495-503.

Svergun, D.I., Barberato, C., Koch M.H.J. (1995). *CRYSOL* - a Program to Evaluate X-ray Solution Scattering of Biological Macromolecules from Atomic Coordinates. *Journal of Applied Crystallography* **28**, 768-773.

Takeda, K., Miyatake, H., Yokota, N., Matsuyama, S., Tokuda, H., Miki, K. (2003). Crystal structures of bacterial lipoprotein localization factors, LolA and LolB. *EMBO Journal* **22**, 3199-3209.

Tam, C., Missiakas, D. (2005). Changes in lipopolysaccharide structure induce the σ^E-dependent response of *Escherichia coli*. *Molecular Microbiology* **55**, 1403-1412.

Taniguchi, N., Matsuyama, S., Tokuda, H. (2005). Mechanisms underlying energy-independent transfer of lipoproteins from LolA to LolB, which have similar unclosed β-barrel structures. *Journal of Biological Chemistry* **280**, 34481-34488.

Terwilliger, T.C. (2000). Maximum-likelihood density modification. *Acta Crystallographica Section D-Biological Crystallography* **56**, 965-972.

Terwilliger, T.C. (2002a). Automated main-chain model building by template matching and iterative fragment extension. *Acta Crystallographica Section D-Biological Crystallography* **59**, 38-44.

Terwilliger, T.C. (2002b). Automated side-chain building and sequence assignment by template matching. *Acta Crystallographica Section D-Biological Crystallography* **59**, 45-49.

Terwilliger, T.C. (2004). Using prime-and-switch phasing to reduce model bias in molecular replacement. *Acta Crystallographica Section D-Biological Crystallography* **60**, 2144-2149.

Terwilliger, T.C., Berendzen, J. (1999). Automated MAD and MIR structure solution. *Acta Crystallographica Section D-Biological Crystallography* **55**, 849-861.

Thompson, J.D., Higginson, J., Gibson, T.J. (1994). CLUSTAL W: improving the sensitivity of progressive multiple sequence alignment through sequence weighting, position-specific gap penalties and weight matrix choice. *Nucleic Acids Research* **22**, 4673-4680.

Tokuda, H., Matsuyama, S. (2004). Sorting of lipoproteins to the outer membrane in *E. coli*. *Biochimica et Biophysica Acta* **1693**, 5-13.

Tsutakawa, S.E., Hura, G.L., Frankel, K.A., Cooper, P.K., Tainer, J.A. (2006). Structural analysis of flexible proteins in solution by small angle X-ray scattering combined with crystallography. *Journal of Structural Biology* **158**, 214-223.

Vale, R.D. (2000). AAA Proteins: Lords of the Ring. *Journal of Cell Biology* **150**, F13-F19.

Vagin, A.A., Teplyakov, A. (1997). MOLREP: an automated program suite. *Journal of Applied Crystallography* **30**, 1022-1025.

Valdar, W.S.J., Thornton, J.M. (2001). Conservation Helps to Identify Biologically Relevant Crystal Contacts. *Journal of Molecular Biology* **313**, 399-416.

van den Berg, B., Clemons, W.M.J., Collinson, I., Modis, Y., Hartmann, E., Harrison, S.C., Rapoport, T.A. (2004). X-ray structure of a protein conducting channel. *Nature* **427**, 34-44.

Waller, P.R., Sauer, R.T. (1996). Characterization of *degQ* and *degS*, *Escherichia coli* genes encoding homologs of the DegP protease. *Science* **271**, 990-993.

Walsh, N.P., Alba, B.M., Bose, B., Gross, C.A., Sauer, R.T. (2003). OMP peptide signals initiate the envelope-stress response by activating DegS protease *via* relief of inhibition mediated by its PDZ domain. *Cell* **113**, 61-71.

Warshel, A., Russel, S.T. (1984). Calculations of electrostatic interactions in biological systems and solutions. *Quarterly Reviews of Biophysics* **17**, 283-422.

Watanabe, S., Matsuyama, S., Tokuda, H. (2006). Roles of the hydrophobic cavity and lid of LolA in the lipoprotein transfer reaction in *Escherichia coli*. *Journal of Biological Chemistry* **281**, 3335-3342.

Weidel, W., Pelzer, H. (1964). Bag-shaped macromolecules - a new outlook on bacterial cell walls. *Advances in Enzymology and Related Areas of Molecular Biology* **26**, 193-232.

Wilken, C., Kitzing, K., Kurzbauer, R., Ehrmann, M., Clausen, T. (2004). Crystal structure of the DegS stress sensor: How a PDZ domain recognizes misfolded protein and activates a protease. *Cell* **117**, 483-494.

Woods, D.F., Bryant, P.J. (1993). ZO-1, DlgA and PSD-95/SAP90: homologous proteins in tight, septate and synaptic cell junctions. *Mechanisms of Development* **44**, 85-89.

Xu, D., Lin, S.L., Nussinov, R. (1997). Protein Binding versus Protein Folding: The Role of Hydrophilic Bridges in Protein Associations. *Journal of Molecular Biology* **265**, 68-84.

Xu, Q., Krishna, S.S., McMullan, D., Schwarzenbacher, R., Miller, M.D., Abdubek, P., Agarwalla, S., Ambing, E., Astakhova, T., Axelrod, H.L. *et al.* (2006). Crystal structure of an ORFan protein (TM1622) from *Thermotoga maritima* at 1.75 Å resolution reveals a fold similar to the Ran-binding protein Mog1p. *Proteins* **65**, 777-782.

Yakushi, T., Masuda, K., Narita, S., Matsuyama, S., Tokuda, H. (2000). A new ABC transporter mediating the detachment of lipid-modified proteins from membranes. *Nature Cell Biology* **2**, 212-218.

Yakushi, T., Tajima, T., Matsuyama, S., Tokuda, H. (1997). Lethality of the covalent linkage between mislocalized major outer membrane lipoprotein and the peptidoglycan of *Escherichia coli*. *Journal of Bacteriology* **179**, 2857-2862.

Ye, J., van den Berg, B. (2004). Crystal structure of the bacterial nucleoside transporter Tsx. *EMBO Journal* **23**, 3187-3195.

Yildiz, O., Vinothkumar, K.R., Goswami, P., Kuhlbrandt, W. (2006). Structure of the monomeric outer-membrane porin OmpG in the open and closed conformation. *EMBO Journal* **25**, 3702-3713.

Young, J.C., Hartl, F.U. (2003). A stress sensor for the bacterial periplasm. Cell **113**, 1-2.

Yura, T., Tobe, T., Ito, K., Osawa, T. (1984). Heat shock regulatory gene (*htpR*) of *Escherichia coli* is required for growth at high temperature but is dispensable at low temperature. *Proceedings of the National Academy of Sciences of the United States of America* **81**, 6803-6807.

Zeth, K. (2004). Structural analysis of DegS, a stress sensor of the bacterial periplasm. *FEBS Letters* **569**, 351-358.

Zvelebil, M.J., Barton, G.J., Taylor, W.R., Sternberg, M.J. (1987). Prediction of protein secondary structure and active sites using the alignment of homologous sequences. *Journal of Molecular Biology* **195**, 957-961.

7. Abbreviations

Å	Angstrom
Amp	ampicillin
ATP	adenosine triphosphate
AU	asymmtric unit
AUC	analytical ultracentrifugation
bp	base pairs
BSA	bovine serum albumine
CL	cross-link
c(s)	sedimentation coefficient distribution
CT	C-terminus
D1	large domain of RseB
D2	small domain of RseB
DDM	dodecyl maltoside
DIM	phthiocerol dimycocerosates
DMSO	dimethylsulfoxide
DNA	deoxyribonucleic acid
dNTP	deoxyribonucleoside triphosphate
DTT	dithiothreitol
E. coli	*Escherichia coli*
EDTA	ethylenediaminetetra acetate
EM	electron microscopy
e.g.	for example
ESI	Electrospray ionization
ESRF	European synchrotron radiation facility
FT	flow through
GTP	guanosine triphosphate
h	hour
HPLC	High Performance Liquid Chromatography
IPTG	isopropyl β-D-thiogalactopyranoside
IM	inner membrane
kDa	kilodalton
LB	Luria Bertani broth
LPS	lipopolysaccharide
MBP	maltose binding protein
MIR	multiple isomorphous replacement
MR	molecular replacement
MS	mass spectrometry
MW	molecular weight
NDS1	dimethylethylammoniumpropane sulfonate
No.	Number
NT	N-terminus
OD	optical density
OG	octyl glycoside
OM	outer membrane
OMP	outer membrane protein
PAGE	polyacrylamide gel electrophoresis
PCR	polymerase chain reaction
PDB	protein data bank
Peg	polyethylene glycol
PegMME	polyethylene glycol monomethylether
poly-Q	poly-glutamines
p(r)	electron pair distribution
RIP	regulated intramembrane proteolysis
RMSD	root mean square deviation
RNA	ribonucleic acid
rpm	rounds per minute
RT	room temperature
Rse	regulator sigmaE
RseA-PP	periplasmic domain of RseA
RseB-D1	large domain of RseB
RseB-D2	small domain of RseB
σ	sigma factor
σ^E	sigma factor for extracytoplasmic stress
S	Svedberg
S2P	site-2-protease
SAXS	small angle X-ray scattering
SDS	sodium dodecyl sulfate
SLS	swiss light source
SREBP	sterol regulator element binding protein
SS	signal sequence
TB	terrific broth
TFA	trifluoroacetic acid
Tris	tris (hydroxymethyl) aminoethanee
UV	ultraviolet
V	voltage

8. Acknowledgement

Zu aller erst gilt mein Dank meinem Doktorvater Prof. Dieter Oesterhelt, der mir die Möglichkeit gegeben hat im anregenden, wissenschaftlichen Umfeld seiner Abteilung unter äußerst fairer und großzügiger Beschirmung zu arbeiten.
Ein spezieller Dank geht an Prof. Karl-Peter Hopfner für seine Bereitschaft das Zweitgutachten zu übernehmen.
Sehr aufrichtig möchte ich mich bei Dr. Kornelius Zeth bedanken, der mich als seine erste Doktorandin aufnahm und mich unwahrscheinlich unterstützt und gefördert hat, zudem jedoch Vertrauen und Raum zur wissenschaftlichen Entfaltung geschenkt hat.
Großer Dank gebührt Prof. Christian Koch (Universität Erlangen-Nürnberg, Institut für Biologie), der mich während meiner Diplomarbeit maßgeblich geschult hat, mir eine wissenschaftliche Denkweise anzueignen. Unbedingt bedanken möchte ich mich für das lange, nette Telefonat mit Prof. Ludger Hengst, der mich ermutigte trotz Kind eine Doktorarbeit zu machen.

Sehr beeindruck hat mich Reinhard Mentele (Abt. Lottspeich), der mit immensem Enthusiasmus versucht hat jegliche Proteinproben auf Sequenz und Masse zu überprüfen. Mit gleicher Liebe und Sorgfalt wurden Proben behandelt, die Elisabeth Weyher-Stingl (Core Facility) analysierte. Als Leiter der Core Facility hat Dr. Stephan Uebel mit großem Zeitaufwand die analytische Ultrazentrifugation von RseB durchgeführt, wofür ich ihm sehr danken möchte.
Für die äußerst amüsante, sehr spontane SAXS Aktion und für die hilfreiche Diskussionsbereitschaft, möchte ich mich ganz herzlich bei Dr. Gregor Witte und Sophia Hartung (Prof. Hopfner, Genzentrum) bedanken.
Zudem danke ich Dr. Reinhard Albrecht, Dr. Heinz Schwarz (MPI Tübingen) und Dr. Beate Rockel (Abt. Baumeister) für EM Aufnahmen und ihre Hilfsbereitschaft, Dr. Martin Grininger für die Klonierung von *rseA* und *rseB* von genomischer DNA, der Core Facility für die Synthese der RseA-Peptides, Monica Zobawa, Sigrid Bauer und Dr. Frank Siedler für Massenanalysen. Ferner danke ich Dr. Yasuhito Shomura (ehem. Abt. Hartl) für den lustigsten Synchrotron Aufenthalt und Assol Arnhold für amüsante Ablenkung und verwaltungstechnische Hilfestellungen.

Ein ganz wichtiger Dank gilt meinem näheren Arbeitsumfeld. Für diverse experimentellen Hilfe- und Fragestellungen danke ich Dr. Hüseyin Besir, Dr. Christian Klein, Stephanie Bleicken, Dr. Patrik Johansson, Dr. Nediljko Budisa, Waldemar Vollmer (MPI Tübingen) und Dr. Andreas Bracher (Abt. Hartl). Auch allen anderen Kollegen möchte ich danken für die schöne Arbeitsatmosphäre, besonders Christoph Schwarz, Henrike Besche, Peter Reichelt, Birgit Bisle und Susanne von Gronau. Für einen reibungslosen Ablauf in der Abteilung danke ich Dr. Jörg Tittor, Dr. Peter Palm, Walter Erhard, Silvia Haslbeck und Eleonore Haack.
Ebenso danke ich Ursula Heider nicht nur für die schöne Zeit in unserem Zweier-Labor, sondern auch für wissenschaftliche Unterstützung in anderen Projekten und für die Durchführung sämtlicher Bestellungen. Christl Weyrauch danke ich für ihre erfrischende direkte Art und ihren speziellen Humor, der mich manchmal noch Tage danach schmunzeln ließ.
Meine beiden Bürokollegen, Iris Asen, danke ich für ihre bemerkenswerte Eigenschaft sich von nichts aus der Ruhe bringen zu lassen und Thomas Meins, für seine uneingeschränkte ehrliche Art. Beiden danke ich auch dafür, dass sie immer ein offenes Ohr für mich hatten und ich sie immer mit Fragen und Gedanken belästigen durfte. Habe ich wirklich genossen mit Euch und es hat sehr Spaß gemacht!!!

Speziell danken möchte ich Stefan Schwarz, der mich ermunterte eine Doktorarbeit zu machen, Opa Richard und Oma Christa für kurzfristige Betreuungs-Termine und meinen Freunden Rachela Mohr, Marion Meinel, Rainer Wienke, Christian Benda und FuSaLuHa, die immer für mich da sind.
Zuletzt danke ich meiner Familie, meiner Mutter Eunhyun und meiner Schwester Beate, die mich immer unterstützt haben und denen ich alles verdanke. Am meisten danke ich meiner Tochter Lara, die mich stets mit frischer Energie und Glück belieferte und die das wichtigste in meinem Leben ist. Martin Grininger danke ich nicht nur für das sorgfältige Durchlesen dieser Arbeit sondern auch für seine treue Unterstützung, unendliche Geduldigkeit und vieles mehr.

Curriculum vitae

Personal Data

Name	Petra Jeanette Lara Wollmann
Date of Birth	4th June 1973
Place of Birth	Karlsruhe, Germany
Nationality	German
Marital Status	unmarried, daughter (born 2000)

Academic Training

Since Nov. 2002	PhD Thesis Max Planck Institute of Biochemistry, Martinsried Department of Membrane Biochemistry Supervisors: Prof. Dr. D. Oesterhelt, and Dr. K. Zeth Title: The Structure of RseB, a Sensor for Periplasmic Stress in *Escherichia coli*
Sept. 1999	Diplom Biologie
1998 to 1999	Diploma Thesis Ludwigs-Maximilians-Universität, Munich Institute of Genetics and Microbiology Supervisor: Prof. Dr. C. Koch Title: START-spezifische Transkription im Zellzyklus der Bäckerhefe *Saccharomyces cerevsiae.* Die Architektur des Ctr9p-Komplexes)
1993 to 1999	Studies in Biology Ludwigs-Maximilians-Universität, Munich
1993	Abitur Rupprecht-Gymnasium, Munich